Mixing and the Jet Flap

B. S. STRATFORD

(National Gas Turbine Establishment)

SUMMARY: One of the main problems associated with the "Jet Flap" concerns the discrepancy in thrust between idealised theory and the experimental results. This discrepancy is attributable to the mixing with the surrounding flow of the thin two-dimensional jet while still in close proximity to the aerofoil. The effect of the mixing may be calculated to a first approximation from a formula derivable from first principles, while certain second order effects, which can be significant, may be considered qualitatively.

It is concluded that

(*i*) the full thrust* should be experienced by a jet flapped aircraft at cruise,

(*ii*) it should be possible to attain a low form drag at cruise in comparison with a conventional aircraft,

(*iii*) at take-off, an aircraft using a shrouded jet flap would have better thrust recovery than one using a pure jet flap (which shows appreciable losses),

(*iv*) the use of by-pass engines would further improve the thrust characteristics,

(*v*) the practical gains from thrust augmentation, as obtained by controlling the mixing, seem likely to be small.

1. Introduction

In the historical sketch[1] which formed the first paper in this series on the "Jet Flap" an outline was given of the mechanism whereby lift was induced. The "Thrust Hypothesis" (according to which the forward thrust on a jet flapped aerofoil remains constant independently of increase in the deflection angle of the jet) also was discussed, but only incompletely, consideration being limited to an inviscid flow having no mixing. Extension of this hypothesis to a real flow is of interest not only because of the scientific curiosity attached to the hypothesis but also because, as has been indicated in Part II of the recent lecture[2], its realisation might be of some economic importance.

*The "full thrust" is here defined as the thrust which would be experienced by that conventional aircraft for which the effects of the mixing of the jet-stream may be assumed negligible and for which certain conditions at the nozzle, namely mass flow, total pressure, and total temperature, are the same as for the jet flapped aircraft.

Received December 1955.

[Aeronautical Quarterly, Vol. VII, May 1956]

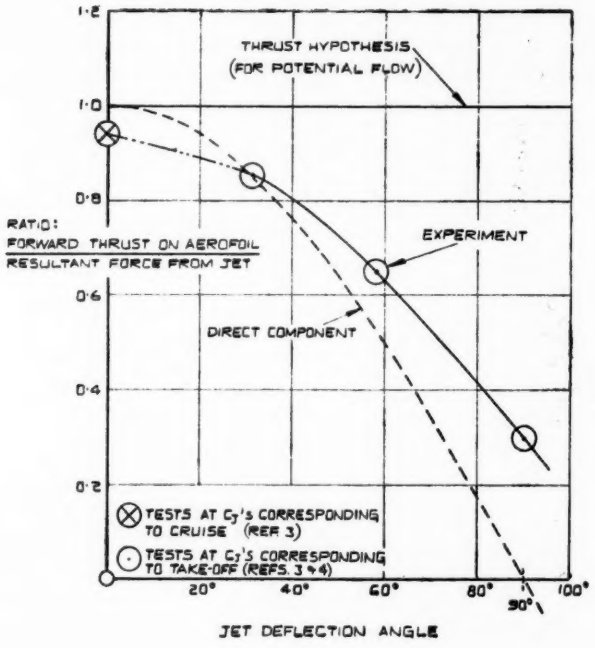

Fig. 1.

Variation of aerofoil thrust with jet deflection angle.

Of the experimental evidence so far available, typical values for the ratio (forward thrust)/(total jet reaction), taken from Dimmock's measurements[3, 4], are shown in Table I and Fig. 1. (These values include losses due to secondary flow from the end wall boundary layers and, for the 90° test, due to separation of the model boundary layer, but the trend indicated is probably correct). It will be seen that, for an angle of deflection greater than about 30°, the forward thrust experienced by the aerofoil is greater than the direct forward component of the reaction; there are, however, for all values of θ, appreciable losses as compared with the prediction of the hypothesis.

Ramifications of the experimental results are apparent. For an aircraft at cruise, when probably the same jet system as at low speeds would be in operation, the jet deflection would be sensibly zero and the results of Table I would suggest a loss of between 5 and 10 per cent. of the cruising thrust—sufficient to influence seriously the economy of the aircraft. For take-off, and to some extent at landing, the effects of a loss of thrust would include a reduction in the usable lift coefficient. This is because the maximum lift that may be used on an aircraft equipped with the jet flap is most probably determined by the thrust that is available for overcoming the induced drag.

TABLE I

VARIATION OF AEROFOIL FORWARD THRUST WITH JET DEFLECTION ANGLE

Jet deflection angle θ	0°	31·4°	58·1°	90°
Ratio $\frac{\text{forward thrust}}{\text{total jet reaction}}$	0·94	0·85	0·65	0·30
$\cos\theta$	1·00	0·855	0·529	0

Notes: (1) The values have been corrected to allow for the direct skin-friction drag.
(2) The results quoted typify ranges of C_J corresponding to cruising conditions for the 0° test, and to take-off for the remainder of the tests.

The problems concerning thrust may therefore be put as follows:—

(*i*) What is the cause of the loss of thrust as shown in Table I?

(*ii*) Can the thrust loss, if any, be predicted for aircraft cruising conditions?

(*iii*) Can the loss be predicted for take-off and landing?

There is also the further problem

(*iv*) Might it be feasible so to combine the jet-aerofoil-flow system as to obtain more thrust than is predicted by the hypothesis?

In answer to the first problem it is suggested that the cause of the thrust loss is the mixing which occurs between the jet and the main stream. This suggestion forms the basis of the present paper and it is found convenient to use three methods for its investigation. The main derivation uses energy considerations, the argument being that the useful power expended on the aircraft for a given engine power must, in some manner, be changed by an amount that will just counterbalance any change in the power dissipated by the mixing. The analysis leads to a simple algebraic formula and one of the points demonstrated is that the density of the jet has an important influence on the thrust in cruising flight. The second and third methods for investigating the mixing respectively use momentum principles and consideration of the sink effect of the jet in absorbing the external stream. The sink effect provides a simple physical picture for the flow, showing, for example, how the increment of thrust or drag is induced on the aerofoil. A later paper[5] will include both the longer analysis based on momentum, as this is perhaps more readily acceptable than are the energy considerations, and also some further details concerning the sink effect.

The theory secures broad agreement with the experimental facts: nevertheless in several types of flow it is still unable to provide a satisfactory prediction. This, it is suggested, is because the surrounding air has a velocity component perpendicular to the jet (in order to reach and mix with it) whereas the basic analysis assumes that the jet and main stream velocities are locally parallel. Thus there is so far only a one-dimensional theory for the flow locally in the mixing region and the effect predicted is accordingly denoted the "primary" change of thrust. An analysis of the second order effects is highly desirable.

When the understanding is sufficiently advanced, aerofoil development might perhaps be assisted by a semi-empirical approach, such as that used by Squire and Young[6] for their analysis of the mixing in a wake.

NOTATION

T_c net thrust on a conventional aerofoil

T_f net thrust on a jet flapped aerofoil

p_0 static pressure in the undisturbed main stream

p_1 static pressure at the position of the mixing

U_0 velocity of the undisturbed main stream

U_1 main stream velocity corresponding to p_1

$U_{j,0} = U_j$, jet velocity at pressure p_0 before mixing

$U_{j,1}$ jet velocity at pressure p_1 before mixing

u_d velocity difference between the jet and the local main stream

ρ, ρ_0, ρ_1 density, or densities, of main stream fluid

ρ_j density of jet fluid

m mass flow rate of the jet

v velocity component of the external flow perpendicular to the boundary of the jet mixing region

n ratio of the mass flow rates of the main stream and of the jet in the mixing process at pressure p_1

y distance measured perpendicular to the jet or boundary layer

u local velocity in the jet or boundary layer

$\delta^* = \int_0^\infty \left(1 - \frac{u}{U_1}\right) dy$, displacement thickness of the bounday layer or jet

c aerofoil chord

$u_{d,1}$ velocity difference between the jet and the main stream at pressure p_1

$u_{d,\infty} = u_{d,0}$, velocity difference between the jet and the main stream at pressure p_0

Suffixes

1 refers to conditions at the position of mixing

0 refers to conditions in the undisturbed main stream

j refers to the jet

KRESGE-HOOKER WAYNE UNIVERSITY SCIENTIFIC LIBRARY

2. Energy Considerations

In conventional jet propulsion the dimensions of the jet are such that most of the mixing occurs so far downstream of the wing as not to affect its pressure distribution; hence the thrust is just that of the engine system. The pressure distribution might, however, be affected on a jet flapped aircraft, since the mixing of its thin jet will occur very close to the wing. This could directly influence the total thrust, a possibility which seems the more likely on recalling that when the jet is deflected a part of the thrust must be transmitted by the external pressure forces. Before looking for a detailed mechanism whereby the thrust might be altered, an examination will be made of the energy balance.

Of the power output from an aircraft jet engine, a part is expended on the aircraft and the remainder is eventually dissipated in the mixing between the jet and the surrounding air. Thus the energy balance may be written

$$\textit{Useful power expended on aircraft} = \textit{Engine power} - \textit{power dissipated in jet mixing}^{*} \quad . \quad . \quad . \quad (1)$$

Since the useful power expended on the aircraft is equal to the product of its thrust and its forward speed, equation (1) gives

$$\textit{Thrust on aircraft} = \frac{\textit{Engine power} - \textit{power dissipated in jet mixing}}{\textit{aircraft speed}} \quad . \quad (2)$$

The conventional aircraft may be taken as a standard and the jet flap system of equal engine power compared with it. Equation (2) then shows that

$$\textit{Change of thrust} = \frac{-(\textit{change of power dissipated in jet mixing})}{\textit{aircraft speed}} \quad . \quad (3)$$

Thus, if the thrust acting on the conventional aircraft is T_c, that on the jet flapped aircraft T_f, and if the aircraft speed is U_0, the proportional change of thrust is

$$\frac{T_f - T_c}{T_c} = \frac{-(\textit{change of power dissipated in jet mixing})}{T_c U_0} \quad . \quad . \quad (4)$$

It is now necessary to examine the mixing process in more detail.

---

*Equation (1) assumes that the thermodynamic reconversion to useful work of the power dissipated is sufficiently small to be neglected. It also assumes for simplicity that both the wake from the aircraft boundary layers and the three-dimensional downwash remain separate from the jet. The second assumption does not affect the principle of the argument, since the force to be overcome could be external to the aerodynamic system, *e.g.* gravity during a climb. The first assumption appears unimportant provided that none of the speeds are appreciably supersonic.

For the jet flapped aircraft the initial stages of the mixing take place within the pressure field of the wing, a process which, in its essence, may be represented by uniform mixing of the jet with n times its own mass flow in a region where the static pressure is p_1, while the remainder of the mixing occurs at the undisturbed pressure p_0. To begin with, this will be simplified by supposing that it is the whole of the mixing which occurs at the pressure p_1; then the change in the power dissipation from that of the conventional aircraft (where sensibly all the mixing occurs downstream at the pressure p_0) is that due to the change $(p_1 - p_0)$ in the static pressure of the mixing region. It will be assumed initially that $(p_1 - p_0)$ is sufficiently small for the use of differentials δp and δu. It will also be assumed that the velocities of the jet and main stream are parallel locally in the mixing region.

Let the velocity difference between the jet and the main stream be u_d. If the mixing is complete, that is if the jet mixes with an infinite mass flow, the whole of the jet energy based on this velocity difference u_d will be dissipated.* Thus, for a mass flow m in the jet,

$$\text{power dissipation} = \tfrac{1}{2} m u_d^2 \qquad (\text{when } n \longrightarrow \infty) \quad . \quad . \quad . \quad (5)$$

If the velocity difference u_d changes by an amount δu_d, due to the change in the static pressure, the change in the power dissipation is given by differentiating equation (5):—

$$\text{change in power dissipation} = m u_d (\delta u_d) \qquad (\text{when } n \longrightarrow \infty) \, . \quad . \quad . \quad (6)$$

Since the change δu_d is supposed small, the value of u_d in equation (6) may be taken either as that before or that after the change. By choosing the value for the conventional aircraft, *i.e.* $u_{d_0} (= U_j - U_0)$, the velocity difference becomes equal to the velocity increase of the jet in passing through the engine system. Thus $m u_d$ in equation (6) may be put equal to the thrust:—

$$m u_d \simeq m u_{d_0} = T_c \quad . \quad . \quad . \quad . \quad . \quad . \quad (7)$$

and then,

$$\text{change in power dissipation} = T_c (\delta u_d) \quad . \quad . \quad . \quad . \quad (8)$$

Equation (4) therefore reduces to

$$\frac{T_f - T_c}{T_c} = -\frac{\delta u_d}{U_0} \qquad (\text{when } n \longrightarrow \infty) \quad . \quad . \quad . \quad (9)$$

This relation, whereby the thrust increases if the velocity difference decreases, (and vice versa), is fundamental to the present discussion, so that the quantity δu_d becomes one of the key considerations in estimating the performance.

*This may be taken as intuitively obvious, by considering axes fixed relative to the main stream, or it may be proved from first principles—for example by means of the result that, when two masses m_1 and m_2 having velocities u_1 and u_2 coalesce, the loss of kinetic energy is $\{\tfrac{1}{2} m_1 (u_1 - u_2)^2\} / \{1 + (m_1/m_2)\}$.

If the more complete picture is considered whereby the jet mixes uniformly with n times its own mass flow at pressure p_1 and with the remainder of the main stream at pressure p_0, the conclusion is that

$$\frac{T_t - T_c}{T_c} = - \frac{\delta u_d}{U_0\left(1 + \frac{U_j}{nU_0}\right)} \quad . \quad . \quad . \quad . \quad . \quad (10)$$

where U_j is the inviscid jet velocity relative to the aircraft in a position where the pressure is p_0. The value of δu_d is readily calculated on inviscid flow principles as follows.

Take axes relative to the aircraft; let U_1 be the velocity of the main stream where the pressure is p_1 and let ρ_j and ρ_0 be the densities of the jet and of the main stream respectively. Now for any inviscid flow, whether compressible or incompressible,

$$dp = - \rho u \, du \quad . \quad . \quad . \quad . \quad . \quad . \quad (11)$$

This follows directly from momentum principles or, for incompressible flow, by differentiating the Bernoulli equation of energy, $p + \frac{1}{2}\rho u^2 = \text{constant}$ along a streamline.

Hence,
$$\delta u = - \frac{\delta p}{\rho u} . \quad . \quad . \quad . \quad . \quad . \quad . \quad (12)$$

Equation (12) illustrates the second feature which is fundamental to the present discussion; for a given change in pressure, the change in velocity is small for a flow of high velocity or density and large for one of low velocity or density, the product ρu being the actual criterion. From equation (12) the values of this product ρu for the jet and for the main stream will determine their respective changes of velocity, and hence the change in their velocity difference, and as already shown, this will determine the thrust.

Thus
$$\delta u_d = \delta U_j - \delta U_{\text{main stream}}$$

i.e.
$$\delta u_d = \delta U_{\text{main stream}} \left(\frac{\delta U_j}{\delta U_{\text{main stream}}} - 1 \right) \quad . \quad . \quad . \quad . \quad (13)$$

The pressure change δp is the same for the jet as for the main stream with which it mixes and so, using equations (12) and (13),

$$\delta u_d = (U_1 - U_0) \left(\frac{\rho_0 U_0}{\rho_j U_j} - 1 \right) \quad . \quad . \quad . \quad . \quad . \quad (14)$$

Thus, from equation (10),

$$\frac{T_t - T_c}{T_c} = \frac{\left(\frac{U_1}{U_0} - 1\right)\left(1 - \frac{\rho_0 U_0}{\rho_j U_j}\right)}{\left(1 + \frac{U_j}{nU_0}\right)} \quad . \quad . \quad . \quad . \quad (15)$$

This result gives the primary change of thrust when a portion of the mixing occurs close to the aerofoil and the remainder downstream, instead of the whole of it occurring downstream as effectively happens for a conventional aircraft.

3. Discussion

3.1. Some Features and Limitations

(*i*) In low speed flight, when U_0/U_j is sufficiently small for the factor $[1-(\rho_0 U_0)/(\rho_j U_j)]$ to be positive, a gain is achieved by allowing the mixing to occur where the pressure is less than the free stream pressure. (The action here may be likened to that of an ejector pump or thrust augmentor, the external aircraft surfces acting in the same way as the internal pump surfaces). On the other hand, a loss would result from mixing which occurs where the pressure is higher than that of the free stream.

(*ii*) If the velocities and densities are such that

$$\rho_0 U_0 = \rho_j U_j \qquad \text{(a possible condition)} . \quad . \quad . \quad . \quad . \quad (16)$$

the primary thrust or drag increment is zero, whatever the position of the mixing.

(*iii*) By multiplication by nU_0/U_j, it will be seen that, when nU_0/U_j is small, the primary change in thrust is proportional to the amount of the mixing which occurs at pressure p_1. More specifically it is proportional to the momentum ratio nU_0/U_j.

(*iv*) For large amounts of mixing the primary change is asymptotic to the value

$$\frac{T_1 - T_e}{T_e} = \left(\frac{U_1}{U_0} - 1\right)\left(1 - \frac{\rho_0 U_0}{\rho_j U_j}\right) \qquad \text{(when } n \longrightarrow \infty\text{)} \quad . \quad . \quad (17)$$

(*v*) Algebraically the formula of equation (15) is only a first approximation to the equations representing the flow model that was initially chosen. Moreover, physically, the chosen model was only a first approximation to the real flow. Now the algebraic approximations are tantamount to the assumption that the quantity $(U_1/U_0 - 1)$ is small, and Ref. 5 shows that this does not introduce a serious error. In contrast the physical approximation is fundamental: it has been assumed that the velocities of the jet and main stream are precisely parallel. In the real flow the main stream is drawn into the jet, so that the two fluids are not travelling in exactly the same direction—a condition which seems likely to cause a superposed loss! This " secondary loss " is not considered quantitatively but will be assumed to increase with increase of the entrainment angle.

(*vi*) Kinetic heating has been neglected in the statement of equation (1) and in the derivation of equation (10), but rough calculation suggests that up to a Mach number of unity the effect will be small.

3.2. The Value of n

To complete the foregoing analysis for the primary increment of thrust, it is necessary to find the rate of mixing and hence the value of the mass flow ratio n.

The standard theory for the mixing between a jet and "still" air has been developed semi-empirically. During the mixing the jet "entrains" the external air, which must therefore have a velocity perpendicular to the jet boundary. (It is effectively this component that is neglected elsewhere in the present treatment). Denoting this entrainment velocity by v, it may be deduced from the standard work that v is given approximately by

$$v = \frac{U_j}{25} \qquad (\rho_j = \rho_0, U_1 = 0) \quad . \quad . \quad . \quad . \quad (18)$$

where U_j is the jet velocity or the peak jet velocity. By integrating v along both sides of the jet the total flow into the jet, and hence the value of n, can be calculated. In equation (18) and the subsequent equations (19) to (21) only, both v and U_j represent local values, which may be deduced from the values at the beginning of the mixing region.

For a jet in moving air, a theory exists[6] but no experimental work is known. The entrainment velocity as given by the theory can be shown to be satisfied very roughly by the relation

$$v = \frac{U_j - U_1}{25} \qquad (\rho_j = \rho_0) \quad . \quad . \quad . \quad . \quad (19)$$

where U_1 is the velocity of the external air. Since equation (19) appears a highly reasonable generalisation of equation (18), it was decided that a crude experimental check would suffice for its confirmation. A comparison of the theoretical and experimental boundaries for a jet of which the initial velocity was just under five times the external main stream velocity is shown in Fig. 2. In the first part of the mixing region there is a discrepancy but, as will be mentioned later, this is probably attributable to the high turbulence level in the oncoming boundary layer. Thereafter the agreement is sufficiently close to justify the use of equation (19) for present requirements. Again, integration of v on both sides of the jet leads to a value for n.

No standard work is known concerning the effects of density, but an experiment which will be described presently has provided incidental information. It was noticed that when a hydrogen jet issued into otherwise still air the suction pressure created in the neighbourhood of the jet, *i.e.* $\frac{1}{2}\rho v^2$, was roughly equal to that created by a similar jet of cold air of the same dynamic head. Thus equation (18) would be replaced by

$$v = \left(\frac{\rho_j}{\rho}\right)^{\frac{1}{2}} \frac{U_j}{25} \qquad (U_1 = 0) \quad . \quad . \quad . \quad . \quad (20)$$

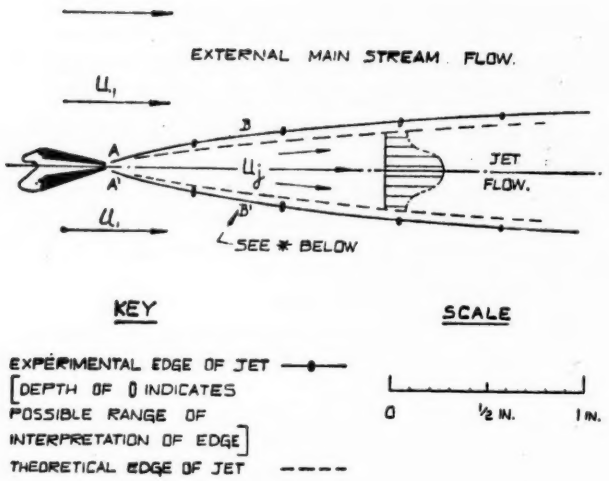

Fig. 2.

A comparison of the experimental and theoretical jet mixing rates.
Jet nozzle velocity $= 4{\cdot}8\ U_1$.
*External boundary layer flow is absorbed by jet in regions AB and $A'B'$.

Until more evidence is available a reasonable generalisation of equation (19) would therefore be

$$v = \left(\frac{\rho_j}{\rho}\right)^{\frac{1}{2}} \frac{U_j - U_1}{25} \quad . \quad . \quad . \quad . \quad . \quad (21)$$

When the jet is flowing along a surface the mixing rate is thereby halved and correspondingly the entrainment velocity v is integrated along only one side. Any reduction in the mixing rate on this one side due to a lower turbulence level in the jet—the turbulence must become zero at the wall—is neglected. Also, any initial laminar mixing region will be neglected, this being counteracted by the increase in mixing caused by the turbulence of the main stream boundary layer. The low velocity in the boundary layer may be allowed for simply by replacing U_1 in equation (21) by the appropriate boundary layer velocity at the position of entrainment.

One final factor arises from the assumption in the main theory that the mixing of the jet with n times its own mass flow is a uniform process in which the velocity profiles are rectangular, both for the jet before mixing and for the jet plus main flow after mixing. In fact the profile after mixing is peaked at the centre and has a "tail" at each side. Some of the entrained air still remains in the tail and so does not significantly contribute to the effect on thrust. Consequently the value for n to be used in the thrust calculation should be somewhat less than that obtained from

equation (21). A factor of 70 per cent. has been adopted. This was chosen after a comparison of certain detailed aspects of the square and peaked jets and it is thought to be probably within 10 per cent. of the true value; although intuitively reasonable, its derivation is by no means rigorous.

Typical values of n obtained by integrating equation (21) and applying the 70 per cent. factor range from 0·5 to 1·5 for cruising conditions and from 0·5 to 2·0 at take-off. It has been assumed that the nozzle width is equal to one third of one per cent. of the chord, and that the mixing occurs on one or both sides of the jet over a distance of between 5 and 10 per cent. of the chord.

3.3. Mixing Between the Aerofoil Boundary Layers and the Jet

The most significant aspect of the mixing with the aerofoil boundary layers is that the form drag of the aerofoil may be removed in cruising flight. Only a summary of points is presented as fuller details will be given in the later paper[5].

(*i*) Because of the lower velocities in the boundary layer, the rate of mixing will be increased, as given by equation (21).

(*ii*) The mixing rate will be further increased by the turbulence of the boundary layer.

(*iii*) Because of the lower velocities in the boundary layer, the angle at which the boundary layer fluid enters the jet will, for a given mixing rate, be greater than the angle at which the main stream enters the jet; this will probably increase the secondary losses mentioned in Section 3.1. The effect would be emphasised by the increases in mixing rate mentioned in points (*i*) and (*ii*) above.

(*iv*) The effect of point (*iii*) would be further emphasised by a high pressure in the mixing region, as the high pressure would reduce the boundary layer velocities. On the other hand a suction, *i.e.* a pressure which is less than in the free stream, would increase the boundary layer velocities and reduce the secondary losses.

(*v*) The previous four points have considered the effects of the boundary layer on the rate of entrainment and on the secondary losses. There is also an effect on the primary increment of thrust considered in the main analysis of Section 2.

Since the boundary layer velocities are smaller than the main stream velocity the boundary layer will react more to changes in pressure than would the main stream, as shown by equation (12). The corresponding factor for equation (15) is $[1 - (\rho_0 u)/(\rho_1 U_1)]$, which remains positive for most of the boundary layer under all conditions of flight. Thus there will be an increase of thrust if the boundary layer mixing is allowed to occur at a high suction, and this increase would hold for cruise as well as at take-off.

(*vi*) The previous effect may be reinterpreted on boundary layer theory as a reduction or removal of the form drag:—

The form drag of an aerofoil, *i.e.* that part of the two-dimensional drag transmitted by the normal pressure forces and not by the skin friction. is given by

$$C_{D,\,\text{form}} = \frac{1}{\frac{1}{2}\rho U_0^2 c}\int_0^\infty \delta^* \frac{dp}{dx}\,dx\,.$$

If the mixing between the jet and the boundary layer occurs at a position of high suction, the decrease in displacement thickness that results from the mixing will persist for the subsequent pressure rise to the trailing edge. Thus the value of the integral and hence of the form drag would be reduced. A crude estimate suggests that at cruise this could reduce the total drag of the aircraft by at least 5 per cent.

3.4. Visualising the Flow

The reasoning so far has suggested that the mixing can affect the thrust acting on an aerofoil, but how it does so has not yet been examined. Again only a summary is presented, Ref. 5 considering the mechanisms more completely.

Consider first a jet issuing from an aerofoil when the main stream fluid is at rest other than for the action of the jet. The jet mixes with the surrounding fluid and absorbs some of it into itself. To do this the jet must create a suction along its boundaries. This creation of a suction pressure may be called the "sink effect" of the jet mixing.

If the sink effect occurs aft of the aerofoil it will cause a suction on the rearward surfaces and this suction will be greater than that produced on the remoter leading surfaces. Consequently there will be a pressure drag, and the net thrust experienced by the aerofoil will be less than the thrust from the jet alone.

When the external fluid is not at rest the sink effect of the mixing changes and becomes proportional to $[1-(\rho_1 U_1)/(\rho_{j,1}U_{j,1})]$ where the suffixes "1" indicate values at the local pressure p_1 before mixing. This follows from a consideration of the total stream tube area before and after mixing. Thus, for example, if $\rho_1 U_1 = \rho_{j,1}U_{j,1}$, it may be shown that the flow occupies the same total cross-sectional area before and after mixing; consequently there is zero sink effect, and zero effect on the aerofoil thrust. This correlates (to a first approximation) with the $\rho_0 U_0 = \rho_{j,0}U_{j,0}$ condition for zero change in thrust as obtained in the main analysis.

The thrust increment induced on the aerofoil by a given sink also becomes changed when the external flow is not at rest. A sink situated downstream of the trailing edge still induces a drag force, but a sink situated on the "body" of the aerofoil induces a thrust force. On the body of the aerofoil the sink tends to

reduce the velocities in the trailing edge region and to increase them at the leading edge, thus causing a forward force. More strictly the sink exerts a thrust or drag on the aerofoil according as the local velocity U_1 at the position of the sink is greater or less than the free stream velocity U_0.

As will be shown in Ref. 5, the foregoing arguments lead to a result which is in agreement with equation (15).

4. Application to the Practical Problems. Low Speed Flight

4.1. Take-off and Landing

The experiments[3, 4] quoted in the Introduction have indicated that a pure jet flapped aerofoil suffers an appreciable loss of thrust when the jet is deflected as for an aircraft at take-off. As a preliminary to a qualitative examination, equation (15) may be simplified to

$$\frac{T_t - T_c}{T_c} \simeq \frac{nU_0}{U_j}\left(\frac{U_1}{U_0} - 1\right) \quad . \quad . \quad . \quad . \quad . \quad (22)$$

since, at take-off, $\rho_0 U_0/(\rho_j U_j)$ is small, while nU_0/U_j is not large. Equation (22) indicates firstly that there is a gain of thrust from mixing where the local main stream velocity U_1 exceeds the free stream velocity U_0, and correspondingly a loss where U_1 is less than U_0; and secondly that each gain or loss is proportional to the amount of mixing which causes it.

With the jet deflected downwards the pressure on its lower side becomes greater than the undisturbed static pressure p_0, and consequently $(U_1/U_0 - 1)$ is negative, while on the upper side the pressure decreases and $(U_1/U_0 - 1)$ is positive. Thus the mixing which occurs on the lower side causes a loss of thrust, while that which occurs on the upper causes an increase. Since $(U_1/U_0 - 1)$ for the upper side will exceed $[-(U_1/U_0 - 1)]$ for the lower, a net gain of thrust might have been expected; but several factors offset this. The velocity difference between the jet and the main stream will be greater on the lower side; thus the amount of mixing there will be greater (equation (21)) and the loss will be increased. Moreover the boundary layer from the lower aerofoil surface is likely to have just experienced a pressure rise, so that its flow might be highly turbulent and its velocity very low. Both factors further increase the amount of mixing and therefore the value of n in equation (22), and so further increase the loss on the lower side as compared with the gain on the upper. Probably more important than these factors, however, is the secondary loss mentioned in Section 3.1 but omitted from the main theory. On the lower side the entrainment velocity v is comparable with the local main stream velocity U_1 and the experiments show that the main flow may go " straight into the jet "; near the nozzle there can be an angle of 120° between the jet and the flow which it is entraining. It is therefore to be expected that the secondary losses would be quite severe for a pure jet flapped aerofoil. It is not yet possible, however, to make a theoretical prediction of these losses.

Two trends seem predictable. Firstly, the use of by-pass engines, which would allow lower jet speeds for a given thrust, should decrease the mixing rate and therefore the net primary losses. It should also decrease the entrainment angles and hence the secondary losses. Secondly, the shroud of the shrouded jet flap also should decrease the mixing losses. The "shrouded jet flap" is a variant of the pure jet flap. The jet issues over a mechanical flap, which may be only a few per cent. in chordal extent, and follows around the upper surface of this flap by "Coanda" action, thereby being deflected when the mechanical flap is deflected. The shrouded jet flap has advantages such as simplicity of jet deflection, increased effectiveness at cruise, and reduction of induced drag if an engine fails at take-off or landing. Its special problems concern the friction and heat transfer between the jet and the flap. The name "shroud," however, was coined because of the action of the mechanical flap in sheltering the jet from the region of very high pressure in the corner, just under the jet exit, where very violent mixing occurs for the pure jet flap. It is because of this sheltering action that the losses from the mixing on the under side should be reduced. The shroud, or mechanical flap, would also increase the region of favourable mixing on the upper side of the jet. Thus, in addition to the advantages just quoted, the thrust characteristics at take-off and landing would be expected to be better for the shrouded than for the pure jet flapped aerofoil. In practice attention would have to be paid to conditions at the leading edge where a boundary layer separation could cause significant losses; for all the present discussion it is assumed that no boundary layer separation occurs.

4.2. Thrust Augmentation

The basic theory of Section 2 has suggested that it would be possible to obtain an increase of thrust at take-off by causing the jet to mix with the main stream in a region of high suction, *i.e.* in a region where the pressure is much less than that in the free stream and where $(U_1/U_0 - 1)$ is large and positive. With the shrouded jet flap a strong suction exists on the upper surface around the "hinge" of the flap so that, by positioning the jet nozzle at say 80 to 90 per cent. of the chord, the desired arrangement would be obtained. With the mixing on only one side of the jet the mass flow ratio n might be expected to reach the value $n = 1{\cdot}0$ in the "useful" region, and if the mean value of $(U_1/U_0 - 1)$ were $2{\cdot}0$, with $U_0/U_j = 1/15$, and $\rho_0/\rho_j = 3{\cdot}0$, the increase of thrust would be given by equation (15) as

$$\frac{T_t - T_c}{T_c} = \frac{2\,(1 - 1/5)}{(1 + 15)} = 10 \text{ per cent.}$$

According to a quick calculation the skin friction between the jet and the aerofoil would largely counteract any gain of this magnitude.

Supposing, on the other hand, that very rapid mixing could be achieved in the suction region. The limit to the gain is given by equation (15) when the value of n becomes infinite, *i.e.*

$$\frac{T_t - T_c}{T_c} = \left(\frac{U_1}{U_0} - 1\right)\left(1 - \frac{\rho_0 U_0}{\rho_j U_j}\right) \qquad (\text{when } n \longrightarrow \infty).$$

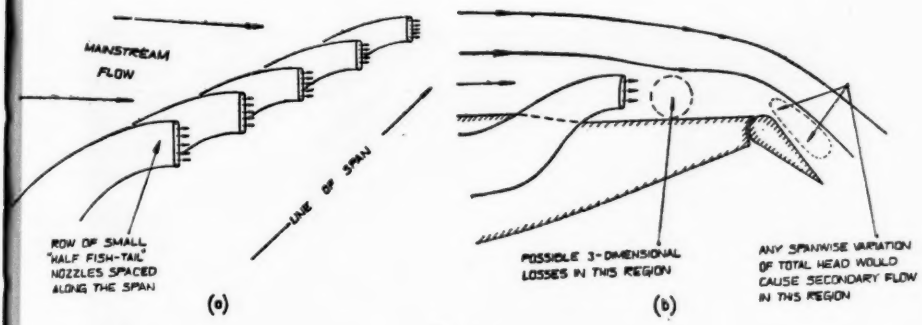
MAINSTREAM FLOW
LINE OF SPAN
ROW OF SMALL "HALF FISH-TAIL" NOZZLES SPACED ALONG THE SPAN
(a)
POSSIBLE 3-DIMENSIONAL LOSSES IN THIS REGION
ANY SPANWISE VARIATION OF TOTAL HEAD WOULD CAUSE SECONDARY FLOW IN THIS REGION
(b)

Fig. 3.

One method of increasing the rate of mixing; additional losses that may result.

For the values just given this would give 160 per cent. augmentation; even for, say, $n=5$ the augmentation would be 40 per cent. A mixing rate giving $n=5$ could be achieved by special arrangement of the jet, for example by the scheme illustrated in Fig. 3, where a row of "half fish-tail" nozzles is placed along the span. The aim in this scheme is to increase the peripheral area between the jet and the main stream, and to reduce the damping effect of the wall on the mixing turbulence. Also the jet skin friction should be less than for a shrouded jet flap.

To test the foregoing suggestion, and to find whether other effects might offset the gain, an experiment was performed with the model shown in Fig. 4. In the experiment it was found that thrust was lost instead of gained over the whole range of jet velocities, although the amount of this loss was slightly less than would have been predicted for a pure jet flap.

At a condition representative of take-off a value was achieved for n of 4·0. The mean value of (U_1/U_0-1) was 1·0 in the mixing region, while $U_0/U_j=1/20$ and $\rho_0/\rho_j=1{\cdot}0$. (The incidence of the aerofoil body was $-4°$ and the upper surface of the flap was at 45° to the aerofoil body; the value of the jet coefficient C_J was 1·3). With these values, equation (15) would predict the primary increase of thrust to be 16 per cent.

The thrust measured on the balance under the given conditions was 83 per cent. of the jet reaction, *i.e.* a loss of 17 per cent. The loss increased slowly to 20 per cent. when C_J was altered either way by a factor of about four. With U_0 equal to zero the measured thrust was 75 per cent. at this incidence.

In the experiment described, some of the losses could be attributed to skin friction and to end effects both from the tunnel wall boundary layers and from the clearance between the model and the tunnel walls. The results quoted have not been corrected for any of these factors. Nevertheless, flow visualisation revealed very little secondary flow in the main stream and it is probably necessary to attribute

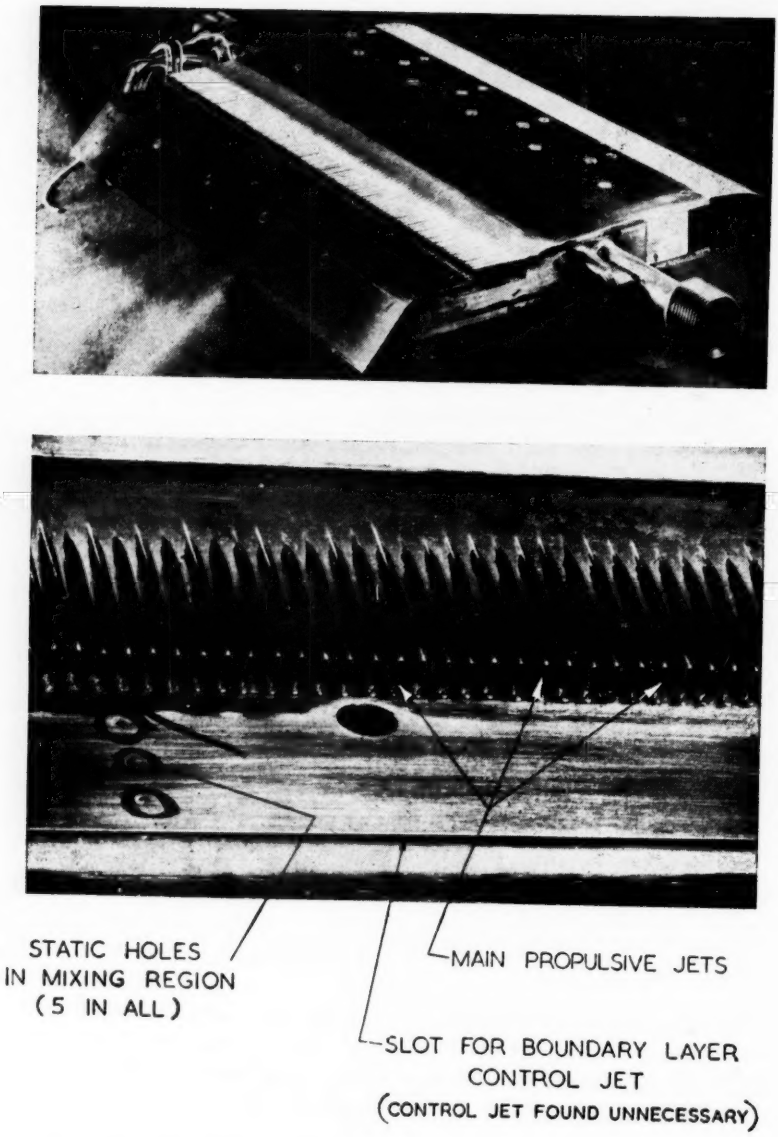

Fig. 4.

The model for the thrust augmentation experiment (*see also* Fig. 3).

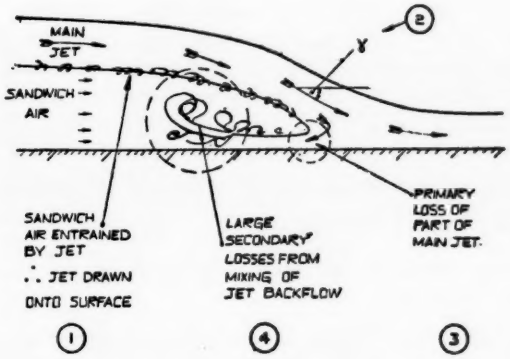

Fig. 5.

The loss of thrust when " sandwich " air causes the jet to impinge on to a surface.

a considerable proportion of the losses to secondary effects connected with the mixing. Experimental confirmation of this would require either a detailed analysis of the jet flow or some arrangement that would eliminate the end effects on the model. The mixing downstream of the nominal mixing region would also need investigation, although its contribution to the thrust loss seems likely to be small.

In addition to the secondary loss that has previously been discussed, *i.e.* that due to the angle at which the external flow is drawn into each jet, various other sources of loss occur in the type of arrangement examined. The essentially three-dimensional flow between neighbouring nozzles may cause a loss. Also there is a possibility of secondary flows at the corner at the flap " hinge," as shown in Fig. 3 (*b*), if the jet total head has not become uniform in a spanwise direction before reaching the corner. (For a non-uniform jet the high momentum air would tend to ignore the corner, while the low momentum air would curl under in order to replace it). An additional possible source of loss occurs where the jet has " sandwich " air between it and the surface, as shown in Fig. 5. The jet will eventually entrain all the sandwich air and impinge on the surface at an appreciable angle, say γ. There will thus be a direct loss of $(1 - \cos\gamma)$ times the jet momentum and, due to the mixing of the reversed flow associated with this momentum loss, there will be, as shown in Fig. 5, subsequent losses that might worsen the situation. In the experiment described there would be some sandwich air, owing to the nozzles being slightly away from the surface, while any arrangement of a jet blowing across the slot of a slotted flap, or of a jet issuing from a nozzle parallel to the surface but away from it, perhaps in order to increase the mixing while avoiding maldistribution along the span, would be likely to meet this difficulty.

Thus, while thrust augmentation, *i.e.* the attainment of an increase in thrust by controlling the mixing, at first seems an attractive proposition, there are many complicating factors to be taken into account. A worthwhile gain would require rapid mixing. It seems likely, though not finally proven, that rapid mixing would

inherently produce various types of secondary flow, and these secondary flows would reduce the gain. The final thrust from the system should be somewhat greater than for a pure jet flapped aerofoil, but unless the details of the flow can be improved the final thrust would probably not exceed the 100 per cent. predicted by the simple thrust hypothesis.

5. Application to the Practical Problems. Cruising Flight

5.1. The Primary Change of Thrust

Under cruising conditions the dominant factor for the primary change of thrust is $[1 - (\rho_0 U_0)/(\rho_1 U_1)]$.

It so happens that for a typical current aircraft at cruise the value of $\rho_1 U_1$ is approximately equal to that of $\rho_0 U_0$ – for example the jet velocity may be double the aircraft velocity and the jet density a half of the ambient. Thus the value of $[1 - (\rho_0 U_0)/(\rho_1 U_1)]$ is close to zero, this being true both for aircraft with pure jet engines and for those with by-pass engines. Consequently, whatever the position of the mixing, the primary loss or gain of thrust as indicated by equation (15) also would be close to zero.

5.2. The Overall Result

In addition to the primary effect, both the secondary loss and also the mixing with the boundary layer must be taken into account when estimating the overall result.

The secondary loss should be small at cruise: with the high main stream velocity the entrainment velocity v perpendicular to the jet would be low, as from equation (21), and consequently the entrainment angle, $\tan^{-1}(v/U_1)$, would be very small.

As regards the mixing between the jet and the aerofoil boundary layers, the discussion of Section 3.3 has suggested that, with care, some gain should be possible. This gain would be achieved by allowing the jet to absorb the boundary layer in a region of high suction—an arrangement that would be practicable on the shrouded jet flap—and the result could be represented as a reduction in the form drag.

Thus, from the foregoing arguments, the net effect from the three aspects of the mixing process should be that an aircraft at cruise will experience effectively the full thrust and possibly some gain.

5.3. The Effect of Jet Temperature

The foregoing conclusion is to be contrasted with the results for a pure jet flapped aerofoil (at zero deflection) using a jet which has the same temperature and density as the main stream.

When the densities of the jet and of the main stream are equal, the factor $[1 - (\rho_0 U_0)/(\rho_1 U_1)]$ approaches unity, instead of being zero as in Section 5.1. Moreover, for the pure jet flap the mixing region is just aft of the trailing edge and so is in

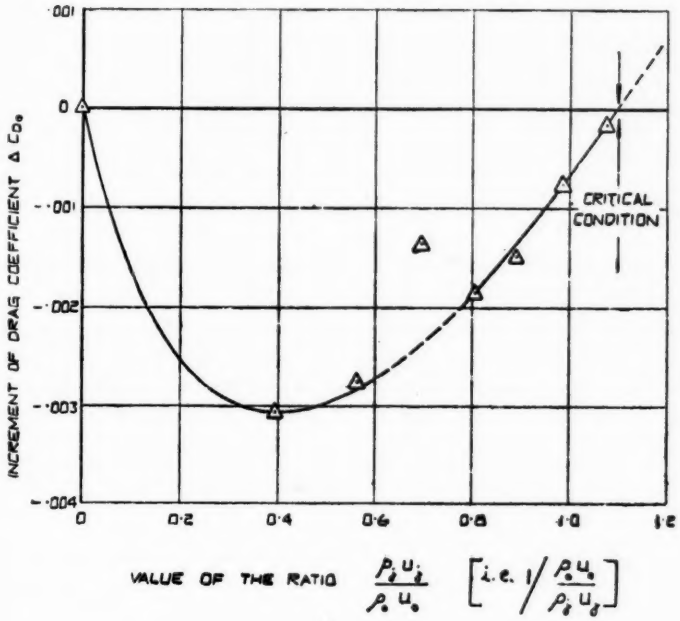

Fig. 6.

Drag/thrust increments under simulated cruising conditions, using a low density (hydrogen) jet.

a position where $U_1/U_0 - 1$ is negative. There is thus no reason to suppose zero loss from the mixing. For example, using $U_0/U_j = \frac{1}{3}$. $U_1/U_0 - 1 = -0{\cdot}1$, and $n = 1{\cdot}5$, equation (15) indicates a primary loss of 2·2 per cent. Since the hot jet would give zero primary loss, it is to be concluded that experiments using a cold air jet would be inadequate for simulating cruising conditions for a jet flapped aircraft. (It will be noticed that the 2·2 per cent. predicted is still a much smaller loss than the 6 per cent. quoted from the experiments of Ref. 3, in Table 1. To this 2·2 per cent. must be added, however, the secondary loss and the additional effects from the boundary layer. The boundary layer effects could cause a significant loss with the pure jet flap of the experiment even although on an aircraft a gain should result).

Since the difference which the theory shows between the behaviour of a hot jet and that of a cold one arises from the difference in density, the reasoning could be tested by using a cold jet of low density gas—assuming that in fact the temperature does not cause other effects. Experiments were therefore performed with a jet of hydrogen issuing undeflected from a pure jet flapped aerofoil and the results are shown, superficially, in Fig. 6. At face value these provide strong confirmation of the theory. The tests were in the nature of a pilot experiment, however, while the effects sought were not only very small but also very sensitive to test conditions.

These results of Fig. 6 were obtained by pressure plotting, whereas the results from tests using a balance were quite inconclusive, the scatter obscuring any definite trend. Thus it would be highly desirable to repeat the experiments using more refined techniques. Provisionally, the evidence suggests that the theory is correct and that under cruising conditions the mixing should still allow the full thrust to be obtained.

6. Conclusions

The foregoing examination has demonstrated certain principles governing the thrust in a jet flap system, but problems still remain.

Concerning the loss of thrust at take-off or landing, only general trends may so far be suggested. It is expected that the shrouded jet flap would have greater thrust recovery than the pure jet flap, and that use of by-pass engines with lower jet velocities and smaller mixing rates would further reduce the losses.

Under cruising conditions the indications are that a jet flapped aircraft should experience effectively the full thrust and possibly some gain, the gain coming from a reduction in the form drag of the wing.

It is fairly definite that any significant augmentation of the take-off thrust (by controlling the mixing) would require a very high mixing rate. It seems likely, but not finally proven, that there are various secondary losses inherent in such rapid mixing and that these would counteract much of the augmentation. The attainable thrust might well be expected to exceed that for a pure jet flapped aerofoil, but it seems unlikely that the prediction of the thrust hypothesis would be surpassed at large flap deflection angles unless a radical improvement is possible in the augmentation system.

These conclusions follow from the arguments of the basic theory, with superposed qualitative considerations of secondary losses and boundary layer effects. The basic theory shows that the primary change of thrust is given by

$$\frac{T_t - T_c}{T_c} = \frac{(U_1/U_0 - 1)\,[1 - (\rho_0 U_0)/(\rho_1 U_1)]}{[1 + U_1/(nU_0)]}.$$

Whereas this primary change is expected to indicate the general trends correctly, the secondary loss, due to the component of velocity of the main flow perpendicular and into the jet, may be important and it would be desirable to develop a theory for its prediction.

The manner in which the thrust or drag increments are induced on the aerofoil may be visualised by considering the sink effect produced by the jet in its absorption of the external flow.

ACKNOWLEDGMENT

All the illustrations used in this paper are Crown Copyright.

REFERENCES

1. STRATFORD, B. S. Early Thoughts on the Jet Flap. *The Aeronautical Quarterly*, February 1956.
2. DAVIDSON, I. M. The Jet Flap. *Journal of the Royal Aeronautical Society*, January 1956.
3. DIMMOCK, N. A. An Experimental Introduction to the Jet Flap. Unpublished Report of the National Gas Turbine Establishment, 1955.
4. DIMMOCK, N. A. Some Further Jet Flap Experiments. Unpublished Memorandum of the National Gas Turbine Establishment, 1956.
5. STRATFORD, B. S. A Further Discussion on Mixing and the Jet Flap. To be published in *The Aeronautical Quarterly*.
6. SQUIRE, H. B. and YOUNG, A. D. The Calculation of the Profile Drag of Aerofoils. R. & M. 1838, November 1937.
7. GOLDSTEIN, S. (Editor). *Modern Developments in Fluid Dynamics*. First Edition. Vol. II, Chapter XIII, pp. 592-4. Oxford University Press, 1938.
8. KUETHE, A. M. Investigations of the Turbulent Mixing Regions formed by Jets. *Journal of Applied Mechanics*, Vol. II, pp. 87-95, 1935.

Numerical Results for the Longitudinal Stability Derivatives and Stability Loci of a Low Aspect Ratio Rectangular Wing in Supersonic Flow

LEE WINOGRAD* and JOHN W. MILES†

(*University of California*)

1. Introduction

The longitudinal stability derivatives and stability loci for a single-degree-of-freedom, pitching oscillation of a rectangular wing having an effective aspect ratio less than unity have been calculated[1] from the results of a previous, analytical investigation[2]. The results extend those previously available for a rectangular wing of effective aspect ratio greater than unity[3, 4].

2. Stability Derivatives

The stability derivatives $C_{L\alpha}$, $C_{L\dot{\alpha}}$, C_{Lq}, $C_{M\alpha}$, $C_{M\dot{\alpha}}$ and C_{Mq} are plotted in Figs. 1 and 2 as functions of the effective aspect ratio ($A=(M^2-1)^{\frac{1}{2}}$ (span/chord)) for a mid-chord ($a=\frac{1}{2}$) axis of rotation; the Mach number M appears as a separate parameter only for $C_{L\dot{\alpha}}$ and $C_{M\dot{\alpha}}$. The notation is that of Ref. 2.

3. Single-Degree-of-Freedom Stability Loci

The stability loci of single-degree-of-freedom pitching oscillations about an axis $x=a$ (the fraction of total chord aft of the leading edge) may be obtained by equating the total damping derivative ($C_{Mq}+C_{M\dot{\alpha}}$) to zero and solving the resulting quadratic equation for a. The pairs of values for a so obtained are plotted as a function of M with A as parameter in Fig. 3. The Mach numbers at which the roots of this quadratic equation coalesce (*i.e.*, the peaks of the curves of a plotted against M) are plotted against *true* aspect ratio (A'=span/chord) to obtain the

*Graduate Student, Department of Engineering, Berkeley.

†Department of Engineering, Los Angeles.

Received March 1955.

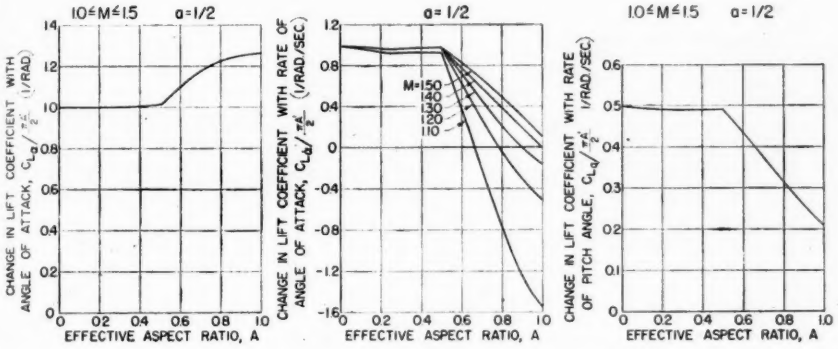
1.0≤M≤1.5 a=1/2
CHANGE IN LIFT COEFFICIENT WITH ANGLE OF ATTACK, $C_{L_\alpha}/\frac{\pi A}{2}$ (1/RAD)
EFFECTIVE ASPECT RATIO, A
a=1/2
CHANGE IN LIFT COEFFICIENT WITH RATE OF ANGLE OF ATTACK, $C_{L_{\dot\alpha}}/\frac{\pi A}{2}$ (1/RAD/SEC)
M=1.50 1.40 1.30 1.20 1.10
EFFECTIVE ASPECT RATIO, A
1.0≤M≤1.5 a=1/2
CHANGE IN LIFT COEFFICIENT WITH RATE OF PITCH ANGLE, $C_{L_q}/\frac{\pi A}{2}$ 1/RAD/SEC)
EFFECTIVE ASPECT RATIO, A

Fig. 1.
Lift coefficient derivatives.

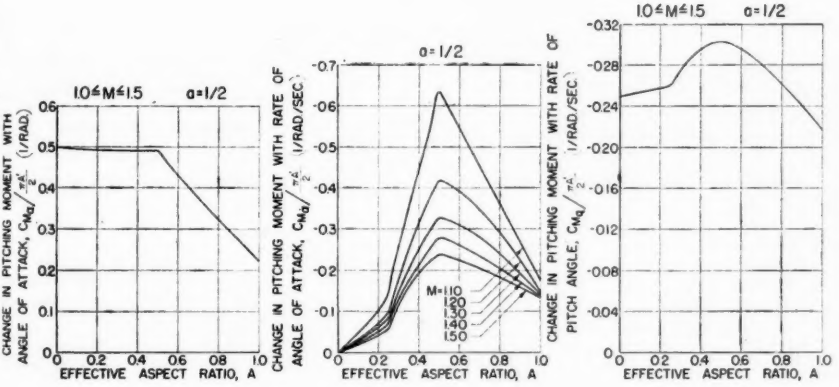
1.0≤M≤1.5 a=1/2
CHANGE IN PITCHING MOMENT WITH ANGLE OF ATTACK, $C_{M_q}/\frac{\pi A}{2}$ (1/RAD)
EFFECTIVE ASPECT RATIO, A
a=1/2
CHANGE IN PITCHING MOMENT WITH RATE OF ANGLE OF ATTACK, $C_{M_{\dot\alpha}}/\frac{\pi A}{2}$ 1/RAD/SEC)
M=1.10 1.20 1.30 1.40 1.50
EFFECTIVE ASPECT RATIO, A
1.0≤M≤1.5 a=1/2
CHANGE IN PITCHING MOMENT WITH RATE OF PITCH ANGLE, $C_{M_q}/\frac{\pi A}{2}$ 1/RAD/SEC)
EFFECTIVE ASPECT RATIO, A

Fig. 2.
Moment coefficient derivatives.

stability envelope of Fig. 4. These results reveal that single-degree-of-freedom instability is impossible for effective aspect ratio less than 0·65 (to two figures), *i.e.*,

$$C_{M_q}+C_{M\dot\alpha/dt}<0 \text{ if } A<0{\cdot}65 \quad . \quad . \quad . \quad . \quad (1)$$

4. Accuracy

The stability locus of Fig. 3 for $A=1$ is in agreement with the exact (linearised) result of Ref. 4 to within 1 – 2 per cent. This, together with the maximum discrepancy of 3 per cent. in centre of pressure at $A=1$ (*cf.* Ref. 2), implies that the foregoing results, which are based on an expansion in the effective aspect ratio A, are adequate for practical application in the range $0<A\leqslant 1$.

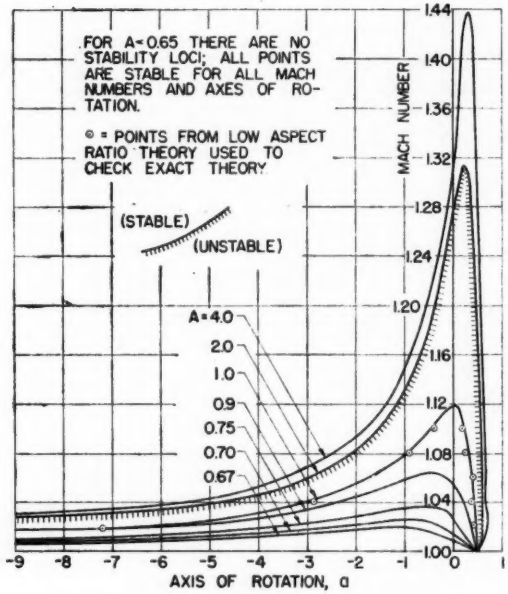

Fig. 3.
Stability loci for pitching oscillations.

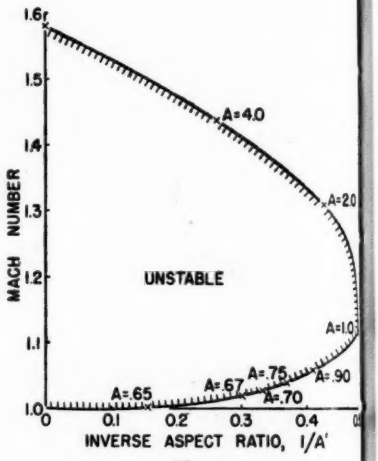

Fig. 4.
Stability envelope for pitching oscillation

References

1. Winograd, Lee. Longitudinal Stability Derivatives of Low Aspect Ratio Rectangular Wings Oscillating in Supersonic Flow. Master of Science Thesis, Department of Mechanical Engineering, University of California, Berkeley, November 1954.

2. Miles, J. W. On the Low Aspect Ratio Oscillating Rectangular Wing in Supersonic Flow. *The Aeronautical Quarterly*, Vol. IV, pp. 231-244, August 1953.

3. Miles, J. W. Aerodynamic Derivatives for an Oscillating Rectangular Airfoil at Supersonic Speeds. U.S. Naval Ordnance Report 1292, Inyokern, California, March 1951.

4. Miles, J. W. The Application of Unsteady Flow Theory to the Calculation of Dynamic Stability Derivatives. North American Aviation Report A.L. 957, Downey, California. September 1950.

Some Integrals Relating to the Vibration of a Cantilever Beam and Approximation for the Effect of Taper on Overtone Frequencies

A. I. MARTIN*

SUMMARY: In the investigation of approximate numerical values of overtone frequencies of a turbine blade it is desirable to know formulae for certain integrals of the modes of vibration of an ordinary cantilever beam. The first object of this paper is to obtain such formulae and to arrange them in tabulated form. By proceeding along the lines of the calculus of perturbations, these results may then be used to obtain new formulae which give second order approximations for the effects of uniform breadth and thickness tapers on the overtone frequencies. The theory gives good agreement with experiments for tapers which do not exceed about 0·5, which is present-day practice for turbine blading.

1. Introduction

The mathematical solution of the ordinary cantilever beam is well known, the frequencies and corresponding modes of vibration being given by elementary formulae quoted in the textbooks. In the theoretical investigation of the flexural vibrations of a turbine blade, or propeller, *e.g.* in the investigation of rotary effects and twist correction factors, it is often desirable to have, in a definite form, formulae for the integrals of these modes. Part I of this paper considers some of these integrals.

If a cantilever beam is uniformly tapered the problem of obtaining its overtone frequencies is much more difficult. The solution is exact in a few cases only; namely, when the beam has a sharp point or a sharp edge at its free end[2, 3, 4, 5]. Several authors have made approximations to the general problem, both by using the theory of integral equations and by extending Rayleigh's device for approximation to the fundamental.† Part II gives second order approximations for the effects

*The work described here was done while the author was with the Bristol Aeroplane Company.

†A list of some of the most efficient methods of approximation will be found on pp. 144-152 of Ref. 1.

Received March 1955.

of uniform breadth and thickness tapers. The formulae may be obtained by proceeding along the lines of the calculus of perturbations and by using the integrals given in Part I. It is assumed that the frequency of vibration can be expressed as a double power series in two taper parameters and that higher powers than two can be neglected. Thus the paper does not cover the range of "extremely large" tapers, but concentrates more on the range applicable to present-day turbine blades.

NOTATION

y	mode of vibration of cantilever beam of length l
η	frequency number
$\rho = \tan \frac{1}{2}\eta$	
l	length of the beam
x	distance measured from fixed end
α, β	breadth and thickness parameters (*see* Section 5)
$F_{bt} = \sqrt{(\lambda/\lambda_0)}$,	ratio between frequencies of tapered and untapered beams
E	Young's modulus
I	moment of inertia of cross section
m	mass per unit length
K_1, K_2	*see* equation (3)
A, B	constants defined by equation (4)
A_1, B_1, C_1, D_1	constants defined by equation (24)
b, t	breadth and thickness of beam
p	angular frequency
$\lambda = m_0 p^2/(EI_0)$	
$a_1, a_2, \ldots$	coefficients in the expansion of F_{bt} in powers of α and β
$k = \alpha/\beta$	
Λ_1, Λ_2 Y_1, Y_2	*see* equation (18)
$\lambda_1, \lambda_2, \ldots$ $y_1, y_2, \ldots$	*see* equation (16)

Suffix 0 denotes values when $\alpha = \beta = 0$, *i.e.* with no taper
Dashes denote differentiation with respect to x

Part I

Some Integrals of the Modes of Vibration of the Ordinary Cantilever Beam

2. Fundamental Relations

The differential equation for flexural vibration of a cantilever beam is

$$y'''' = \frac{\eta^4}{l^4} y; \qquad . \quad . \quad . \quad . \quad . \quad . \quad (1)$$

with boundary conditions $y = y' = 0$, at $x = 0$,
and $y'' = y''' = 0$, at $x = l$. $\Big\}$ . . . . . (2)

Dashes denote differentiations with respect to x, l is the length of the beam which is supposed to be rigidly fixed at $x = 0$ and free at $x = l$, and the dimensionless number η is related to the angular frequency p by the formula

$$p = \frac{\eta^2}{l^2} \sqrt{\left(\frac{EI}{m}\right)}.$$

The solution of equations (1) and (2) is

$$y = K_1(x) - K_2(x), \qquad . \quad . \quad . \quad . \quad . \quad (3)$$

where

$$K_1(x) = A \cos \eta \frac{x}{l} + B \sin \eta \frac{x}{l}$$

$$K_2(x) = A \cosh \eta \frac{x}{l} + B \sinh \eta \frac{x}{l},$$

and A and B are constants to be determined from the pair of equations

$$\left.\begin{aligned} A(\cos \eta + \cosh \eta) + B(\sin \eta + \sinh \eta) &= 0, \\ A(-\sin \eta + \sinh \eta) + B(\cos \eta + \cosh \eta) &= 0. \end{aligned}\right\} \quad . \quad . \quad . \quad (4)$$

Elimination of A and B gives the well-known equation

$$\cos \eta \cosh \eta = -1; \qquad . \quad . \quad . \quad . \quad . \quad (5)$$

the first few roots of which are given by Table I.

TABLE I

Mode of Vibration	*Fundamental or Null Harmonic*	*1st Overtone or 1st Harmonic*	*2nd Overtone or 2nd Harmonic*	*3rd Overtone or 3rd Harmonic*	*4th Overtone or 4th Harmonic*
η	1·875	4·694	7·855	10·996	14·137
$\rho = \tan \frac{1}{2}\eta$	1·362	−1·019	1·001	− 1·000	1·000

The formulae may be greatly simplified by introducing the parameter $\rho = \tan \frac{1}{2}\eta$, giving

$$\sin \eta = \frac{2\rho}{1+\rho^2}, \quad \cos \eta = \frac{1-\rho^2}{1+\rho^2} \text{ and } \cosh \eta = \frac{\rho^2+1}{\rho^2-1} \quad . \quad . \quad . \quad (6)$$

The last of equations (6), which is obtained from equation (5), shows that $\rho^2 > 1$. From the graphs of $\cos \eta$ and $-1/\cosh \eta$ it readily follows that $\rho > 1$ for the even harmonic and $\rho < -1$ for the odd harmonics. Also

$$\sinh \eta = \pm \frac{2\rho}{\rho^2-1},$$

where the upper sign is taken for the even harmonics and the lower sign for the odd harmonics.

The first of equations (4) now gives $\beta = -(1/\rho)A$ for the even harmonics and $\beta = \rho A$ for the odd harmonics. The constant A, which may be chosen arbitrarily, will be taken equal to $l^{-\frac{1}{2}}$.

Then $\int_0^l y^2 dx = 1$, as shown later. The formulae for $K_1(x)$ and $K_2(x)$ now become

$$\left.\begin{aligned} K_1(x) &= l^{-1/2}\left(\cos \eta \frac{x}{l} - \frac{1}{\rho} \sin \eta \frac{x}{l}\right), \\ K_2(x) &= l^{-1/2}\left(\cosh \eta \frac{x}{l} - \frac{1}{\rho} \sinh \eta \frac{x}{l}\right), \end{aligned}\right\} \quad . \quad . \quad (7)$$

for even harmonics. With odd harmonics ρ should be replaced by $-1/\rho$.

In the sections which follow certain integrals involving y and its derivatives are given in terms of η and ρ. The results are presented for the even harmonics: for the odd harmonics the corresponding expressions can be derived by replacing ρ by $-1/\rho$.

3. Integrals of K_1 and K_2

Now $$K_1''(x) = -\frac{\eta^2}{l^2} K_1(x) \text{ and } K_2''(x) = \frac{\eta^2}{l^2} K_2(x) \quad . \quad . \quad . \quad (8)$$

Also, by equations (6) and (7),

$$\left.\begin{aligned} K_1(0) = K_2(0) &= l^{-1/2}, \quad K_1'(0) = K_2'(0) = -\eta\rho^{-1} l^{-3/2} \\ K_1(l) = -K_2(l) &= -l^{-1/2}, \quad K_1'(l) = -K_2'(l) = -\eta\rho^{-1} l^{-3/2} \end{aligned}\right\} \quad . \quad . \quad (9)$$

for even harmonics.

Using Green's formula $\int_0^l (uv'' - u''v)\, dx = [uv' - u'v]_0^l$, which may easily be

verified by integrating by parts, first with $u=K_1$, $v=K_2$ and then with $u=K_1'$, $v=K_2'$, equations (8) and (9) show that

$$\int_0^l K_1(x)\,K_2(x)\,dx=\int_0^l K_1'(x)\,K_2'(x)\,dx=0 \quad . \quad . \quad . \quad (10)$$

Thus K_1, K_2 and K_1', K_2' form two pairs of orthogonal functions.

Direct integration of the functions in equation (7) yields

$$\left.\begin{aligned}
&\int_0^l K_1(x)^2dx=\frac{1}{2}\left(1+\frac{1}{\rho^2}-\frac{2}{\eta\rho}\right), \quad \int_0^l K_2(x)^2dx=\frac{1}{2}\left(1-\frac{1}{\rho^2}+\frac{2}{\eta\rho}\right),\\
&\int_0^l K_1'(x)^2dx=\frac{\eta^2}{2l^2}\left(1+\frac{1}{\rho^2}+\frac{2}{\eta\rho}\right), \quad \int_0^l K_2'(x)^2\,dx=\frac{\eta^2}{2l^2}\left(-1+\frac{1}{\rho^2}+\frac{2}{\eta\rho}\right).
\end{aligned}\right\} \quad (11)$$

It is also a simple matter to obtain repeated integrals of $K_1(x)^2$, etc. Some results are given by

$$\left.\begin{aligned}
&\int_0^l\int_0^x K_1(x)^2dx\,dx=\frac{1}{4}\,l\left(1+\frac{1}{\rho^2}-\frac{2}{\eta\rho}\right),\\
&\int_0^l\int_0^x K_2(x)^2dx\,dx=\frac{1}{4}\,l\left(1-\frac{1}{\rho^2}+\frac{2}{\eta\rho}\right),\\
&\int_0^l\int_0^x K_1'(x)^2dx\,dx=\frac{1}{4}\,\frac{\eta^2}{l}\left(1+\frac{1}{\rho^2}+\frac{2}{\eta\rho}\right)\\
\text{and}\quad &\int_0^l\int_0^x K_2'(x)^2dx\,dx=\frac{1}{4}\,\frac{\eta^2}{l}\left(-1+\frac{1}{\rho^2}+\frac{2}{\eta\rho}\right).
\end{aligned}\right\} \quad . \quad . \quad . \quad (12)$$

In addition, the two formulae

$$\left.\begin{aligned}
&\int_0^l\int_0^x\int_0^x K_1'(x)^2dx\,dx\,dx=\frac{1}{8}\,\eta^2\left\{\frac{2}{3}\left(1+\frac{1}{\rho^2}\right)+\frac{2}{\eta\rho}-\frac{1}{\eta^2}\left(1-\frac{1}{\rho^2}\right)-\frac{2}{\eta^3\rho}\right\}\\
\text{and}\\
&\int_0^l\int_0^x\int_0^x K_2'(x)^2dx\,dx\,dx=\frac{1}{8}\,\eta^2\left\{-\frac{2}{3}\left(1-\frac{1}{\rho^2}\right)+\frac{2}{\eta\rho}-\frac{1}{\eta^2}\left(1+\frac{1}{\rho^2}\right)+\frac{2}{\eta^3\rho}\right\}
\end{aligned}\right\} \quad (13)$$

are required.

4. Integrals of y and its Derivatives

Using equations (3), (8) and (9) it is a simple matter to evaluate y and its derivatives at either end of the beam. Thus, in addition to equation (2),

$$\left.\begin{aligned} y''&=-2\eta^2 l^{-5/2}, & y'''&=2\eta^3\rho^{-1}l^{-7/2}, & &\text{at } x=0,\\ \text{and}\quad y&=-2l^{-1/2}, & y'&=-2\eta\rho^{-1}l^{-3/2}, & &\text{at } x=l. \end{aligned}\right\} \quad . \quad . \quad (14)$$

The integrals given in Table II can be obtained without difficulty by using equations (1), (2), (3), (8), (10), (11), (12), (13) and (14). Details of the work are given in Appendix I.

TABLE II*

(1)	$\int_0^l y^2 dx = 1$
(2)	$\int_0^l yy' dx = \frac{2}{l}$
(3)	$\int_0^l yy'' dx = \frac{\eta^2}{l^2}\left(-\frac{1}{\rho^2}+\frac{2}{\eta\rho}\right)$
(4)	$\int_0^l yy''' dx = -\frac{2\eta^2}{\rho^2 l^3}$
(5)	$\int_0^l (y')^2 dx = \frac{\eta^2}{l^2}\left(\frac{1}{\rho^2}+\frac{2}{\eta\rho}\right)$
(6)	$\int_0^l y'y'' dx = \frac{2\eta^2}{\rho^2 l^3}$
(7)	$\int_0^l y'y''' dx = -\frac{\eta^4}{l^4}$
(8)	$\int_0^l (y'')^2 dx = \frac{\eta^4}{l^4}$
(9)	$\int_0^l y''y''' dx = -\frac{2\eta^4}{l^5}$
(10)	$\int_0^l (y''')^2 dx = \frac{\eta^6}{l^6}\left(\frac{1}{\rho^2}+\frac{2}{\eta\rho}\right)$

*For even harmonics; for odd harmonics replace ρ by $-1/\rho$.

TABLE II (*continued*)

(11)	$\int_0^l xy^2dx = l\left(\frac{1}{2} + \frac{2}{\eta^2\rho^2}\right)$
(12)	$\int_0^l xyy'dx = \frac{3}{2}$
(13)	$\int_0^l xyy''dx = \frac{\eta^2}{2l}\left(-\frac{1}{\rho^2} + \frac{2}{\eta\rho}\right)$
(14)	$\int_0^l xyy'''dx = -\frac{\eta^2}{l^2}\left(\frac{1}{2\rho^2} + \frac{1}{\eta\rho}\right)$
(15)	$\int_0^l x(y')^2dx = \frac{\eta^2}{2l}\left(\frac{1}{\rho^2} + \frac{6}{\eta\rho} - \frac{4}{\eta^2}\right)$
(16)	$\int_0^l xy'y''dx = \frac{\eta^2}{l^2}\left(\frac{3}{2\rho^2} - \frac{1}{\eta\rho}\right)$
(17)	$\int_0^l xy'y'''dx = -\frac{\eta^4}{2l^3}$
(18)	$\int_0^l x(y'')^2dx = \frac{\eta^4}{l^3}\left(\frac{1}{2} - \frac{2}{\eta^2\rho^2}\right)$
(19)	$\int_0^l xy''y'''dx = -\frac{\eta^4}{2l^4}$
(20)	$\int_0^l x(y''')^2dx = \frac{\eta^6}{2l^5}\left(\frac{1}{\rho^2} - \frac{2}{\eta\rho} + \frac{4}{\eta^2}\right)$
(21)	$\int_0^l x^2y^2dx = l^2\left(\frac{1}{3} + \frac{3}{2\eta^2\rho^2} + \frac{1}{\eta^3\rho}\right)$
(22)	$\int_0^l x^2yy'dx = l\left(\frac{3}{2} - \frac{2}{\eta^2\rho^2}\right)$
(23)	$\int_0^l x^3y'ydx = \frac{3}{2}l^2\left(1 - \frac{3}{2\eta^2\rho^2} - \frac{1}{\eta^3\rho}\right)$

By equation (1), the results (1) to (10) in the table determine any integral of the type

$$\int_0^l \frac{d^m y}{dx^m}\,\frac{d^n y}{dx^n}\,dx$$

in terms of η and ρ, where m and n are positive integers or zero. Similarly, the results (11) to (20) yield

$$\int_0^l x\,\frac{d^m y}{dx^m}\,\frac{d^n y}{dx^n}\,dx.$$

The integrals (21), (22) and (23) are required in Part II.

Part II

Second Order Approximation for the Effect of Double Taper on Overtone Frequencies

5. Method of Solution

By using the integrals in Table II, second order approximations may be obtained for the effects of uniform breadth and thickness tapers on the frequencies of vibration of a cantilever beam. Let the breadth b and thickness t of the beam vary according to the linear relations

$$b=b_0\left(1-\alpha\frac{x}{l}\right) \quad \text{and} \quad t=t_0\left(1-\beta\frac{x}{l}\right),$$

where α, β, b_0 and t_0 are constants, l is the length of the beam, and x is measured from the fixed end. Thus, the breadth parameter α is equal to the ratio between the difference in breadths at the two ends of the beam and the breadth at the fixed end; and similarly for the thickness parameter β. The moment of inertia I and the mass per unit length m then vary according to the relations

$$I=I_0\left(1-\alpha\frac{x}{l}\right)\left(1-\beta\frac{x}{l}\right)^3 \quad \text{and} \quad m=m_0\left(1-\alpha\frac{x}{l}\right)\left(1-\beta\frac{x}{l}\right).$$

Hence, since the ordinary differential equation of flexural vibration is given by $(Ely'')''=mp^2y$, where p is the angular frequency, we obtain

$$\left\{\left(1-\alpha\frac{x}{l}\right)\left(1-\beta\frac{x}{l}\right)^3 y''\right\}''=\lambda\left(1-\alpha\frac{x}{l}\right)\left(1-\beta\frac{x}{l}\right)y, \qquad (15)$$

where $\lambda=m_0p^2/(EI_0)$. The boundary conditions are again given by equation (2).

It is assumed that λ and y can be expanded in powers of α and β; that is

$$\left.\begin{aligned} &\lambda = \lambda_0 + \lambda_1\alpha + \lambda_2\beta + \lambda_3\alpha^2 + \lambda_4\alpha\beta + \lambda_5\beta^2 + \dots \\ \text{and} \quad &y = y_0 + y_1\alpha + y_2\beta + y_3\alpha^2 + y_4\alpha\beta + y_5\beta^2 + \dots \end{aligned}\right\} \quad . \quad . \quad . \quad (16)$$

where $\lambda_0, \lambda_1, \dots$ are constants and $y_0, y_1, \dots$ functions of x. Substituting the values of λ and y given by (16) in equation (15) and equating like powers of α and β, gives a series of differential equations from which the numbers $\lambda_0, \lambda_1, \dots$ may be determined as simple expressions involving η and ρ. Details of the work are given in Appendix II.

Having thus obtained the numbers $\lambda_0, \lambda_1, \dots$, the equation $F_{bt} = \sqrt{(\lambda/\lambda_0)}$ then gives the ratio of the frequency of vibration of the tapered beam to the corresponding frequency of vibration of the untapered beam. The final result, as far as terms of the second order, is given in Table III.

TABLE III*

$$F_{bt} = 1 + a_1\alpha + a_2\beta + a_3\alpha^2 + a_4\alpha\beta + a_5\beta^2 + \dots$$

$$a_1 = \frac{2}{\eta^2\rho^2}, \qquad a_2 = -\frac{1}{2} + \frac{4}{\eta^2\rho^2}$$

$$a_3 = \frac{5}{4\eta^2\rho^2} + \frac{1}{2\eta^3\rho} - \frac{1}{\eta^3\rho^5} - \frac{1}{\eta^4\rho^4}$$

$$a_4 = \frac{2}{\eta^3\rho} - \frac{4}{\eta^3\rho^5} - \frac{4}{\eta^4\rho^4}$$

$$a_5 = -\frac{1}{16} + \frac{19}{16\eta^2\rho^2} + \frac{13}{8\eta^3\rho} - \frac{4}{\eta^3\rho^5} - \frac{4}{\eta^4\rho^4}$$

Some approximate numerical values are given in Table IV.

TABLE IV

Mode of Vibration	*Fundamental or Null Harmonic*	*1st Overtone or 1st Harmonic*	*2nd Overtone or 2nd Harmonic*	*3rd Overtone or 3rd Harmonic*	*4th Overtone or 4th Harmonic*
a_1	0·3066	0·0943	0·0324	0·0163	0·01
a_2	0·114	−0·3115	−0·4353	−0·4673	−0·48
a_3	0·1914	0·051	0·019	0·0099	0·006
a_4	0·0013	−0·0317	−0·0052	−0·002	−0·0008
a_5	0·077	−0·0419	−0·0593	−0·0548	−0·0575

*Even harmonics; for odd harmonics replace ρ by $-1/\rho$.

6. Examination of the Numerical Results*

For thickness taper, a comparison has been made between theoretical results given in Table III and corresponding experimental values. In the experiment, several specimens of various thickness tapers were put into a state of vibration by an Electro-Magnetic Induction Exciter, and natural frequencies were obtained by resonance. The root thickness of each specimen was $\frac{1}{8}$ in., the constant breadth was 2 in. and the length 6 in. From a knowledge of the material properties, density = 0·283 lb./in.^{3} and Young's modulus = 29·2 lb./in.^{2}, the untapered frequencies were calculated. The experimental values of F_{bt} were then obtained by dividing the natural frequencies by the corresponding untapered frequencies. The theoretical results were obtained by taking $F_{bt} = 1 + a_2\beta + a_3\beta^2$, where a_2 and a_3 have the values given in Table IV. Table V gives the approximate values ($\alpha = 0$).

TABLE V

COMPARISON BETWEEN THEORY AND EXPERIMENT FOR THICKNESS TAPER

	Mode of Vibration	*Fundamental or Null Harmonic*	*1st Overtone or 1st Harmonic*	*2nd Overtone or 2nd Harmonic*	*3rd Overtone or 3rd Harmonic*	*4th Overtone or 4th Harmonic*
$\beta = 0{\cdot}1$	*Theory*	1·012	0·9684	0·9559	0·9528	0·9514
	Experiment	1·0	0·9772	0·9512	0·9450	0·9424
$\beta = 0{\cdot}2$	*Theory*	1·026	0·9359	0·9106	0·9044	0·9017
	Experiment	1·027	0·9487	0·9054	0·9045	0·9298
$\beta = 0{\cdot}3$	*Theory*	1·041	0·9026	0·8642	0·855	0·8508
	Experiment	1·054	0·9202	0·8596	0·8515	0·8701
$\beta = 0{\cdot}4$	*Theory*	1·056	0·8685	0·8165	0·8044	0·7988
	Experiment	1·08	0·9031	0·8179	0·8032	0·8136
$\beta = 0{\cdot}5$	*Theory*	1·076	0·8335	0·7677	0·7528	0·7456
	Experiment	1·116	0·8718	0·7752	0·7555	0·7539
$\beta = 0{\cdot}6$	*Theory*	1·096	0·7977	0·7177	0·7002	0·6913
	Experiment	1·152	0·8063	0·7253	0·7009	0·7005
$\beta = 0{\cdot}7$	*Theory*	1·118	0·7611	0·6664	0·6463	0·6358
	Experiment	1·205	0·7806	0·6775	0·6438	0·6408

It is also interesting to compare the values given by taking the first six terms in the series for F_{bt} with known theoretically exact values in the case when either α or β (or both) is equal to unity, *i.e.* when the cantilever has a sharp edge (or a sharp point), at its free end. The results are contained in the tables (*a*), (*b*) and (*c*) which follow.

*The experimental results were kindly supplied by Mr. K. B. Chamberlain of the Bristol Aeroplane Company. For the comparison between theory and experiment, the author is indebted to Mr. J. Runcie.

(*a*) $\alpha=0$, $\beta=1$; $F_{bt}=1+a_2+a_5$. Ward[4] gives the exact values.

Mode of Vibration	*Fundamental or Null Harmonic*	*1st Overtone or 1st Harmonic*	*2nd Overtone or 2nd Harmonic*	*3rd Overtone or 3rd Harmonic*	*4th Overtone or 4th Harmonic*
$F_{bt}=1+a_2+a_5$ Exact value (Ward)	1·191 1·512	0·6466 0·6903	0·5054 0·4873	0·4779 0·4116	0·4625 —

(*b*) $\alpha=1$, $\beta=0$; $F_{bt}=1+a_1+a_3$. Meyer[3] gives the exact values.

Mode of Vibration	*Fundamental or Null Harmonic*	*1st Overtone or 1st Harmonic*	*2nd Overtone or 2nd Harmonic*	*3rd Overtone or 3rd Harmonic*	*4th Overtone or 4th Harmonic*
$F_{bt}=1+a_1+a_3$ Exact value (Meyer)	1·498 2·035	1·145 1·409	1·051 1·223	1·026 1·153	1·016 1·118

(*c*) $\alpha=\beta=1$; $F_{bt}=1+a_1+a_2+a_3+a_4+a_5$. Ward's paper gives the exact values for a sharply pointed pyramid on a square base. Dr. Dorothy Wrinch[5] has considered a thin conical cantilever bar of circular section. The two cases agree with one another.

Mode of Vibration	*Fundamental or Null Harmonic*	*1st Overtone or 1st Harmonic*	*2nd Overtone or 2nd Harmonic*	*3rd Overtone or 3rd Harmonic*	*4th Overtone or 4th Harmonic*
$F_{bt}=1+a_1+a_2+a_3+a_4+a_5$ Exact value (Ward and Wrinch)	1·69 2·48	0·7602 0·9599	0·5516 0·6242	0·5021 —	0·4777 —

The worst case is (*c*) in which the first six terms of the series for F_{bt} may differ by nearly as much as 32 per cent. of the total sum.

As an example in the case of breadth taper, let $\alpha=0{\cdot}5$ and $\beta=0$. Equations (15) and (30) on pp. 146 and 157 of Ref. 1 show that the exact value of F_{bt}, for the fundamental mode of vibration, lies between 1·202 and 1·240. The value obtained by taking the first six terms of the series is 1·201, which gives an error of less than $3\frac{1}{2}$ per cent.

The foregoing considerations show that the results of Table III may be expected to give a sufficiently good approximation for tapers which do not exceed 0·5; the results appear to be somewhat better for the overtone frequencies than for the fundamental. As either α or β approaches unity, the approximation can no longer be expected to be satisfactory.

References

1. Biezeno, C. B. and Grammel, R. *Engineering Dynamics*, Blackie, Vol. III, 1954.
2. Kirchhoff, G. Uber die Transversalschwingungen eines Stabes von veränderlichen Querschnitt. *Annalen der Physik und Chemie*, Vol. X, p. 501, 1880.
3. Meyer, F. Mathematische Theorie der Transversalen Schwingungen eines Stabes von veränderlichen Querschnitt. *Annalen der Physik und Chemie*, Vol. XXXIII, p. 661, 1888.
4. Ward, P. F. The Transverse Vibration of a Rod of Varying Cross Section. *Phil. Mag.* (6), Vol. 25, p. 85, 1913.
5. Wrinch, D. M. The Lateral Vibrations of Bars of Conical Type. *Proc. Roy. Soc.* A, Vol. 101, p. 493, 1922.

Appendix I

Construction of Table II

Entries (1) *to* (10): Integral (1) follows from the first result in equation (10) and the first two of equations (11). Integral (2) is immediate by the relation for y in equation (14). Integral (3) follows from equations (3), (8) and (11). By integrating by parts, the left hand side of integral (4) is equal to

$$\left[yy''\right]_0^l - \int_0^l y'y''dx = -\frac{1}{2}y'(l)^2 = -\frac{2\eta^2}{\rho^2 l^3}.$$

The equations (3), (10) and the second line of equation (11) yield integral (5). Next, integral (6) is immediate by the second line of equation (14), and (7) and (8) follow from equations (3), (8) and (11). Integral (9) is immediate by the first equation in the first line of equation (14) and, finally, (10) follows from equations (3), (8), (10) and (11).

Entries (11) *to* (20): To obtain integral (11), use equation (1) and integrate by parts. Thus the left hand side is equal to

$$\frac{l^4}{\eta^4}\int_0^l xyy''''dx = \frac{l^4}{\eta^4}\left\{\left[xyy'''\right]_0^l - \int_0^l yy'''dx - \int_0^l xy'y'''dx\right\}.$$

The first term in the curly brackets is zero and the second is given by integral (5) in the table. By equations (3) and (8), the third term is equal to

$$\frac{\eta^2}{l^2}\int_0^l x\{(K_1')^2-(K_2')^2\}dx = \frac{\eta^2}{l}\int_0^l \{(K_1')^2-(K_2')^2\}dx - \frac{\eta^2}{l^2}\int_0^l\int_0^x \{(K_1')^2-(K_2')^2\}dxdx,$$

by integrating by parts. Integral (11) now follows from equations (11) and (12). By integrating by parts, integral (12) is equal to

$$\left[\frac{1}{2}xy^2\right]_0^l - \frac{1}{2}\int_0^l y^2dx = \frac{3}{2},$$

from equations (2) and (14) and integral (1).

Using equations (3) and (8), integral (13) becomes

$$-\frac{\eta^2}{l^2}\int_0^l x(K_1^2-K_2^2)\,dx=-\frac{\eta^2}{l^2}\left\{ l\int_0^l (K_1^2-K_2^2)\,dx-\int_0^l\int_0^x (K_1^2-K_2^2)\,dx\,dx\right\},$$

and the result follows by equations (11) and (12).

Integrating by parts twice and using equation (2), integral (14) is equal to

$$-\int_0^l yy''\,dx-\frac{1}{2}ly'(l)^2+\frac{1}{2}\int_0^l (y')^2\,dx,$$

and the right hand side is obtained from equation (14) and integrals (3) and (5). For integral (15), integrating by parts gives

$$\left[xy'y\right]_0^l-\int_0^l y'y\,dx-\int_0^l xyy''\,dx,$$

and the result follows from equations (2) and (14) and integrals (2) and (13).

Integral (16) is equal to $\frac{1}{2}ly'(l)^2-\frac{1}{2}\int_0^l (y')^2\,dx,$

and the result follows from equation (14) and integral (5). Integral (17) has already been considered in the derivation of integral (11). For integral (18), integrating by parts gives

$$\left[xy'y''\right]_0^l-\int_0^l y'y''\,dx-\int_0^l xy'y'''\,dx,$$

and these integrals have already been evaluated.

Integral (19) is equal to minus one half the value of integral (8), by integrating by parts. Finally, a further integration by parts shows that integral (20) is equal to

$$-\int_0^l y''y'''\,dx-\int_0^l xy''y''''\,dx,$$

and the result follows by equation (1) and integrals (9) and (13).

Entries (21), (22) *and* (23): Integration by parts shows that integral (22) is a consequence of equation (14) and integral (11), and that integral (23) follows from equation (14) and integral (21). Lastly, using equation (1), integral (21) is equal to

$$\frac{l^4}{\eta^4}\int_0^l x^2yy''''dx = -\frac{l^4}{\eta^4}\left\{2\int_0^l xyy'''dx + \int_0^l x^2y'y'''dx\right\},$$

by integrating by parts. The first integral within the brackets is integral (14). By equations (3) and (8), the second integral is equal to

$$-\frac{\eta^2}{l^2}\int_0^l x^2\{(K_1')^2-(K_2')^2\}dx = -\frac{\eta^2}{l^2}\left[l^2\int_0^l\{(K_1')^2-(K_2')^2\}dx - \right.$$

$$\left. -2l\int_0^l\int_0^x\{(K_1')^2-(K_2')^2\}dxdx + 2\int_0^l\int_0^x\int_0^x\{(K_1')^2-(K_2')^2\}dxdxdx\right],$$

by integrating by parts twice. The required result now follows from equations (11), (12) and (13).

Appendix II

Determination of the Coefficients λ_0, λ_1, λ_2, λ_3, λ_4 and λ_5

Clearly, on putting $\alpha=\beta=0$, equation (15) must go over to equation (1). Hence $\lambda_0=\eta^4/l^4$, and y_0 is the function which represents the mode of vibration of the ordinary cantilever beam, *i.e.* the function y in Part I. Also, the equations obtained by substituting the second of equations (16) in equation (2) must hold for all values of α and β; hence, each y_0, y_1, y_2, ... satisfies equation (2).

The work may be simplified by writing $\alpha=k\beta$, and regarding k as fixed and β as a variable. From (15) we then have

$$\left\{\left(1-k\beta\frac{x}{l}\right)\left(1-\beta\frac{x}{l}\right)^3 y''\right\}'' = \lambda\left(1-k\beta\frac{x}{l}\right)\left(1-\beta\frac{x}{l}\right)y, \quad . \quad (17)$$

and from equation (16)
$$\left.\begin{aligned}\lambda &= \lambda_0+\Lambda_1\beta+\Lambda_2\beta^2+\dots\\ \text{and}\qquad y &= y_0+Y_1\beta+Y_2\beta^2+\dots\end{aligned}\right\} \quad . \quad . \quad . \quad (18)$$

where $\Lambda_1=\lambda_1k+\lambda_2$, $\Lambda_2=\lambda_3k^2+\lambda_4k+\lambda_5$,

$Y_1=y_1k+y_2$ and $Y_2=y_3k^2+y_4k+y_5$.

Substituting equation (18) in (17) and comparing powers of β up to the second degree gives

$$y_0'''' - \lambda_0 y_0 = 0, \quad . \quad . \quad . \quad . \quad . \quad . \quad (19)$$

$$Y_1'''' - \lambda_0 Y_1 = \Lambda_1 y_0 + \frac{2}{l} x\lambda_0 y_0 + \frac{2}{l}(3+k)\, y_0''' \quad . \quad . \quad . \quad (20)$$

and $$Y_2'''' - \lambda_0 Y_2 = \Lambda_2 y_0 + \Lambda_1 Y_1 + \frac{2}{l} x\lambda_0 Y_1 + \frac{2}{l}(3+k)\, Y_1''' +$$

$$+ \frac{2}{l} x\Lambda_1 y_0 + \frac{3}{l^2} x^2 \lambda_0 y_0 + \frac{2}{l^2}(3+k^2)\, xy_0''' - \frac{6}{l^2}(1+k)\, y_0''. \quad . \quad (21)$$

Equation (20) is obtained by comparing coefficients of β and using equation (19). Equation (21) follows by comparing coefficients of β^2 and using equations (19) and (20).

Multiply equation (20) by y_0 and integrate over $0 \leqslant x \leqslant l$. The left hand side vanishes since, on integrating by parts and remembering that y_0 and Y_1 both satisfy equation (2), it is equal to

$$\int_0^l (y_0'''' - \lambda_0 y_0)\, Y_1 dx = 0.$$

For the integrals on the right hand side, use the integrals (1), (4) and (11) of Table II.

Then $$\Lambda_1 = \frac{\eta^4}{l^4}\left(-1 + \frac{8}{\eta^2\rho^2} + \frac{4}{\eta^2\rho^2} k\right). \quad . \quad . \quad . \quad (22)$$

Hence, since λ_1 and λ_2 are independent of k, it follows that

$$\lambda_1 = \frac{4\eta^2}{l^4\rho^2}, \quad \text{and} \quad \lambda_2 = \frac{2\eta^4}{l^4}\left(-\frac{1}{2} + \frac{4}{\eta^2\rho^2}\right). \quad . \quad . \quad (23)$$

To obtain Λ_2, equation (20) must first be solved for Y_1 subject to the boundary conditions that $y = Y_1$ satisfies equation (2). By using equation (19), it may be verified that the general solution of equation (20) is given by

$$Y_1 = \frac{\Lambda_1}{4\lambda_0} xy_0' + \frac{1}{4l} x^2 y_0' + \frac{1}{4l}(3+2k)\, xy_0 + A_1 y_0' + B_1 y_0'' + C_1 y_0''' + D_1 y_0, \quad (24)$$

where A_1, B_1, C_1 and D_1 are constants. The first three terms on the right hand side of this expression give a particular integral, and the last four terms supply the complementary function. The boundary conditions give

$$B_1 y_0''(0) + C_1 y_0'''(0) = 0, \qquad A_1 y_0''(0) + B_1 y_0'''(0) = 0,$$

$$B_1 y_0(l) + C_1 y_0'(l) = -\frac{2+k}{l\lambda_0} y_0'(l) \quad \text{and} \quad A_1 y_0(l) + B_1 y_0'(l) = -\frac{l}{4}\left(\frac{\Lambda_1}{\lambda_0} + 1\right) y_0(l).$$

For these four equations to be consistent,

$$\frac{\Lambda_1}{\lambda_0} + 1 = -\frac{4(2+k)}{\lambda_0 l^2}\,\frac{y_0'''(0)\,y_0'(l)}{y_0''(0)\,y_0(l)}.$$

This equation reduces to equation (22) on using equation (14). Also

$$A_1 = -\left(1+\frac{1}{2}k\right)\frac{l}{\eta^2\rho^2}, \qquad B_1 = -\left(1+\frac{1}{2}k\right)\frac{l^2}{\eta^3\rho} \quad \text{and} \quad C_1 = -\left(1+\frac{1}{2}k\right)\frac{l^3}{\eta^4}. \qquad (25)$$

The following equation may be obtained from equations (21) and (24)

$$\begin{aligned} Y_2'''' - \lambda_0 Y_2 = {} & \Lambda_2 y_0 + \frac{2}{l}(3+k)\,A_1\lambda_0 y_0 + \frac{1}{4l}(17+4k)\,\Lambda_1 x y_0 + \frac{3}{2l^2}(4+k)\,\lambda_0 x^2 y_0 + \\ & + \left\{A_1\Lambda_1 + \frac{2}{l}(3+k)\,B_1\lambda_0\right\} y_0' + \left(\frac{\Lambda_1^2}{4\lambda_0} + \frac{2\lambda_0}{l}A_1\right) x y_0' + \frac{3}{4l}\Lambda_1 x^2 y_0' + \\ & + \frac{\lambda_0}{2l^2}x^3 y_0' + \left[B_1\Lambda_1 + \frac{2}{l}(3+k)\left\{\frac{3}{4l}(5+2k) + C_1\lambda_0\right\} - \frac{6}{l^2}(1+k)\right] y_0'' + \\ & + \frac{2}{l}B_1\lambda_0 x y_0'' + \left\{C_1 + \frac{3}{2l\lambda_0}(3+k)\right\}\Lambda_1 y_0''' + \\ & + \frac{1}{l}\left\{2C_1\lambda_0 + \frac{1}{2l}(3+k)(9+2k) + \frac{2}{l}(3+k^2)\right\} x y_0''' + \\ & + D_1\left[\Lambda_1 y_0 + \frac{2\lambda_0}{l}x y_0 + \frac{2}{l}(3+k)\,y_0'''\right]. \end{aligned}$$

Multiply this equation by y_0 and integrate over $0 \leqslant x \leqslant l$. The left hand side vanishes as with equation (20). The coefficient of D_1 also vanishes by equation (22). The remaining integrals are given by the integrals (1), (2), (3), (4), (11), (12), (13), (14), (21), (22) and (23) in Table II. Hence, substituting the values for A_1, B_1, C_1, λ_0 and Λ_1 (*see* equations (22) and (25)) and simplifying the resulting expression, it follows that

$$\begin{aligned} \frac{\Lambda_2}{\lambda_0} = {} & \frac{1}{8} - \frac{13}{8\eta^2\rho^2} + \frac{13}{4\eta^3\rho} - \frac{8}{\eta^3\rho^5} + \frac{8}{\eta^4\rho^4} + \\ & + \left(-\frac{2}{\eta^2\rho^2} + \frac{4}{\eta^3\rho} - \frac{8}{\eta^3\rho^5} + \frac{8}{\eta^4\rho^4}\right)k + \\ & + \left(\frac{5}{2\eta^2\rho^2} + \frac{1}{\eta^3\rho} - \frac{2}{\eta^3\rho^5} + \frac{2}{\eta^4\rho^4}\right)k^2. \end{aligned}$$

The quantities λ_3, λ_4 and λ_5 are then given, respectively, by the coefficients of k^2, k and k^0 in this expression for Λ_2.

Buckling of Columns in the Presence of Creep

SHARAD A. PATEL

(Polytechnic Institute of Brooklyn)

SUMMARY: This paper is concerned with the solution of the creep buckling of columns. Instantaneous elastic and plastic deformations, as well as the transient and secondary creep, are considered. Formulae for the critical time at which a column fails are presented for integral values of the exponents appearing in the creep law.

1. Introduction

During the past few years much work has been published on the subject of creep buckling. A reasonably complete list of publications can be found in Ref. 3. In the present work, Hoff's theory of creep buckling, in which the instantaneous elastic and plastic deformations as well as the transient and secondary creep phenomena are taken into account, is used and a general solution for integral values of the exponents appearing in the creep law is found. From this solution the critical time, that is, the time required for a column to collapse after load application, can be calculated.

Notation

A dot over a symbol denotes differentiation with respect to time.

A	total cross-sectional area of column
$B = (\bar{\sigma}/\mu)^{m+1}/(\bar{\sigma}/\lambda)^n$	
$C = 2(\varepsilon_E - \bar{\sigma}/E)/(\bar{\sigma}/\lambda)^n$	
E	Young's modulus
L	length of column
M	bending moment
P	axially compressive load
a	amplitude of non-dimensional deflection
a_1, a_2	particular values of amplitude a
a_{cr}, a_{cr}'	critical values of amplitude a
h	distance between flanges of idealised H-section
m, n	exponents in plastic and viscous terms of creep law
r	radius of curvature
t, t_{cr}, t_{lim}	time, critical time and limit time respectively

Received June 1955.

$w = 2y/h$, non-dimensional deflection parameter

y lateral deflection of column

$\alpha_k = (-1)^k [\cos(k\pi/n)]^{n-2}$

$\beta_p = m!/[(m-p)!\,p!]$

ε strain

ε_c, ε_t strains on concave and convex sides of column

$\varepsilon_E = \pi^2 h^2/(4L^2)$

$\gamma_k = (-1)^{(n-k-1)/2} [\sin(k\pi/2n)]^{n-2} \cot(k\pi/2n)$

λ, μ coefficients of viscous and plastic terms in creep law

σ stress

σ_c, σ_t stresses on concave and convex sides of column

$\bar{\sigma}$ average compressive stress

2. Creep Law

The creep law is assumed as

$$\dot{\varepsilon} = \frac{\dot{\sigma}}{E} + k_1 \left(\frac{\sigma}{\mu}\right)^m \left(\frac{\dot{\sigma}}{\mu}\right) + k_2 \left(\frac{\sigma}{\lambda}\right)^n . \quad . \quad . \quad . \quad (1)$$

This relation is the same as that given in Ref. 1. In the present analysis the stress σ is considered positive when compressive (instead of tensile as in Ref. 1). The first term in the right hand member represents the recoverable elastic deformations. The second term takes into account the instantaneous non-recoverable plastic deformations and also, in an approximate manner, the transient creep. The quantities μ and m are so chosen that the second term represents the intercept of the straight line portion of the secondary creep curve on the strain axis less the elastic deformation (*see* Fig. 1). The symbols m and n stand for integers and the values of k_1 depend on the conditions of loading.

When $\sigma > 0$, $\dot{\sigma} > 0$ (loading in compression): $k_1 = 1$

$\sigma > 0$, $\dot{\sigma} < 0$ (unloading in compression): $k_1 = 0$.

$\sigma < 0$, $\dot{\sigma} < 0$ (loading in tension): $k_1 = (-1)^m$

$\sigma < 0$, $\dot{\sigma} > 0$ (unloading in tension): $k_1 = 0$.

Finally, the third term in the right hand member represents the non-recoverable creep deformations of the secondary phase. The values of k_2 are:—

when $\sigma > 0$ (compression), $k_2 = 1$;

when $\sigma < 0$ (tension), $k_2 = (-1)^{n+1}$.

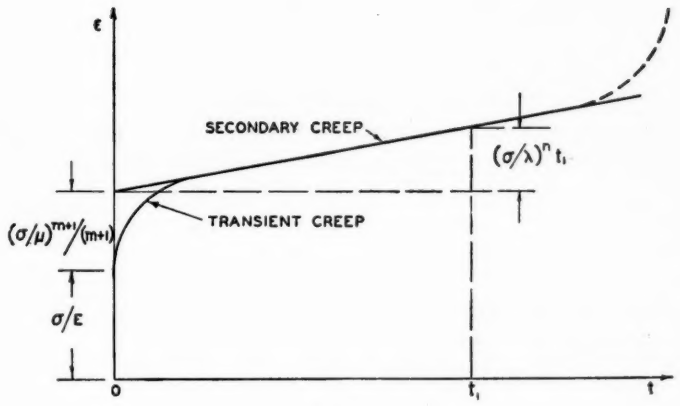

Fig. 1.
Representation of compressive creep curve.

3. The Column Problem

If an axially compressive load P is applied to an idealised H-section column, as shown in Fig. 2, the stress-load relation can be given as

$$\left.\begin{aligned}\sigma_c &= \frac{P}{A} + \frac{2M}{Ah} \\ \sigma_t &= \frac{P}{A} - \frac{2M}{Ah}\end{aligned}\right\} \quad . \quad . \quad . \quad . \quad . \quad . \quad . \quad (2)$$

where σ_c and σ_t, respectively, are the stresses in the concave and convex flanges, A is the cross-sectional area of the column, h is the distance between the two flanges and M is the bending moment at the point under consideration, given by

$$M = Py \quad . \quad . \quad . \quad . \quad . \quad . \quad . \quad (3)$$

in which y is the deflection. Introducing a non-dimensional deflection parameter $w = 2y/h$ equations (2), together with equation (3), become

$$\left.\begin{aligned}\sigma_c &= \bar{\sigma}(1+w) \\ \sigma_t &= \bar{\sigma}(1-w)\end{aligned}\right\} \quad . \quad . \quad . \quad . \quad . \quad . \quad (4)$$

Hence

$$\left.\begin{aligned}\dot{\sigma}_c &= \bar{\sigma}\dot{w} \\ \dot{\sigma}_t &= -\bar{\sigma}\dot{w}\end{aligned}\right\} \quad . \quad . \quad . \quad . \quad . \quad . \quad (5)$$

where $\bar{\sigma} = P/A$ is the average compressive stress.

The relation between the strains and the curvature can be given by

$$\varepsilon_c - \varepsilon_t = \frac{h}{r} \quad . \quad . \quad . \quad . \quad . \quad . \quad . \quad (6)$$

in which ε_c and ε_t are respectively strains in the concave and convex flanges of the column and r is the radius of curvature. For small deflections, r can be related to w by

$$\frac{1}{r} = -\frac{h}{2} w_{xx} \quad . \quad . \quad . \quad . \quad . \quad . \quad (7)$$

where x is the axial co-ordinate of a point on the column axis, as shown in Fig. 2, and the suffix x indicates differentiation with respect to x.

Equations (6) and (7) yield

$$-\frac{h^2}{2} \dot{w}_{xx} = \dot{\varepsilon}_c - \dot{\varepsilon}_t. \quad . \quad . \quad . \quad . \quad . \quad . \quad (8)$$

When the column begins to creep, the compressive strain ε_c on the concave side increases because of the increasing curvature. For this flange of the column the deformation law is therefore

$$\dot{\varepsilon}_c = \frac{\dot{\sigma}_c}{E} + \left(\frac{\sigma_c}{\mu}\right)^m \left(\frac{\dot{\sigma}_c}{\mu}\right) + \left(\frac{\sigma_c}{\lambda}\right)^n \quad . \quad . \quad . \quad . \quad . \quad (9)$$

At the same time on the convex side of the column the increasing curvature diminishes the absolute value of the compressive strain ε_t. Hence for this flange

$$\dot{\varepsilon}_t = \frac{\dot{\sigma}_t}{E} + \left(\frac{\sigma_t}{\lambda}\right)^n \quad . \quad . \quad . \quad . \quad . \quad . \quad (10)$$

Equations (4), (5), (9) and (10), together with equation (8), yield

$$\left(-\frac{h^2}{2}\right) \dot{w}_{xx} = 2\left(\frac{\bar{\sigma}}{E}\right) \dot{w} + \left(\frac{\bar{\sigma}}{\mu}\right)^{m+1} (1+w)^m \dot{w} + \left(\frac{\bar{\sigma}}{\lambda}\right)^n [(1+w)^n - (1-w)^n]. \quad (11)$$

Solution of equation (11) will give the deflection-time characteristics for the column as long as the strains remain compressive in both flanges. The initial non-dimensional deviation $w = w_0$, at time $t = 0$, of the centre line of the column from the straight line along which the load P is applied (Fig. 2) can be represented as[1, 6]

$$w_0 = a_0 \sin\left(\frac{\pi x}{L}\right). \quad . \quad . \quad . \quad . \quad . \quad . \quad (12)$$

For the solution of equation (11) the deflection w at any time t is assumed as

$$w = a \sin\left(\frac{\pi x}{L}\right). \quad . \quad . \quad . \quad . \quad . \quad . \quad (12a)$$

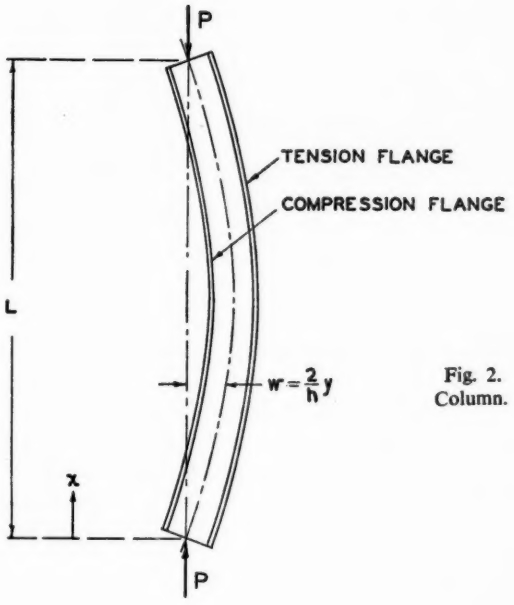

Fig. 2. Column.

Using the collocation method and satisfying the differential equation (11) at the mid-height of the column leads to

$$\frac{dt}{da}=\frac{(\lambda/\bar{\sigma})^n\{2[\varepsilon_E-(\bar{\sigma}/E)]-(\bar{\sigma}/\mu)^{m+1}(1+a)^m\}}{(1+a)^n-(1-a)^n} \quad . \quad (13)$$

where ε_E is the Euler buckling strain

$$\varepsilon_E=\frac{\pi^2}{4}\left(\frac{h}{L}\right)^2 \quad . \quad (14)$$

Integrating,

$$t=\frac{C-B}{2n}\left[\log\frac{a}{a_0}+\sum_{k=1,2,3}^{n'}\alpha_k\log\frac{a^2+\tan^2(k\pi/n)}{a_0^2+\tan^2(k\pi/n)}\right]-\frac{B}{2n}\sum_{p=1,2,3}^{m}\frac{\beta_p}{p}(a^p-a_0^p)-$$

$$-\frac{B}{n}\sum_{k=1,2,3}^{n'}\left\{\sum_{p=1,3,5}^{m_1'}\alpha_k\beta_p[\tan(k\pi/n)]^p\left[\sum_{q=0,1,2}^{(p-1)/2}\frac{(-1)^q}{p-2q}[\cot(k\pi/n)]^{p-2q}(a^{n-2q}-a_0^{p-2q})+\right.\right.$$

$$\left.+(-1)^{(p+1)/2}\tan^{-1}\frac{(a-a_0)\cot(k\pi/n)}{1+aa_0\cot^2(k\pi/n)}\right]+\sum_{p=2,4,6}^{m_2'}\alpha_k\beta_p[\tan(k\pi/n)]^p\times$$

$$\left.\times\left[\sum_{t=0,1,2}^{(p/2)-1}\frac{(-1)^q[\cot(k\pi/n)]^{p-2q}}{p-2q}(a^{p-2q}-a_0^{p-2q})+(-1)^{p/2}\frac{1}{2}\log\frac{1+a^2\cot^2(k\pi/n)}{1+a_0^2\cot^2(k\pi/n)}\right]\right\}$$

. . . (15)

where $C=2\left(\frac{\lambda}{\bar{\sigma}}\right)^n\left[\varepsilon_E-\frac{\bar{\sigma}}{E}\right]$, $\quad \alpha_k=(-1)^k[\cos(k\pi/n)]^{n-2}$

$B=\left(\frac{\lambda}{\bar{\sigma}}\right)^n\left(\frac{\bar{\sigma}}{\mu}\right)^{m+1}$. $\quad \beta_p=\frac{m!}{(m-p)!\,p!}$

$n'=\frac{n}{2}-1$ for n even, $\quad m_1'=m-1$ for m even

$=m$ for m odd

$=\frac{n-1}{2}$ for n odd, $\quad m_2'=m$ for m even

$=m-1$ for m odd.

It follows from equation (4) that the compression changes to tension in the middle of the column when $a=1$. Since equation (13) was derived under the assumption of compression in both the flanges, it is valid only for values of $a\leqslant 1$. The equation has a singular point at which da/dt increases indefinitely; hence, equation (15) is not valid beyond this point. The singularity occurs when the numerator of the right hand side of equation (13) vanishes, that is when

$$a=a_{cr}=\left\{2\left(\frac{\mu}{\bar{\sigma}}\right)^{m+1}\left[\varepsilon_E-\frac{\bar{\sigma}}{E}\right]\right\}^{1/m}-1. \quad . \quad . \quad . \quad (16)$$

If the value of $a=a_{cr}\leqslant 1$ as obtained from equation (16), the lateral velocity of the column increases beyond all limits as the deflection a approaches a_{cr}. If the value exceeds unity, equation (15) ceases to be valid. In case a_{cr} exceeds unity, substitution of a_{cr} into equation (15) yields an upper limit of the critical time $t_{cr\,u}$, since compression is assumed to be present in the tension flange throughout the buckling process, which reduces the rate of increase in curvature and consequently yields a larger time of failure. The time corresponding to $a=1$ is designated as the limit time t_{lim}. Upon substitution of $a=1$ equation (15) reduces to

$$t_{lim}=\frac{C-B}{2n}\left[\log\frac{1}{a_0}+\sum_{k=1,2,3}^{n'}\alpha_k\log\frac{1+\tan^2(k\pi/n)}{a_0^2+\tan^2(k\pi/n)}\right]-\frac{B}{2n}\sum_{p=1,2,3}^{m}\frac{\beta_p}{p}(1-a_0^p)-$$

$$-\frac{B}{n}\sum_{k=1,2,3}^{n'}\left\{\sum_{p=1,3,5}^{m_1'}\alpha_k\beta_p[\tan(k\pi/n)]^p\left[\sum_{q=0,1,2}^{(p-1)/2}\frac{(-1)^q}{p-2q}[\cot(k\pi/n)]^{p-2q}(1-a_0^{p-2q})+\right.\right.$$

$$\left.+(-1)^{(p+1)/2}\tan^{-1}\frac{(1-a_0)\cot(k\pi/n)}{1+a_0\cot^2(k\pi/n)}\right]+$$

$$+\sum_{p=2,4,6}^{m_2'}\alpha_k\beta_p[\tan(k\pi/n)]^p\left[\sum_{q=0,1,2}^{(p/2)-1}(-1)^q\frac{[\cot(k\pi/n)]^{p-2q}}{p-2q}(1-a_0^{p-2q})+\right.$$

$$\left.\left.+(-1)^{p/2}\frac{1}{2}\log\frac{1+\cot^2(k\pi/n)}{1+a_0^2\cot^2(k\pi/n)}\right]\right\} \quad . \quad . \quad . \quad . \quad . \quad (17)$$

Beyond this limit, in the tensile part of the convex flange, equation (10) should be replaced by

$$\dot{\varepsilon}_t = \frac{\dot{\sigma}_t}{E} + (-1)^m \left(\frac{\sigma_t}{\mu}\right)^m \left(\frac{\dot{\sigma}_t}{\mu}\right) + (-1)^{n+1} \left(\frac{\sigma_t}{\lambda}\right)^n . \quad . \quad . \quad (18)$$

In the remainder, equation (10) is still valid because the stress there is still compressive. Solution of the problem under these conditions is difficult. But if it is assumed that equation (18) is valid in the entire tension flange from this limit time on, then equation (11) must be replaced by

$$-\frac{h^2}{2}\dot{w}_{xx} = 2\frac{\bar{\sigma}}{E}\dot{w} + \left(\frac{\bar{\sigma}}{\mu}\right)^{m+1} \dot{w}\left[(1+w)^m + (-1)^m (1-w)^m\right] + \\ + \left(\frac{\bar{\sigma}}{\lambda}\right)^n \left[(1+w)^n - (-1)^{n+1}(1-w)^n\right] . \quad . \quad (19)$$

Again, solution by the collocation method yields

$$\frac{dt}{da} = \frac{(\lambda/\bar{\sigma})^n \{2[\varepsilon_E - (\bar{\sigma}/E)] - (\bar{\sigma}/\mu)^{m+1}[(1+a)^m + (-1)^m (1-a)^m]\}}{(1+a)^n - (-1)^{n+1}(1-a)^n} . \quad (20)$$

Integration gives the time required for the increase in the amplitude of the non-dimensional deflection from a_1 to a_2: —

(*i*) For n odd and m even: —

$$t = \frac{C-2B}{2n}\left[\log\frac{a_2}{a_1} + \sum_{k=1,2,3}^{(n-1)/2} \alpha_k \log\frac{a_2^2 + \tan^2(k\pi/n)}{a_1^2 + \tan^2(k\pi/n)}\right] - \frac{B}{n}\sum_{p=2,4,6}^{m}\frac{\beta_p}{p}(a_2^p - a_1^p) - \\ - \frac{2B}{n}\sum_{k=1,2,3}^{(n-1)/2}\sum_{p=2,4,6}^{m}\alpha_k\beta_p[\tan(k\pi/n)]^p\left[\sum_{q=0,1,2}^{(p/2)-1}\frac{(-1)^q[\cot(k\pi/n)]^{p-2q}}{p-2q}(a_2^{p-2q} - a_1^{p-2q}) + \right. \\ \left. + (-1)^{p/2}\frac{1}{2}\log\frac{1+a_2^2\cot^2(k\pi/n)}{1+a_1^2\cot^2(k\pi/n)}\right] . \quad . \quad . \quad (21a)$$

(*ii*) For n odd and m odd: —

$$t = \frac{C}{2n}\left[\log\frac{a_2}{a_1} + \sum_{k=1,2,3}^{(n-1)/2}\alpha_k\log\frac{a_2^2 + \tan^2(k\pi/n)}{a_1^2 + \tan^2(k\pi/n)}\right] - \frac{B}{n}\sum_{p=1,3,5}^{m}\frac{\beta_p}{p}(a_2^p - a_1^p) - \\ - \frac{2B}{n}\sum_{k=1,2,3}^{(n-1)/2}\sum_{p=1,3,5}^{m}\alpha_k\beta_p[\tan(k\pi/n)]^p\left[\sum_{q=0,1,2}^{(p-1)/2}\frac{(-1)^q[\cot(k\pi/n)]^{p-2q}}{p-2q} \times \right. \\ \left. \times (a_2^{p-2q} - a_1^{p-2q}) + (-1)^{(p+1)/2}\tan^{-1}\frac{(a_2-a_1)\cot(k\pi/n)}{1+a_2a_1\cot^2(k\pi/n)}\right] . \quad . \quad (21b)$$

(*iii*) For n even and m even: —

$$t=\frac{C-2B}{n}\sum_{k=1,3,5}^{n-1}\gamma_k[\tan(k\pi/2n)]\tan^{-1}\frac{(a_2-a_1)\tan(k\pi/2n)}{1+a_2a_1\tan^2(k\pi/2n)}-$$

$$-\frac{2B}{n}\sum_{k=1,3,5}^{n-1}\sum_{p=1,3,5}^{m-1}\gamma_k\beta_{p+1}[\cot(k\pi/2n)]^p\left\{\sum_{q=0,1,2}^{(p-1)/2}\frac{(-1)^q[\tan(k\pi/2n)]^{p-2q}}{p-2q}\times\right.$$

$$\left.\times(a_2^{p-2q}-a_1^{p-2q})+(-1)^{(p+1)/2}\tan^{-1}\frac{(a_2-a_1)\tan(k\pi/2n)}{1+a_2a_1\tan^2(k\pi/2n)}\right\}\quad .\quad .\quad .\quad (21c)$$

(*iv*) For n even and m odd: —

$$t=\frac{C}{n}\sum_{k=1,3,5}^{n-1}\gamma_k[\tan(k\pi/2n)]\tan^{-1}\frac{(a_2-a_1)\tan(k\pi/2n)}{1+a_2a_1\tan^2(k\pi/2n)}-$$

$$-\frac{Bm}{n}\sum_{k=1,3,5}^{n-1}\gamma_k\log\frac{a_2^2+\cot^2(k\pi/2n)}{a_1^2+\cot^2(k\pi/2n)}-\frac{2B}{n}\sum_{k=1,3,5}^{n-1}\sum_{p=2,4,6}^{m-1}\gamma_k\beta_{p+1}[\cot(k\pi/2n)]^p\times$$

$$\times\left\{\sum_{q=0,1,2}^{(p/2)-1}\frac{(-1)^q[\tan(k\pi/2n)]^{p-2q}}{p-2q}(a_2^{p-2q}-a_1^{p-2q})+\right.$$

$$\left.+(-1)^{p/2}\frac{1}{2}\log\frac{1+a_2^2\tan^2(k\pi/2n)}{1+a_1^2\tan^2(k\pi/2n)}\right\}\quad .\quad .\quad .\quad .\quad .\quad (21d)$$

where $$\gamma_k=(-1)^{(n-k-1)/2}[\sin(k\pi/2n)]^{n-2}\cot(k\pi/2n).$$

Beyond the limiting value of time, for the deflection to reach a_2, the substitution $a_1=1$ should be made. The singularity of equation (20) corresponds to a displacement a_{cr}' which satisfies the relation

$$(1+a_{cr}')^m+(-1)^m(1-a_{cr}')^m=2\left(\frac{\mu}{\bar{\sigma}}\right)^{m+1}\left[\varepsilon_E-\frac{\bar{\sigma}}{E}\right].\quad .\quad .\quad (22)$$

Substitution of a_{cr}' for a_2, with $a_1=1$, in equations (21) yields the time t_{ad} necessary for the lateral deflection amplitude a to increase from unity to a_{cr}'. Since tension is assumed to be present in the entire tension flange throughout the buckling process, this adds to the rate of increase of curvature and consequently decreases the time of failure. Hence $t_{cr\,l}$, the lower limit of the time required for buckling, is

$$t_{cr\,l}=t_{lim}+t_{ad}.\quad .\quad .\quad .\quad .\quad .\quad (23)$$

If the initial deflection a_0 is greater than unity, then tension is present on the convex side of the column from the beginning of creep. Equation (20) is valid during the entire buckling process in such cases provided it is assumed that the entire convex flange is in tension. Equation (15) with the a_{cr} value from equation (16) gives again the upper limit $t_{cr\,u}$ of the critical time. The lower limit $t_{cr\,l}$ can be calculated by using a_0 for a_1 and a_{cr}' for a_2 in equations (21).

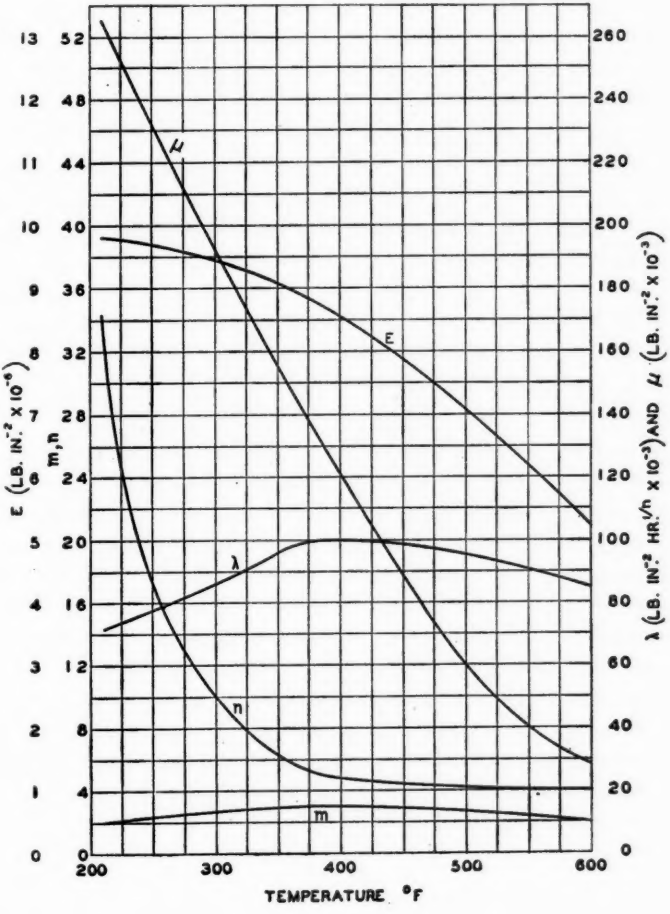

Fig. 3.
Variation of material constants with temperature for 75S-T6 aluminium alloy.

4. Example

A column with a slenderness ratio of 99·34 ($\varepsilon_E = 0{\cdot}001$) and an initial deflection $a_0 = 0{\cdot}1$ is considered. It is assumed that the column is made of 75S-T6 aluminium alloy. Further, it is assumed that the applied average compressive stress $\bar{\sigma}$ is equal to half the Euler stress. Material constants, E, μ, m, λ and n are found with the aid of the data presented in Refs. 7 and 8. Fig. 3 shows how these constants vary with temperature in the range 211 - 600°F. The results obtained by the use of the formulae presented in the paper are given in Table I.

TABLE I

Temperature (°F)	211	300	375	600
$t_{cr\,u}$ (hr.)	$4{\cdot}02\times10^{32}$	$1{\cdot}93\times10^{8}$	$1{\cdot}01\times10^{3}$	2
$(t_{cr\,u}-t_{cr\,l})$ (hr.)	$2{\cdot}25\times10^{6}$	4×10^{4}	5×10	$a_{cr}<1$

The results clearly indicate that for relatively small variation of temperature there may be a significant change in the critical time. For example, when the temperature is varied from 300°F. to 375°F. the consequent change in the critical time is 22,000 years to 6 weeks.

5. Conclusion

The foregoing analysis can be used to find the upper and lower limits of the critical time. The critical time is defined as the time at which the magnitude of the transverse velocity of the column becomes infinitely large. This differs from the analyses of Refs. 4, 5 and 6 where the deflections themselves become infinitely large. The infinite velocity occurs at a finite deflection. This analysis may give a lower critical time than the non-linear visco-elastic analysis of Ref. 5. If the term expressing the plastic deformations is neglected, the solution is reduced to that of the non-linear visco-elastic analysis of Ref. 5. It may be noted that in the present work it is assumed that the deflection a_0 at time $t=0$ is known. If the shape of the column before load application is known, a_0 can be determined in a manner similar to that described in Ref. 1.

ACKNOWLEDGMENTS

This paper is based on a portion of a dissertation submitted to the Polytechnic Institute of Brooklyn in partial fulfilment of the requirements for the degree of Doctor of Philosophy. The author is grateful to Professor N. J. Hoff and to Professor Joseph Kempner for their valuable criticism.

REFERENCES

1. HOFF, N. J. Creep Buckling. *Aeronautical Quarterly*, Vol. VII, February 1956.
2. ODQVIST, FOLKE K. G. Influence of Primary Creep on Column Buckling. *Journal of Applied Mechanics*, Vol. 21, No. 3, p. 295, September 1954.
3. HOFF, N. J. Rapid Creep in Structures. *Journal of the Aeronautical Sciences*, Vol. 22, No. 10, p. 661, October 1955.
4. LIBOVE, CHARLES. Creep Buckling of Columns. *Journal of the Aeronautical Sciences*, Vol. 19, No. 7, pp. 459-467, July 1952.
5. KEMPNER, JOSEPH and PATEL, SHARAD, A. Creep Buckling of Columns. N.A.C.A. T.N. 3138, January 1954; *see* also P.I.B.A.L. Report No. 205, November 1952.
6. HOFF, N. J. Buckling and Stability. Forty-First Wilbur Wright Memorial Lecture. *Journal of the Royal Aeronautical Society*, Vol. 58, No. 1, p. 1, January 1954; *see* also P.I.B.A.L. Report No. 227, July 1953.
7. MATHAUSER, ELDON E. and BROOKS, WILLIAM A., Jr. An Investigation of the Creep Lifetime of 75S-T6 Aluminum-Alloy Columns. N.A.C.A. T.N. 3204, July 1954.
8. Strength of Metal Aircraft Elements. ANC-5, Munitions Board Aircraft Committee, Dept. of Defense. Revised edition, June 1951.

Supersonic Bangs

Part II

P. SAMBASIVA RAO

(*Department of Mathematics, The University, Manchester*)

SUMMARY: The non-linear theory of supersonic bangs, obtained in Part I[1] for a body accelerating along a straight path, is extended to include curved paths. The basic theory remains the same. The important parameter, which appears in the theory, is the acceleration component along the ray, the rays being lines drawn from points on the flight path at an angle $\cos^{-1}(1/M)$ with the direction of motion. It is found that the only essential effect of the curvature of the path is in the modification of this acceleration component to include a term due to the transverse acceleration. With this modification the main results are formally the same as in Part I.

The strength of the bow shock is obtained, and it is found that the effect of the curvature of the path is more pronounced at points on the inside of the curve, and in general it becomes greater as the distance from the body increases. A simple asymptotic formula is obtained which predicts the strength of the shock with an error of less than five per cent. at distances of the order of a hundred body-lengths. Finally, the theory is compared and contrasted with the recent work by Warren[3].

1. Introduction

In Part I of this paper[1] the Whitham theory[2] of the shocks produced by a body in uniform supersonic flight was extended to include bodies moving with variable velocity. However, for simplicity in developing the theory, only the case of a straight flight path was considered. In this paper, the necessary modifications are obtained for application of the theory to the shocks produced by a body moving along a curved path. Also, in this paper, the opportunity is taken to compare this theory with the results obtained by Warren[3], whose recent paper was published after Part I had been written.

NOTATION

$\mathbf{x}$	position vector of the field point
$\mathbf{X}$	position vector of an element of the body
$\mathbf{X}_0$	position vector of the nose of the body

Received September 1955.

r	distance measured perpendicular to the axis of the body
ξ	distance of an element of the body from the nose
ξ_1	maximum value of ξ
η	function defining more accurate wavelets
η_0	first zero of $F(\eta)$ apart from $\eta=0$
η'	dummy variable
θ	angular co-ordinate determining the position of a plane round the path
κ	curvature of the path
t	time variable
τ	time when a disturbance leaves the body
τ_0	time when the nose of the body crosses the ray
$\delta\theta, \delta\tau$	small increments in θ and τ
U	speed of the body
l	length of the body
δ	thickness ratio
a	local sound speed
a_0	speed of sound in the undisturbed flow
M	Mach number, U/a_0
μ	Mach angle, $\sin^{-1}(1/M)$
ϕ	velocity potential
A	acceleration component along the ray
s	distance along the ray
$E(s)$	expansion ratio
$S(\xi)$	cross-sectional area of the body
$\lambda = a_0^2(M^2-1)/A$	
b	defined by equation (3)
F	function describing the wave profile
p	pressure
p_0, ρ_0	pressure and density in the undisturbed flow
γ	ratio of specific heats of air

2. Basic Theory

The basic method is unchanged from Part I. The linear (acoustic) theory provides a first rough approximation of the geometry of the shocks; the wave fronts, *i.e.* the envelopes of sound wavelets, are the linear approximations to the shocks. But the linear theory gives only an inaccurate estimate of the shock strengths. In fact, the pressure is continuous across a wave front and the estimate of the shock strength is taken from the maximum pressure which is attained in the flow behind the wave front (Warren[4]). To obtain an accurate evaluation of the shock strengths, it is necessary to incorporate certain crucial non-linear features. In the first instance, this involves the introduction of the correct propagation speed (equal to the local speed of sound relative to the fluid) for the individual wavelets. Then, since the wavelets move with different speeds, they pile up in compression regions to form shocks. Thus, shocks are necessarily introduced as an essential part of the theory.

In applying these ideas, it is possible and also desirable to work mainly with the geometrical acoustic approximation to the full linear theory; the reasons for this were discussed in detail in Part I. In geometrical acoustics an important part is played by the rays, which are defined as the orthogonal trajectories of the wave fronts and in a sense are the carriers of the disturbance. In this paper the theory is developed for a uniform atmosphere, but the method may be extended to other cases. It is easily shown that, for a uniform medium, the rays are straight lines drawn from each point of the supersonic part of the flight path at an angle $\frac{1}{2}\pi - \sin^{-1}(1/M)$ to the direction of motion, where M is the Mach number of the body at the point concerned. Thus, the component of the velocity of the body along a ray is equal to the sound speed. This provides the approximate criterion that an observer subsequently hears a bang if at any time the velocity component towards him is sonic; for in that case he would be on a ray. The wave front and the rays are shown in Fig. 1 for the typical case of an accelerating point source. Fig. 1 shows that a novel feature of accelerated flow is that the wave front is cusped and has a rear portion which may be called the rear shock. This is considered later. For a real body, which is more like a doublet, shocks will arise from both the nose and the tail of the body. Thus, it may be expected that the shock system in Fig. 1 would be duplicated. In practice, however, the rear shock seems to be single, and the flow pattern is as shown in Fig. 2 (*see* Ref. 5).

The theory of geometrical acoustics also provides an approximate determination of the amplitude of the disturbance as it moves along a narrow tube formed by neighbouring rays. The assumption is made that the energy of the disturbance remains constant; that is, energy is not reflected or diffracted. Then, since energy is proportional to the square of the amplitude multiplied by the cross-sectional area of the ray tube, the amplitude is proportional to $\{E(s)\}^{-\frac{1}{2}}$, where $E(s)$ is the expansion ratio at a distance s along the ray tube and is defined as the ratio of the cross-sectional area at s to the value at some reference position. More precisely, $E(s)$ would be taken as the limiting value of this ratio as the ray tube shrinks up to a

single ray. The determination of E is a simple geometrical calculation and the details are given in Section 3. It is found that, omitting a constant of proportionality, we may take

$$E(s)=s\left(1-\frac{s}{\lambda}\right) \quad . \quad . \quad . \quad . \quad . \quad (1)$$

with $$\lambda=\frac{a_0^2(M^2-1)}{A}, \quad . \quad . \quad . \quad (2)$$

where a_0 is the speed of sound in the undisturbed fluid and A is the component of acceleration of the body along the ray. Equations (1) and (2) are of the same form as for the straight path. The only difference is in the expression for A, which now includes a term due to the acceleration perpendicular to the path; thus A depends on the curvature of the path and the angular co-ordinate determining the position of the plane containing the field point around the path. E obviously tends to zero at the cusp (corresponding to $s=\lambda$ in equation (1)), and the approximation of geometrical acoustics breaks down. Therefore, near the cusp it is necessary to consider the full linear solution; this is considered in detail in Section 6. For a non-uniform medium it would be necessary to include the factor $\rho_0 a_0$ in the expression for the energy, since it would vary with position.

In geometrical acoustics reflection and diffraction of energy are neglected. But, even when this is justified, the theory requires modification to include the non-linear effects already mentioned; correct allowance for the dissipation of energy by the shocks is essential. It is found that, at large distances, the additional fall-off in amplitude due to this effect is represented by a factor $\{b(s)\}^{-\frac{1}{2}}$ in the amplitude, where

$$b(s)=\int_0^s \frac{ds}{[E(s)]^{\frac{1}{2}}}, \quad . \quad . \quad . \quad . \quad . \quad (3)$$

so that at large distances the shock strength varies with s as

$$\left\{E\int_0^s \frac{ds}{E^{\frac{1}{2}}}\right\}^{-\frac{1}{2}} \quad . \quad . \quad . \quad . \quad . \quad . \quad (4)$$

To obtain this modified theory, a more detailed description of the flow is required and it is obtained by taking any flow quantity, the pressure increase for example, in the form

$$p-p_0=E^{-\frac{1}{2}}f\left(t-\tau_0-\frac{s}{a_0}\right), \quad . \quad . \quad . \quad (5)$$

where τ_0 is the time when the nose of the body is on the ray through the point. The function f describes the wave profile and is determined from the initial disturbance at the body, while the factor $E^{-\frac{1}{2}}$ accounts for the change in amplitude as the disturbance propagates along the ray tube. It should be stressed, however, that the present unrigorous formulation of this result is used for simplicity and in order

to highlight the basic ideas. In fact, it was shown in Part I that, near the wave front, the approximate form of the full linear solution is in accord with (5); the actual form is

$$p-p_0=\frac{M^{5/2}}{\{2(M^2-1)\}^{\frac{1}{4}}}\frac{\rho_0 a_0^2 F(\xi_1)}{E^{\frac{1}{4}}}, \qquad (6)$$

where ρ_0 is the density of undisturbed fluid and

$$\xi_1=U\left(t-\tau_0-\frac{s}{a_0}\right). \qquad (7)$$

The F function depends on the shape of the body and is determined in the full linear theory. However, if the changes in the direction and magnitude of velocity in the time taken by the body to fly its own length are small, the F function is not affected by the acceleration and is the same as for uniform motion; it is

$$F(\xi_1)=\frac{1}{2\pi}\int_0^{\xi_1}\frac{S''(\xi)\,d\xi}{(\xi_1-\xi)^{\frac{1}{2}}}. \qquad (8)$$

where $S(\xi)$ is the area of cross section of the body at a distance ξ from the nose. In Section 4 these conclusions are checked briefly for the extension to curved paths.

For the improved non-linear theory, ξ_1 is replaced by η, which is now chosen so that the wavelets specified by η=constant are determined with the more accurate speed of propagation in place of a_0. This follows the standard method explained in Ref. 2 and used in Part I. Then, where the wavelets would otherwise overlap, a shock is introduced and its position and strength are determined from the condition that the shock speed is the mean of the speeds of the wavelets on either side of the shock. The details are set out in Section 5.

The main result is the expression for the shock strength as a function of s. This now depends on the angular co-ordinate round the flight path, the shock being stronger on the concave side of the path than on the convex side. Graphs showing the results of numerical computations of the shock strength for different curvatures of the path and in different planes through the tangent at a point of the path are then given. From the graphs it may be noted that, compared with the case of a straight flight path, the shock is stronger on the inside of the curve and is weaker on the outside. This effect becomes increasingly more pronounced as s increases. In a particular case (Fig. 6), when the curvature of the path is (1/3000)m.$^{-1}$, the ratio of the shock strength on the inside of the path for $\theta=\frac{1}{3}\pi$ to that on the outside for $\theta=\frac{2}{3}\pi$ varies from 1·1 to 2, as s increases from about 300 to 1,200 body-lengths. (The shock strength at the nose is independent of the curvature of the path). For larger curvatures this factor can be greater. The effect of the curvature is felt more on the inside of the path than on the outside. For example, in Fig. 6, at a distance equal to about 1,200 body-lengths, the shock is stronger for $\theta=\frac{1}{3}\pi$ by a factor 1·6

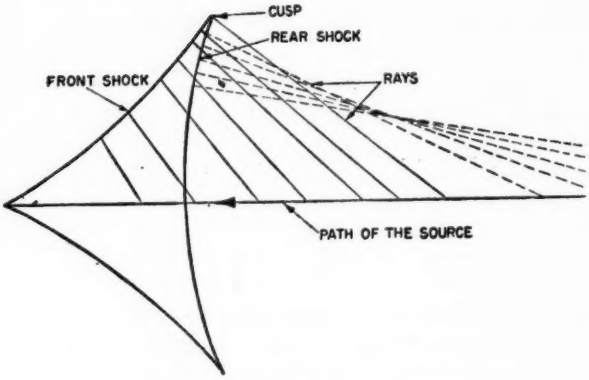

Fig. 1.

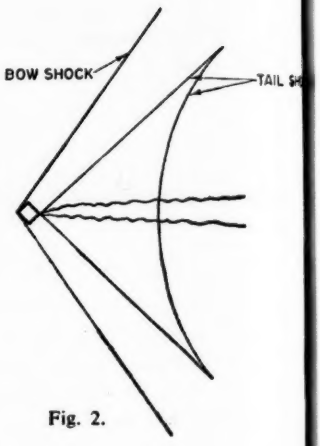

Fig. 2.

compared with the case of no curvature ($\theta=\frac{1}{2}\pi$); it is weaker for $\theta=\frac{2}{3}\pi$ only by a factor 0·8. As the cusp is approached, of course, the shock on the inside becomes much stronger.

It is shown in Part I that, when the acceleration component of the body along a ray is positive, the wave front will have a cusp at one point on that ray and there will be a rear shock as in Fig. 1. As already noted, geometrical acoustics, and hence the correction based thereon, do not apply in the neighbourhood of a cusp. But it seems reasonable to suppose that on the rear shock, well beyond the cusp, the theory again gives a correct description of the shock decay. It may well be, of course, that some energy is lost in the neighbourhood of a cusp, and that in continuing across the cusp the shock strength may be appreciably reduced. Nevertheless, it is felt that at least the variation of strength of the shock with s will be given correctly. Under these assumptions the pressure rise at the rear shock can be estimated, and the details are given in Section 6. An asymptotic formula for the shock strength for large distances is deduced, and it is found that as s tends to infinity the shock strength decays like $s^{-1}(\log s)^{-\frac{1}{4}}$, which is typical of spherical shocks.[6]

Finally, Section 6 is concluded with a study of the neighbourhood of a cusp, working with the full linear theory. In the full linear theory the disturbance does not become infinite at a cusp; it is only the approximation of geometrical acoustics which breaks down. By incorporating some of the non-linear effects a rough estimate of the pressure to be expected near a cusp is suggested. Of course, it is not clear what the detailed motion in the neighbourhood of a cusp is really like. For example, from the results given by Lilley and others[5], the flow pattern appears to be as shown in Fig. 2, with the bow shock simply ending in the fluid. In these circumstances, evaluation of the shock strength in this region is necessarily of a very tentative nature.

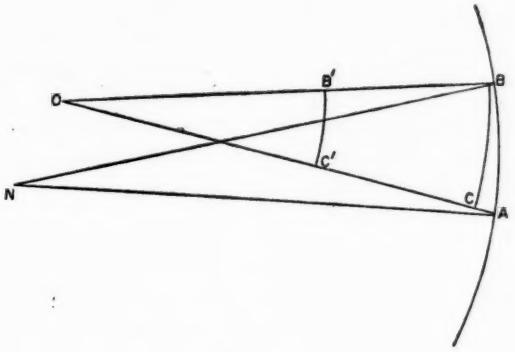

Fig. 3.

3. Expansion Ratios of Ray Tubes

As explained in Section 2, as the disturbance propagates along a ray, its amplitude varies like $E^{-\frac{1}{2}}$. In this section the expansion ratio E is determined for a general flight path.

In Fig. 3, A and B are the positions of the body on the flight path at times τ and $\tau+\delta\tau$ respectively. Consider a plane through AB inclined at an angle θ to the instantaneous plane of motion at A. In this plane the rays at A and B are AC' and BB', and AN and BN are the intersections of this plane with the normal planes to the path at A and B. If κ is the curvature of the path at A then $AN\cos\theta=(1/\kappa)$. The arc $AB=U\delta\tau$, where U is the speed of the body; hence the angle $ANB=U\delta\tau\,\kappa\cos\theta$. If μ is the Mach angle $\sin^{-1}(a_0/U)$, the rays AC' and BB' make angles $\frac{1}{2}\pi-\mu$ and $\frac{1}{2}\pi-\mu-\delta\mu$ with tangents at A and B respectively. Therefore the angle BOA between the rays is $U\delta\tau\,\kappa\cos\theta-\delta\mu$, and at distance $s=AC'$ along the ray, the distance between the rays is

$$B'C'=BC-s\,(U\delta\tau\kappa\cos\theta-\delta\mu) \quad . \quad . \quad . \quad . \quad (9)$$

where BC is the initial distance.

Since
$$BC=AB\cos\mu=U\delta\tau\cos\mu, \quad . \quad . \quad . \quad . \quad (10)$$

it follows that
$$B'C'=\left[U\cos\mu-s\left(U\kappa\cos\theta-\frac{d\mu}{d\tau}\right)\right]\delta\tau. \quad . \quad . \quad (11)$$

At a distance s, the cross-sectional area of the ray tube, bounded by the cones of rays at A and B and the planes making angles θ and $\theta+\delta\theta$ with the instantaneous plane of motion, is given by $\delta\theta\,B'C's\cos\mu$. From (11) this is

$$s\cos\mu\left[U\cos\mu-s\left(U\kappa\cos\theta-\frac{d\mu}{d\tau}\right)\right]\delta\theta\,\delta\tau, \quad . \quad . \quad (12)$$

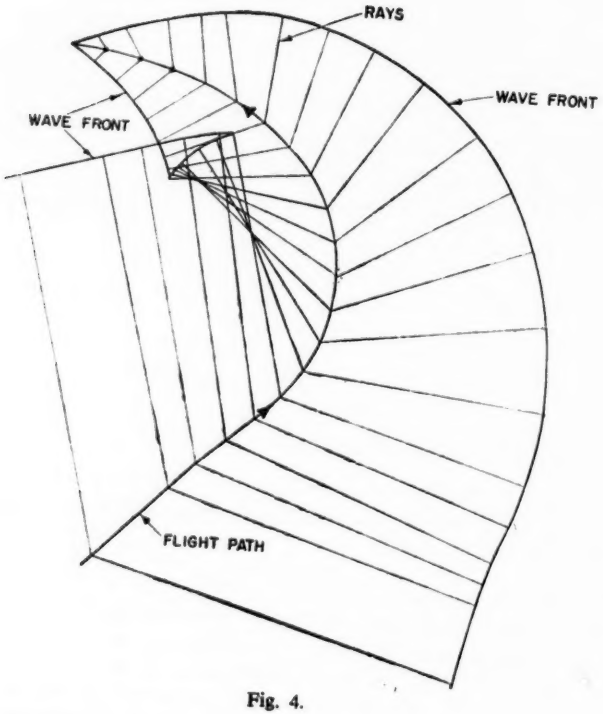

Fig. 4.

Omitting a factor independent of s, we may now take

$$E = s\left(1 - \frac{s}{\lambda}\right), \qquad (13)$$

where

$$\lambda = \left[\frac{\kappa \cos\theta}{\cos\mu} - \frac{1}{U\cos\mu}\frac{d\mu}{d\tau}\right]^{-1} \qquad (14)$$

Writing $M = \dfrac{U}{a_0}$, $A = a_0^2 (M^2 - 1)^{\frac{1}{2}} M\kappa \cos\theta + \dfrac{a_0}{M}\dfrac{dM}{d\tau}$, (15)

relation (14) gives

$$\lambda = \frac{a_0^2 (M^2 - 1)}{A}. \qquad (16)$$

The components of acceleration along and perpendicular to the path are respectively $a_0 dM/d\tau$ and $a_0^2 M^2 \kappa$; whence it is easily seen that A defined in (15) is the component of acceleration along the ray.

Finally, the amplitude is proportional to

$$\left[s\left(1 - \frac{s}{\lambda}\right)\right]^{-\frac{1}{2}}. \qquad (17)$$

Comparing (17) with the corresponding result in Part I, it is seen that they are of the same form and that the curvature of the path only modifies the expression for the acceleration component A. In the plane for which $\theta=\frac{1}{2}\pi$ the curvature has no effect; and the amplitude has its maximum value for $\theta=0$ and its minimum value for $\theta=\pi$. It is observed from (17) that, when $A>0$, and consequently $\lambda>0$, the amplitude tends to infinity as s tends to λ; this corresponds to the cusp of the wave front on this ray. Since λ varies with θ, the occurrence of a cusp on any ray depends on the value of θ. In particular, if the speed of the body is constant, a cusp occurs only on the rays directed towards the inside of the curve, that is, those rays for which $|\theta|<\frac{1}{2}\pi$. Fig. 4 shows the wave front, with the rays, for a source which moves with Mach number 2 from a straight path into a curved one. The cusp is seen to occur on the rays drawn towards the inside of the path, while there is none on the rays drawn outwards.

4. Linear Theory

Following the procedure outlined in Section 2, a check is now made that, in the neighbourhood of the wave front, the flow quantities can be taken proportional to $E^{-\frac{1}{4}}F(\xi_1)$, with $\xi_1=U(t-\tau_0-s/a_0)$ in the linear theory. Furthermore, it was found in Part I that $F(\xi_1)$ is given by

$$\frac{1}{2\pi}\int_0^{\xi_1}\frac{S''(\xi)\,d\xi}{(\xi_1-\xi)^{\frac{1}{2}}},$$

where $S(\xi)$ is the area of cross section of the body at a distance ξ from the nose; in this section it is also verified that this remains true even for the general flight path. The fact that the amplitude agrees with the result of geometrical acoustics shows that the assumptions of geometrical acoustics are valid near the wave front.

This paper is concerned only with the description of the flow at reasonably large distances from the body. The flow is represented by a source distribution along the path of the body. This will be sufficient for slender bodies, but for an aircraft of arbitrary shape a doublet distribution may also be required.

Let the nose of the body be at $\mathbf{X}_0$ at time τ and let U be its speed. Then an element of the path $|d\mathbf{X}|$ at the point $\mathbf{X}$ is occupied at time τ by an element of the body at a distance ξ from its nose, where

$$\xi=|\mathbf{X}-\mathbf{X}_0(\tau)|, \quad . \quad . \quad . \quad . \quad . \quad (18)$$

and, since at distance ξ the cross-sectional area is expanding at the rate $S'(\xi)$, the appropriate source strength at the point $\mathbf{X}$ is $US'(\xi)\,|d\mathbf{X}|$.

Hence at the point **x** at time t the velocity potential of the flow is given by

$$\phi = \frac{1}{4\pi} \int \frac{US'(\xi)\,|d\mathbf{X}|}{|\mathbf{x}-\mathbf{X}|} \quad . \quad . \quad . \quad . \quad . \quad (19)$$

the integration being over all those points **X** on the path from which the disturbance can reach the point **x** at time t. Accordingly τ is given by

$$|\mathbf{x}-\mathbf{X}| = a_0(t-\tau). \quad . \quad . \quad . \quad . \quad . \quad (20)$$

Assuming that the changes in magnitude and direction of the velocity of the body in the time taken to fly its own length are small, the velocity and the distance from the point **x** of any element of the body in (19) can be replaced by the corresponding values for the nose when the nose was on the ray through the point **x**. If the nose was on the ray at time τ_0, then (19) becomes

$$\phi = \frac{-U(\tau_0)}{4\pi\,|\mathbf{x}-\mathbf{X}_0(\tau_0)|} \int S'(\xi)\,|d\mathbf{X}| \,. \quad . \quad . \quad . \quad (21)$$

To obtain ϕ in the form given in (5), the variable of integration is changed to ξ and this can be done conveniently by using τ as an intermediate variable. Now $d\mathbf{X}/d\tau$ differs from the velocity of the body only due to the change of ξ with τ. However, it may be shown as in Part I that $d\xi/d\tau$ is relatively small and we have approximately

$$|d\mathbf{X}| = U(\tau_0)\,d\tau. \quad . \quad . \quad . \quad . \quad . \quad (22)$$

The variables ξ and τ are related by (18) and (20). It was pointed out in Part I that the major part of the contribution to the integral in (21) is made by the supersonic part of the flight path. Among the elements of the body that contribute to the disturbance at the point **x** at time t, the one farthest from the nose, *i.e.* with the greatest ξ, is at the foot of the ray through **x**. Let ξ_1 be this maximum value of ξ. If the point **x** is chosen on the wave front at time t, the corresponding value of ξ_1 is zero; hence ξ_1 is a measure of the distance behind the wave front. Let τ_1 be the time at which the element, at distance ξ_1 from the nose, is on the ray through the point **x**. Expanding ξ as Taylor series near $\tau = \tau_1$, we obtain

$$\xi - \xi_1 = \frac{1}{2}\ddot{\xi}_1(\tau-\tau_1)^2 + \ldots\ldots \quad . \quad . \quad . \quad . \quad (23)$$

The higher order terms are neglected, as in Part I, under the assumption, which is true near the shock, that $\xi_1/|\mathbf{x}-\mathbf{X}_0|$ is small. Differentiating (23) it is seen that

$$\frac{d\xi}{d\tau} = \{2(\xi-\xi_1)\ddot{\xi}_1\}^{\frac{1}{2}}. \quad . \quad . \quad . \quad . \quad . \quad (24)$$

From (21), (22) and (24), the expression for ϕ becomes

$$\frac{-U^2}{(-2\ddot{\xi}_1)^{\frac{1}{2}}\,s}\int_0^{\xi_1}\frac{S'(\xi)\,d\xi}{2\pi(\xi_1-\xi)^{\frac{1}{2}}}, \qquad (25)$$

where $$s=|\mathbf{s}|=|\mathbf{x}-\mathbf{X}_0(\tau_0)|. \qquad (26)$$

The relation between ξ and τ is given from (18) and (20) as

$$(\mathbf{s}+\xi\mathbf{i})^2 \simeq a_0^2(t-\tau)^2, \qquad (27)$$

where $\mathbf{i}$ is the unit vector along the flight path; from this, $-\ddot{\xi}_1$ is found to be

$$-\ddot{\xi}_1 \simeq \frac{a_0^2M(M^2-1)-MAs}{s^3}. \qquad (28)$$

where A is the acceleration component defined in (15). (In deriving (28), use is again made of the assumption that ξ_1/s and the change of direction in a distance ξ_1 are both small). Substituting from (28) for $\ddot{\xi}_1$, the potential function ϕ is finally written in the form

$$\phi=\frac{-a_0M^{3/2}}{\left\{2(M^2-1)s\left(1-\frac{s}{\lambda}\right)\right\}^{\frac{1}{2}}}\int_0^{\xi_1}\frac{S'(\xi)\,d\xi}{2\pi(\xi_1-\xi)^{\frac{1}{2}}}, \qquad (29)$$

where $\lambda=a_0^2(M^2-1)/A$, as before, and M is the Mach number at time τ_0. It remains to determine ξ_1 in terms of t, τ_0, and s. Now, ξ_1 is the distance travelled by the body during the time $(\tau_1-\tau_0)$; it is therefore approximately equal to $U(\tau_0)(\tau_1-\tau_0)$ and, since $(t-\tau_1)\,a_0=s$, we have

$$\xi_1 \simeq U\left(t-\tau_0-\frac{s}{a_0}\right). \qquad (30)$$

From (29) and (30) it is found, neglecting terms of order ξ_1/s, that

$$\phi_s=\frac{M^{3/2}a_0F(\xi_1)}{\left\{2(M^2-1)s\left(1-\frac{s}{\lambda}\right)\right\}^{\frac{1}{2}}}, \qquad (31)$$

$$p-p_0=-\rho_0\phi_t=\frac{M^{5/2}\rho_0a_0^2F(\xi_1)}{\left\{2(M^2-1)s\left(1-\frac{s}{\lambda}\right)\right\}^{\frac{1}{2}}}, \qquad (32)$$

where $$F(\xi_1)=\frac{1}{2\pi}\int_0^{\xi_1}\frac{S''(\xi)\,d\xi}{(\xi_1-\xi)^{\frac{1}{2}}}. \qquad (33)$$

Thus the amplitude is given in accordance with geometrical acoustics and the F function is the same as in Part I.

Perhaps it is worthwhile summarising the co-ordinates now adopted. The position $\mathbf{x}$ of a point is specified by the " ray co-ordinates " τ_0, θ and s; τ_0 determines the point on the path through which the ray is drawn (this point being the position of the nose at time τ_0), and θ determines the plane around the path in which the ray lies, while s gives the distance along the ray. In terms of these co-ordinates the particle velocity and pressure at time t are given by (30), (31) and (32). The expression in (31) is the component of the velocity of the fluid along the ray. In the region near the wave front, the component tangential to the wave front is small compared to ϕ_s, since across the wave front the tangential component is continuous; hence, in this region the flow is approximately along the rays. Thus the flow along each ray tube can be considered independently, and in each ray tube the flow is similar to propagation in a duct of variable cross section $E(s)$.

5. Non-Linear Theory

The expressions in (31) and (32) for the particle velocity ϕ_s and the excess pressure $p - p_0$ only differ from the corresponding formulae of Part I in the definition of λ. Now, from (15) and (16), λ is given by

$$\lambda = \frac{a_0^2 (M^2 - 1)}{\left[a_0^2 (M^2 - 1)^{\frac{1}{2}} M\kappa \cos\theta + \frac{a_0}{M} \frac{dM}{d\tau} \right]};$$

thus, a term due to the acceleration perpendicular to the path is included. Thus the non-linear improvement of these results is exactly as in Part I, and it is unnecessary to reproduce the details here. Introducing the excess pressure ratio $(p - p_0)/p_0$, since $\gamma p_0 = \rho_0 a_0^2$, where γ is the ratio of specific heats, the flow quantities are given by

$$\left.\begin{aligned} \phi_s &= \frac{M^{5/2} a_0 F(\eta)}{\left[2(M^2 - 1) s \left(1 - \frac{s}{\lambda} \right) \right]^{\frac{1}{4}}} \\ \frac{p - p_0}{p_0} &= \frac{M^{5/2} \gamma F(\eta)}{\left[2(M^2 - 1) s \left(1 - \frac{s}{\lambda} \right) \right]^{\frac{1}{4}}} \end{aligned}\right\} \quad . \quad . \quad . \quad (34)$$

where the wavelets, defined by $\eta(t, s) = \text{constant}$, are now determined from the accurate speed of propagation $a + \phi_s$, a being the local speed of sound. Only the dependence of η on t and s is shown explicitly, but it also depends on the parameters* τ and θ defining the ray.

*The suffix of τ_0 is dropped hereafter.

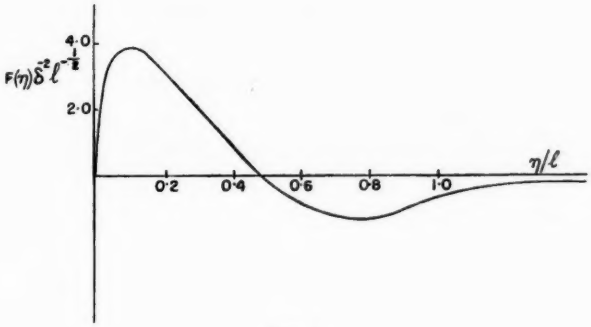

Fig. 5.

The relation determining η is found to be

$$U(t-\tau-s/a_0)+\frac{(\gamma+1)M^{7/2}}{\{8(M^2-1)\}^{\frac{1}{4}}}F(\eta)\,b(s)=\eta \quad . \quad . \quad (35)$$

where
$$b(s)=\int_0^s -\frac{ds}{s^{\frac{1}{2}}\left(1-\frac{s}{\lambda}\right)^{\frac{1}{4}}}. \quad . \quad . \quad . \quad (36)$$

Evaluating the integral for b, we have

$$\left.\begin{aligned} b&=2\lambda^{\frac{1}{4}}\sin^{-1}(s/\lambda)^{\frac{1}{2}}, \quad \lambda>0 \\ b&=2(-\lambda)^{\frac{1}{4}}\sinh^{-1}(s/-\lambda)^{\frac{1}{2}}, \quad \lambda<0. \end{aligned}\right\} \quad . \quad . \quad . \quad (37)$$

Finally, it is necessary to know the relation between s and η at the shock, *i.e.* the distance along the ray at which the wavelet η=constant runs into the shock. For, when this is known, equation (35) gives the position of the shock at time t and (34) gives the pressure behind it. If the shock is moving into the undisturbed fluid, the required relation between s and the value of η at the shock is (*see* Part I)

$$\frac{(\gamma+1)M^{7/2}}{\{32(M^2-1)\}^{\frac{1}{4}}}b(s)=\frac{\int_0^{\eta}F(\eta')\,d\eta'}{F^2(\eta)}. \quad . \quad . \quad . \quad (38)$$

Figure 5 shows the F-curve of an axi-symmetric body of length l, thickness ratio δ and shape given by

$$r=\delta l\left\{1-\left(1-\frac{x}{l}\right)^3\right\}, \quad 0\leqslant\frac{x}{l}\leqslant 1, \quad . \quad . \quad (39)$$

where x is measured from the nose along the axis and r is measured perpendicular to the axis. It is clear from (38) that large values of s (when b is large) correspond to

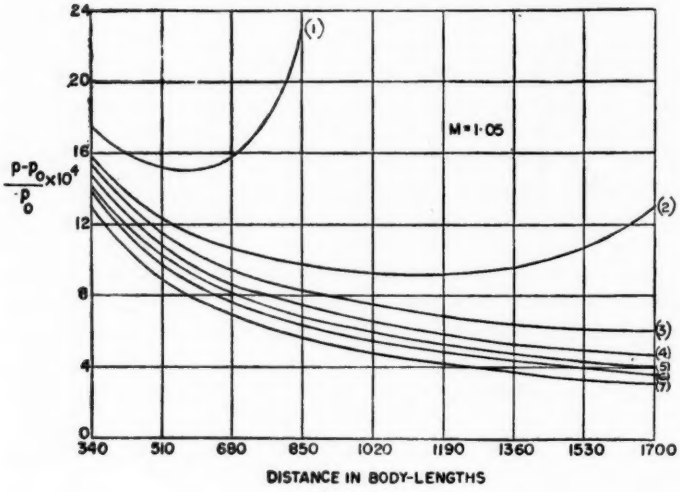

Fig. 6.

values of η near to η_0, the zero of $F(\eta)$ (when there is more than one zero, η_0 is the first one apart from $\eta=0$). This leads to a simple asymptotic formula valid for large s. For, from (38),

$$F(\eta) \simeq \frac{2^{5/4}(M^2-1)^{\frac{1}{4}}}{(\gamma+1)^{\frac{1}{2}}M^{7/4}}\left\{\frac{\int_0^{\eta_0} F(\eta')\,d\eta'}{b(s)}\right\}^{\frac{1}{2}}; \qquad (40)$$

hence the shock strength for large s is given by

$$\frac{p-p_0}{p_0} = \frac{2^{3/4}M^{3/4}\gamma}{(\gamma+1)^{\frac{1}{2}}(M^2-1)^{\frac{1}{4}}}\left\{\frac{\int_0^{\eta_0} F(\eta')\,d\eta'}{b(s)\,s\left(1-\frac{s}{\lambda}\right)}\right\}^{\frac{1}{2}}. \qquad (41)$$

It should be noted that in this formula only a single numerical factor depends on the shape of the body. For the body defined in (39) with $\delta=0{\cdot}06$ (as in Part I)

$$\int_0^{\eta_0} F(\eta')\,d\eta' = 0{\cdot}00391 l^{3/2}.$$

Thus, accepting this as a typical value and taking $\gamma=1{\cdot}4$, (41) becomes

$$\frac{p-p_0}{p_0} = \frac{0{\cdot}095\,M^{3/4}l^{3/4}}{(M^2-1)^{\frac{1}{4}}}\left\{b(s)\,s\left(1-\frac{s}{\lambda}\right)\right\}^{-\frac{1}{2}}. \qquad (42)$$

TABLE I

(i)	(ii)	(iii)	(iv)	(v)	(vi)
		Straight path	*Curved path with constant speed*		
Curve No.	*Value of λ in body-lengths*	*Acceleration in m./sec.²*	*Radius of curvature 3,000 m. Value of θ*	*Radius of curvature 1,500 m. Value of θ*	*$\theta=0$ Radius of curvature in m.*
(1)	914·8	13·6	0°	60°	3,000
(2)	1829·6	6·8	60°	75° 31′	6,000
(3)	3659·2	3·4	75° 31′	82° 49′	12,000
(4)	∞	0	90°	90°	∞
(5)	−3659·2	− 3·4	104° 29′	97° 11′	−12,000
(6)	−1829·6	− 6·8	120°	104° 29′	− 6,000
(7)	− 914·8	−13·6	180°	120°	− 3,000

When s is much smaller than λ (although still large enough for the asymptotic formula to apply), (36) and (41) show that the shock strength falls off like $s^{-3/4}$; this result is typical of cylindrical waves and it was also found in the case of zero acceleration[2]. But, in contrast, when $s >> |\lambda|$, from (36) $b(s) \sim \lambda^{\frac{1}{2}} \log(s)$ (*see* Section 6) and we have the result

$$\frac{p - p_0}{p_0} \propto s^{-1} (\log s)^{-\frac{1}{2}}, \qquad (43)$$

which is typical of the decay of spherical shocks (*see* Ref. 6); this final decay is a special feature of accelerated motion.

It is of interest now to compare formula (42) with the one suggested by Warren[3] and to consider his results from the present point of view. Warren also starts with the linear theory and he uses a formula which is essentially (34) with a typical value inserted for $F(\eta)$. Then, for the special case of uniform velocity, he compares this result with the accurate value obtained by Whitham[2] and finds that a further factor $(M^2-1)^{\frac{1}{4}} M^{-7/4} s^{-\frac{1}{4}}$ is required to take account of the non-linear effects. He then retains this factor in the formula for the accelerating body. It can be seen from (42) that the correct factor is $(M^2-1)^{\frac{1}{4}} M^{-7/4} [b(s)]^{-\frac{1}{4}}$. Thus the effect of acceleration appears not only in the original linear formula (34) but also through $b(s)$ in the modifying factor; Warren's formula does not have this latter effect. For small $s/|\lambda|$, it is true that $b(s)$ is proportional to $s^{\frac{1}{4}}$, so that Warren's formula is initially correct. Ultimately, however, $b(s)$ is proportional to $\log s$, leading to the law of decay of spherical shocks, whereas Warren's formula leads to

$$\frac{p - p_0}{p_0} \propto s^{-5/4} \qquad (44)$$

for large s.

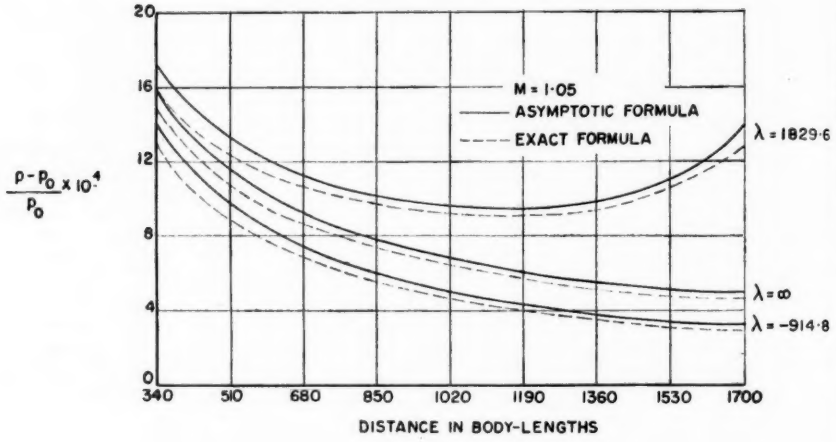

Fig. 7.

Calculations of the variation of shock strength with s have been made for the body defined in (39) in the case when $M = 1{\cdot}05$. The strength has been computed for various values of λ, both from the exact result given by (34) and (38) and from the asymptotic formula (42). The results of the exact calculations are shown in Fig. 6; the values of s are measured as multiples of body-length l and the values of λ (again measured in body-lengths) are shown in column (*ii*) of Table I.

In Fig. 7 the values of shock strength obtained from the asymptotic and actual formulae are compared for the values of λ equal to 1829·6, ∞ and $-914{\cdot}8$, measured in body-lengths. It should be noted that the error, which is about five per cent., does not vary much over the range of s shown. This is because η approaches η_0 only slowly and consequently $\int_0^{\eta} F(\eta')\,d\eta'$ is approximately constant over an appreciable range, although it is still not equal to $\int_0^{\eta_0} F(\eta')\,d\eta'$.

Thus, even at distances of the order of a hundred body-lengths, the law of variation with s of the shock strength is given quite accurately by the asymptotic formula, but the "constant of proportionality" is to be reduced.

Now, λ is determined by the component of acceleration of the body along the ray, and this may be derived from various combinations of the accelerations along and normal to the path. Thus, for example, a given value of λ may be interpreted as corresponding to a body accelerating along a straight path or to a body moving with constant speed on a curved path.

In columns (*iii*) to (*vi*) of Table I, various possible interpretations of the set of values of λ have been given.

Since the sound speed a_0 enters into the expression for λ, it is necessary for *these* results to specify a definite value for the body-length; here l is chosen to be one metre. In column (*iii*) the values of λ are interpreted as different accelerations of the body along a straight path. In columns (*iv*) and (*v*) they are associated with different angles θ about the flight path for a body moving with constant speed on a curved path; in column (*iv*) the path has a radius of curvature of 3,000 m. while in column (*v*) it is 1,500 m. The infinite value of λ corresponds to uniform velocity and also to the plane $\theta=\frac{1}{2}\pi$. The rays for which $|\theta|<\frac{1}{2}\pi$ correspond to the inside of the path and the rays for which $|\theta|>\frac{1}{2}\pi$ correspond to the outside. It may be noted from Fig. 6 that the effect of the curvature is more pronounced on the inside than on the outside of the path. For example, when the radius of curvature of the path is 3,000 m., at a distance of 1,200 m. from the nose, the shock is stronger for $\theta=\frac{1}{3}\pi$ than for $\theta=\frac{1}{2}\pi$ by a factor 1·6, while it is weaker for $\theta=\frac{2}{3}\pi$ only by a factor 0·8. Finally, in column (*vi*) the values of λ are interpreted for points in the plane of flight for different values of the curvature.

6. Rear Shock and Neighbourhood of a Cusp

This section deals with the application of the theory to the rear shock and indicates a method of obtaining an estimate of the shock strength near a cusp. It has already been mentioned that, if the acceleration component along a ray is positive, the wave front has a cusp on the ray and there is a rear shock. On the rear shock, well beyond the cusp, it is expected that the geometrical acoustics, as modified in Section 5, can again be applied. It is therefore assumed that the shock strength decays with s according to the asymptotic formula (41). The formula for $E(s)$ given in (13) becomes negative beyond the cusp ($s>\lambda$) and, of course, the sign must be changed; similarly for $b(s)$ we now have

$$b(s)=\int_0^s \frac{ds}{|E|^{\frac{1}{4}}}=2\lambda^{\frac{1}{4}}\left[\tfrac{1}{2}\pi+\cosh^{-1}(s/\lambda)^{\frac{1}{2}}\right], \qquad (45)$$

when $s>\lambda$. Hence, the asymptotic formula becomes

$$\frac{p-p_0}{p_0}=\frac{2^{1/4}M^{3/4}\gamma a_0^{\frac{1}{2}}}{(\gamma+1)^{\frac{1}{2}}A^{\frac{1}{4}}}\left\{\frac{\int_0^{\eta_0}F(\eta')\,d\eta'}{[\frac{1}{2}\pi+\cosh^{-1}(s/\lambda)^{\frac{1}{2}}]\,s(s-\lambda)}\right\}^{\frac{1}{4}} \qquad (46)$$

However, it may well be that the " constant of proportionality " will now be smaller, since there may be a loss of energy at the cusp. Certainly, experiments seem to indicate that the rear shock is always very much weaker than the main shocks.

For very large s ($s>>\lambda$), we have

$$\frac{p-p_0}{p_0}=\frac{2^{3/4}M^{3/4}\gamma a_0^{\frac{1}{2}}}{(\gamma+1)^{\frac{1}{2}}A^{\frac{1}{4}}}\,\frac{\left\{\int_0^{\eta_0}F(\eta')\,d\eta'\right\}^{\frac{1}{4}}}{s(\log s)^{\frac{1}{4}}} \qquad (47)$$

This form applies very soon at the point where the rear shock meets the axis, since λ tends to zero there. Again, for very large s, formula (47) indicates a decay of shock strength typical of spherical shocks.

Figure 8 shows the shock strengths plotted against s for the front and rear

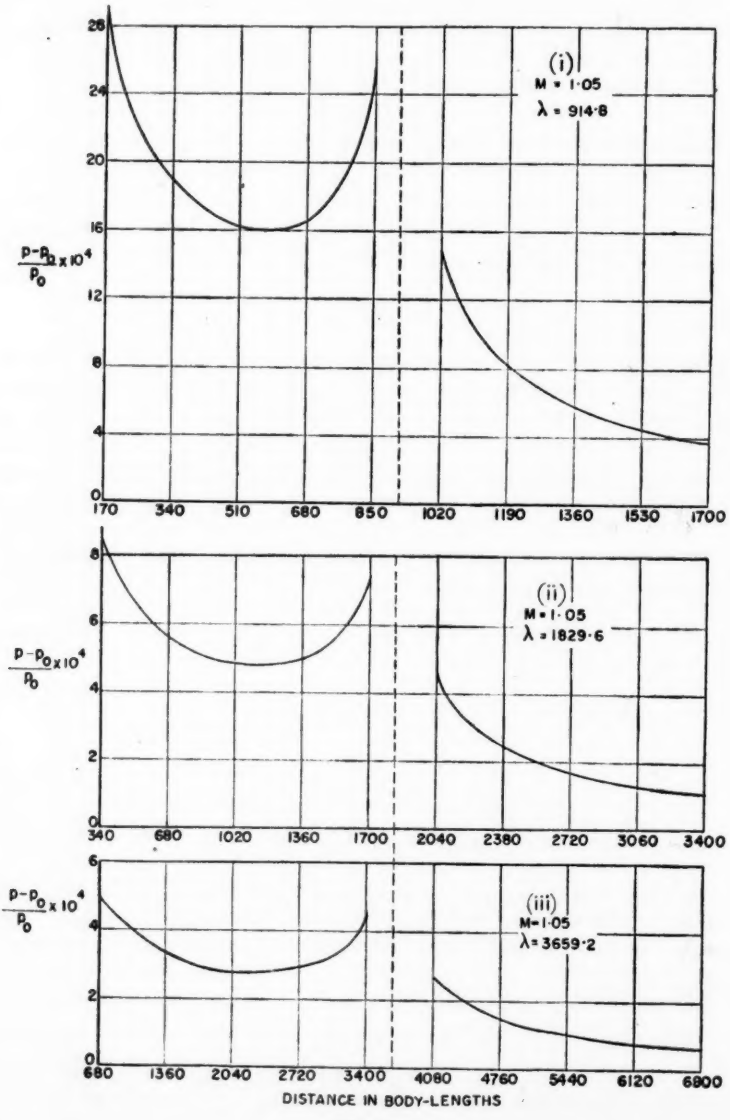

Fig. 8.

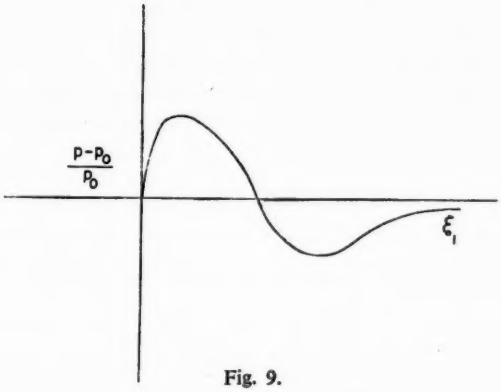

Fig. 9.

shocks for $\lambda = 914{\cdot}8$, 1829·6, and 3659·2, the unit of length being the body length. The shock strength is seen to fall off very rapidly on the rear shock, so that this again predicts that the rear shock will be very much weaker than the main shock.

As mentioned in Section 1, geometrical acoustics, and hence the corrected theory, break down near a cusp. But the full linear theory gives a finite value for the pressure rise and, if a method can be found of modifying this to include the non-linear effects, some estimate of the shock strength near a cusp can be obtained.

Figure 9 is a typical graph of the pressure rise plotted against $\xi_1 = U(t - \tau - s/a_0)$, (*i.e.* U times the time that has elapsed since the wave front passed the point). Now, in the linear theory $\xi_1 = 0$ corresponds to the wave front and the pressure is continuous there. But in the improved theory, which is applied away from the cusp, the appropriate value of ξ_1 is simply the η determined from (38). The portion of the pressure curve ($0 \leqq \xi_1 \leqq \eta$), which is cut out in this way, corresponds to the wavelets which have been absorbed by the shock. Near the cusp, where the approximate formula of geometrical acoustics breaks down, the appropriate pressure curve must be obtained from the full linear theory. (The pressure is again plotted against $\xi_1 = U(t - \tau - s/a_0)$). Then, having found the pressure curve, the problem reduces to choosing the appropriate point on the curve which corresponds to the value just behind the shock.

Now, since wavelets are absorbed by the shock at a relatively slow rate, it seems reasonable to neglect this effect just in the neighbourhood of the cusp, and to determine the required point on the pressure curve from the value of ξ_1 given by the theory away from the cusp. In fact, since the integral defining $b(s)$ is convergent as s tends to λ, the value of η determined by (38) should still be taken. In many cases considered the cusp will be at a large distance, and the approximate determination with η near to η_0 may then be used. Since, for points in the neighbourhood of a cusp, the exact linear expression for $p - p_0$ does not vanish for $\eta = \eta_0$, it is perhaps possible simply to choose η *equal to* η_0 for much of this region.

The expression for ϕ in the full linear theory has been given in Section 4 but the formula for the pressure increase $p - p_0 = -\rho_0 \phi_t$ is now required. The disturbance is represented by a distribution of sources on the flight path and at any point $\mathbf{X}$ the source strength is $US'(\xi) \mid d\mathbf{X} \mid$, where ξ measures the distance of $\mathbf{X}$ from the nose (*i.e.* the point $\mathbf{X}_0(\tau)$) at time τ. The contribution of this source to the value of ϕ at the point $\mathbf{x}$ at time t is

$$\frac{US'(\xi) \mid d\mathbf{X} \mid}{4\pi \mid \mathbf{x} - \mathbf{X} \mid},$$

where the retarded time τ, used in the determination of ξ, satisfies

$$\mid \mathbf{x} - \mathbf{X} \mid = a_0 (t - \tau). \quad . \quad . \quad . \quad . \quad . \quad (48)$$

Clearly, the rate of change of this contribution with time is due to the rate of change of $S'(\xi)$ as the body passes the point $\mathbf{X}$ and this is $US''(\xi)$. Hence, the contribution of the elementary source to ϕ_t is

$$\frac{-U^2 S''(\xi) \mid d\mathbf{X} \mid}{4\pi \mid \mathbf{x} - \mathbf{X} \mid},$$

and ϕ_t is given by the integral of this quantity over all the sources. Making similar approximations used in (21) gives

$$\frac{p - p_0}{p_0} = \frac{-\gamma \phi_t}{a_0^2} = \frac{\gamma M^2}{4\pi s} \int S''(\xi) \mid d\mathbf{X} \mid . \quad . \quad . \quad (49)$$

Then, using the approximation $\mid d\mathbf{X} \mid \simeq U\, d\tau$ (*see* (22)), we write

$$\frac{p - p_0}{p_0} = \frac{\gamma M^3 a_0}{4\pi s} \int S''(\xi)\, d\tau, \quad . \quad . \quad . \quad . \quad . \quad (50)$$

where $\xi = \mid \mathbf{X} - \mathbf{X}_0(\tau) \mid$ and $\mathbf{X}$ is determined in terms of τ by (48).

The method just suggested, although possible in principle, would be cumbersome in practice unless some approximation going beyond geometrical acoustics can be used for (50). This sort of difficulty arises in many applications of geometrical optics and acoustics; near certain curves, called "caustics," the theory of geometrical acoustics is invalid and a more accurate approximation is required. Methods for overcoming these difficulties have been developed for some of these cases and it may be that similar ones may be applied here. On the other hand, it may be possible to obtain adequate results by retaining further terms in (23) (the second order term vanishes at a cusp). However, it is felt that such investigations would be more appropriate when a reasonable qualitative account of what happens in the neighbourhood of cusps is available.

In Warren's[3] approach to the problem, it is not necessary to have such an accurate estimate of (50) and he obtains a rough formula as follows. He suggests a method for estimating the shock strength at the cusp which is derived from a formula corresponding to (50). From the present point of view it may be explained

in the following way. First, the integral (50) is approximated by some mean value of $S''(\xi)$ multiplied by $\Delta\tau$, where $\Delta\tau$ is the change in the retarded time τ over the range of integration. At a fixed point **x**, $\Delta\tau$ varies with the time t and Warren chooses the maximum value, giving the maximum pressure rise as the linear estimate of the shock strength. Then, as before, he introduces the factor $(M^2-1)^{\frac{1}{4}}M^{-7/4}s^{-\frac{1}{2}}$ to account for the extra decrease in strength due to non-linear effects. In contrast, in the method explained, this extra decrease from the linear result arises because, not only is the whole pressure curve of Fig. 9 diminished as s is increased, but the point on the pressure curve which represents conditions behind the shock tends to the zero of $p-p_0$ as s tends to infinity.

ACKNOWLEDGMENT

The author is greatly indebted to Dr. G. B. Whitham for his continued guidance and encouragement and to Professor M. J. Lighthill, F.R.S., for his keen interest and advice throughout the preparation of this paper. He is also grateful to the Government of India and to the authorities of the Andhra University, India, for the award of an overseas scholarship.

REFERENCES

1. SAMBASIVA RAO, P. Supersonic Bangs, Part I. *The Aeronautical Quarterly*, February 1956.
2. WHITHAM, G. B. The Flow Pattern of a Supersonic Projectile. *Communications on Pure and Applied Mathematics*, Vol. 5, pp. 301-48, August 1952.
3. WARREN, C. H. E. An Estimation of the Occurrence and Intensity of Sonic Bangs. R.A.E. Technical Note Aero. 2334, 1954.
4. WARREN, C. H. E. Sonic Bangs. A Qualitative Explanation. R.A.E. Technical Note Aero. 2192, 1952.
5. LILLEY, G. M., WESTLEY, R., YATES, A. H. and BUSING, J. R. On Some Aspects of the Noise Propagation from Supersonic Aircraft. *Journal of the Royal Aeronautical Society*, Vol. 57, pp. 396-414, June 1953.
6. WHITHAM, G. B. The Propagation of Spherical Blast. *Proc. Roy. Soc.* A., Vol. 203, pp. 571-581, 1950.

The expression for ϕ in the full linear theory has been given in Section 4 but the formula for the pressure increase $p - p_0 = -\rho_0 \phi_t$ is now required. The disturbance is represented by a distribution of sources on the flight path and at any point $\mathbf{X}$ the source strength is $US'(\xi) \mid d\mathbf{X} \mid$, where ξ measures the distance of $\mathbf{X}$ from the nose (*i.e.* the point $\mathbf{X}_0(\tau)$) at time τ. The contribution of this source to the value of ϕ at the point $\mathbf{x}$ at time t is

$$\frac{US'(\xi) \mid d\mathbf{X} \mid}{4\pi \mid \mathbf{x} - \mathbf{X} \mid},$$

where the retarded time τ, used in the determination of ξ, satisfies

$$\mid \mathbf{x} - \mathbf{X} \mid = a_0 (t - \tau). \quad . \quad . \quad . \quad . \quad . \quad (48)$$

Clearly, the rate of change of this contribution with time is due to the rate of change of $S'(\xi)$ as the body passes the point $\mathbf{X}$ and this is $US''(\xi)$. Hence, the contribution of the elementary source to ϕ_t is

$$\frac{-U^2 S''(\xi) \mid d\mathbf{X} \mid}{4\pi \mid \mathbf{x} - \mathbf{X} \mid},$$

and ϕ_t is given by the integral of this quantity over all the sources. Making similar approximations used in (21) gives

$$\frac{p - p_0}{p_0} = \frac{-\gamma \phi_t}{a_0^2} = \frac{\gamma M^2}{4\pi s} \int S''(\xi) \mid d\mathbf{X} \mid . \quad . \quad . \quad (49)$$

Then, using the approximation $\mid d\mathbf{X} \mid \simeq U \, d\tau$ (*see* (22)), we write

$$\frac{p - p_0}{p_0} = \frac{\gamma M^2 a_0}{4\pi s} \int S''(\xi) \, d\tau, \quad . \quad . \quad . \quad . \quad . \quad (50)$$

where $\xi = \mid \mathbf{X} - \mathbf{X}_0(\tau) \mid$ and $\mathbf{X}$ is determined in terms of τ by (48).

The method just suggested, although possible in principle, would be cumbersome in practice unless some approximation going beyond geometrical acoustics can be used for (50). This sort of difficulty arises in many applications of geometrical optics and acoustics; near certain curves, called "caustics," the theory of geometrical acoustics is invalid and a more accurate approximation is required. Methods for overcoming these difficulties have been developed for some of these cases and it may be that similar ones may be applied here. On the other hand, it may be possible to obtain adequate results by retaining further terms in (23) (the second order term vanishes at a cusp). However, it is felt that such investigations would be more appropriate when a reasonable qualitative account of what happens in the neighbourhood of cusps is available.

In Warren's[3] approach to the problem, it is not necessary to have such an accurate estimate of (50) and he obtains a rough formula as follows. He suggests a method for estimating the shock strength at the cusp which is derived from a formula corresponding to (50). From the present point of view it may be explained

in the following way. First, the integral (50) is approximated by some mean value of $S''(\xi)$ multiplied by $\Delta\tau$, where $\Delta\tau$ is the change in the retarded time τ over the range of integration. At a fixed point **x**, $\Delta\tau$ varies with the time t and Warren chooses the maximum value, giving the maximum pressure rise as the linear estimate of the shock strength. Then, as before, he introduces the factor $(M^2-1)^{\frac{1}{4}}M^{-7/4}s^{-\frac{1}{4}}$ to account for the extra decrease in strength due to non-linear effects. In contrast, in the method explained, this extra decrease from the linear result arises because, not only is the whole pressure curve of Fig. 9 diminished as s is increased, but the point on the pressure curve which represents conditions behind the shock tends to the zero of $p-p_0$ as s tends to infinity.

ACKNOWLEDGMENT

The author is greatly indebted to Dr. G. B. Whitham for his continued guidance and encouragement and to Professor M. J. Lighthill, F.R.S., for his keen interest and advice throughout the preparation of this paper. He is also grateful to the Government of India and to the authorities of the Andhra University, India, for the award of an overseas scholarship.

REFERENCES

1. SAMBASIVA RAO, P. Supersonic Bangs, Part I. *The Aeronautical Quarterly*, February 1956.
2. WHITHAM, G. B. The Flow Pattern of a Supersonic Projectile. *Communications on Pure and Applied Mathematics*, Vol. 5, pp. 301-48, August 1952.
3. WARREN, C. H. E. An Estimation of the Occurrence and Intensity of Sonic Bangs. R.A.E. Technical Note Aero. 2334, 1954.
4. WARREN, C. H. E. Sonic Bangs. A Qualitative Explanation. R.A.E. Technical Note Aero. 2192, 1952.
5. LILLEY, G. M., WESTLEY, R., YATES, A. H. and BUSING, J. R. On Some Aspects of the Noise Propagation from Supersonic Aircraft. *Journal of the Royal Aeronautical Society*, Vol. 57, pp. 396-414, June 1953.
6. WHITHAM, G. B. The Propagation of Spherical Blast. *Proc. Roy. Soc.* A., Vol. 203, pp. 571-581, 1950.

The Behaviour of Damped Linear Systems in Steady Oscillation

R. E. D. BISHOP

(University Engineering Laboratory, Cambridge)

SUMMARY: The classical theory of small harmonic vibrations of a linear damped system embodies the notion of "viscous damping." The equations of motion which result are somewhat complicated and, when there are more than two degrees of freedom, they are usually too unwieldy to be of much practical value. When the damping is small, however, approximating assumptions may be made which permit the treatment of systems which are near resonance as if they possess but one degree of freedom.[1] But the effects of making these assumptions are by no means easily assessed, and even their justification is tedious.

It is shown that these difficulties may be greatly diminished by postulating hysteretic damping instead of viscous damping; the concept of hysteretic damping has been dealt with in two previous papers.[2], [3] The equations then take a much simpler form and the justification for, and validity of, the foregoing approximations are more easily seen. Moreover, the effects of damping upon the principal modes which the system possesses in the absence of its damping may be elucidated in this way.

1. Introduction

When a mechanical system having a finite number of degrees of freedom executes steady forced harmonic vibration, the motion that the system would perform if it were conservative is modified by the existence of damping forces. If the excitation frequency is remote from a natural frequency of the undamped system, this modification is not great unless the damping is very heavy; but the damping forces play a dominant part in determining the amplitude of the response when the impressed frequency is approximately equal to a natural frequency. The engineer is most concerned with this latter problem, particularly when the damping is light, since it is intimately connected with the liability of components and structures to fracture by fatigue and with the other objectionable features of violent oscillation.

The usual way of tackling the problem of small dissipation is to postulate the existence of viscous damping forces. This leads to a theory which is very complicated when applied to any but the simplest systems. As a result, practical vibration analysis[1] usually involves the assumption that the system may be thought of as possessing one degree of freedom when it oscillates at, or near, resonance. That is to say, it is supposed that the response at the principal co-ordinates of the system (as they are defined in the absence of damping) may be

Received March 1955.

analysed independently such that, at each resonance, one of these co-ordinates only varies. The maximum response in each of the modes is assumed to occur when the excitation frequency equals a natural frequency of the system (which is calculated in the absence of its damping) and the variations of the amplitudes of the principal co-ordinates with frequency is supposed to be the same as that of the displacement of a simple damped spring-mass system.

This method of approach is justified when the damping is light. But in fact there is always coupling between the modes, although one of them predominates at each resonance. Also the maximum responses do occur at frequencies which are very close to the natural frequencies. These results are not easily demonstrated with any generality and an algebraic discussion of their consequences in a given system is usually out of the question as a result of mathematical complexity.

The purpose of this paper is to show that the qualitative results just mentioned may be arrived at with comparative ease by changing the damping theory to that of hysteretic damping[2, 3]. Moreover, the algebra is materially simplified by this change of hypothesis and provides greater insight into the nature of the mathematical theory of damped vibration; it also greatly simplifies the analysis of systems whose damping is not small. The method which is used to demonstrate this is to show how the introduction of damping modifies certain of the simple results of the standard theory for conservative systems. The first part of this paper is therefore devoted to a brief summary of the relevant features of the theory of undamped systems.

The reader should note that it is not the author's purpose to present a practical technique of vibration analysis for use with known systems. It is, rather, to discuss the *nature* of damped vibration in general terms.

NOTATION

$_mA_{rs}$	real constants defined in equation (14)
$_mB_{rs}$	complex constants defined in equation (25)
a_{rs}	inertia coefficients for kinetic energy
c_{rs}	stability coefficients for potential energy
d_{rs}	hysteretic damping coefficients
$i = \sqrt{(-1)}$	
n	number of degrees of freedom
Q_r	generalised force corresponding to q_r
q_r	r^{th} generalised co-ordinate
T	kinetic energy
V	potential energy
α_{rs}	receptance function (*see* equations (7) and (18))

Δ	determinant defined in equation (6), but which may have c_{rs} replaced by $c_{rs}+id_{rs}$
$\eta_1, \eta_2, \ldots \eta_{n-1}$	complex roots of $\Delta_{rr}=0$
$\xi_1, \xi_2, \ldots \xi_n$	complex roots of $\Delta=0$
Φ_r	amplitude of Q_r
Ψ_r	amplitude of q_r
$\Omega_1, \Omega_2, \ldots \Omega_{n-1}$	anti-resonance frequencies
ω	excitation frequency
$\omega_1, \omega_2, \ldots \omega_n$	natural frequencies

2. The Conservative System

2.1. The General Solution

The kinetic and potential energies of a linear oscillatory system with n degrees of freedom have the form

$$\left.\begin{aligned} T &= \tfrac{1}{2}\left[a_{11}\dot{q}_1^2 + a_{22}\dot{q}_2^2 + \ldots + a_{nn}\dot{q}_n^2 + 2a_{12}\dot{q}_1\dot{q}_2 + \ldots\right] \\ V &= \tfrac{1}{2}\left[c_{11}q_1^2 + c_{22}q_2^2 + \ldots + c_{nn}q_n^2 + 2c_{12}q_1q_2 + \ldots\right] \end{aligned}\right\} \quad . \quad (1)$$

If these functions are used in conjunction with Lagrange's equations, the general equations of motion are found; namely,

$$(a_{1r}\ddot{q}_1 + c_{1r}q_1) + (a_{2r}\ddot{q}_2 + c_{2r}q_2) + \ldots + (a_{nr}\ddot{q}_n + c_{nr}q_n) = Q_r \quad . \quad (2)$$

where $r=1, 2, \ldots n$. Suppose that the excitation is harmonic such that

$$Q_s = \Phi_s e^{i\omega t} \qquad (s=1, 2, \ldots n) \quad . \quad . \quad . \quad (3)$$

and that the harmonic response is sought in the form

$$q_r = \Psi_r e^{i\omega t} \quad . \quad . \quad . \quad . \quad . \quad . \quad (4)$$

Equation (2) now gives, for the amplitudes Ψ_r,

$$(c_{1r} - \omega^2 a_{1r})\Psi_1 + (c_{2r} - \omega^2 a_{2r})\Psi_2 + \ldots + (c_{nr} - \omega^2 a_{nr})\Psi_n = \Phi_r \quad . \quad (5)$$

To solve this set of n equations, it is convenient to form the determinant

$$\Delta = \begin{vmatrix} c_{11}-\omega^2 a_{11} & c_{12}-\omega^2 a_{12} & \cdot & \cdot & \cdot & \cdot & c_{1n}-\omega^2 a_{1n} \\ c_{21}-\omega^2 a_{21} & c_{22}-\omega^2 a_{22} & \cdot & \cdot & \cdot & \cdot & c_{2n}-\omega^2 a_{2n} \\ \cdot & \cdot & \cdot & \cdot & \cdot & \cdot & \cdot \\ \cdot & \cdot & \cdot & \cdot & \cdot & \cdot & \cdot \\ c_{n1}-\omega^2 a_{n1} & c_{n2}-\omega^2 a_{n2} & \cdot & \cdot & \cdot & \cdot & c_{nn}-\omega^2 a_{nn} \end{vmatrix} . \quad (6)$$

Suppose first that Q_s is the only non-zero generalised disturbing force; the amplitude of q_r is then given by

$$\Psi_r = (-1)^{r+s} \frac{\Delta_{rs}}{\Delta} \Phi_s = \alpha_{rs} \Phi_s \quad . \quad . \quad . \quad . \quad (7)$$

where Δ_{rs} is that determinant which is formed from Δ by omitting the r^{th} column and s^{th} row. In general all the Φ's will be non-zero and, in that case, the Ψ's must be found by adding solutions of the type (7).

The quantities α_{rs} have been called "receptances"; they are functions of the energy coefficients of equations (1) and of ω^2 and they have been shown by Duncan[4] and others[5, 6] to possess properties which are both interesting and useful. It may be mentioned that these same properties are still available when linear damping is incorporated in the theory. Attention will now be paid to the algebraic form of these receptances.

The natural frequencies of the system may be regarded as those excitation frequencies for which an infinite response is obtained from a finite amplitude of disturbance. They are thus given by the roots $\omega_1^2, \omega_2^2, \ldots\ldots \omega_n^2$ (in order of increasing magnitude) of the frequency equation

$$\Delta = 0. \quad . \quad . \quad . \quad . \quad . \quad . \quad (8)$$

The quantity Δ is a polynomial of degree n in ω^2 and the roots of (8) are all real and positive provided that the system is a stable one; mathematically, this is because the expressions (1) for T and V are "positive definite." The receptance α_{rs} may therefore be written in the form

$$\alpha_{rs} = \frac{f(\omega^2)}{(\omega_1^2-\omega^2)(\omega_2^2-\omega^2) \ldots\ldots (\omega_n^2-\omega^2)} \quad . \quad . \quad . \quad (9)$$

where $f(\omega^2)$ is a polynomial of maximum degree $n-1$ in ω^2. This general result will now be used to demonstrate two general results of vibration theory.

2.2. Direct Receptances

Suppose that it is required to measure the response at q_r caused by excitation Q_r; the receptance of equation (7) would be denoted by α_{rr} and is referred to as "the direct receptance" at q_r. It is given by

$$\alpha_{rr}=\frac{\Delta_{rr}}{\Delta} \quad . \quad . \quad . \quad . \quad . \quad . \quad . \quad (10)$$

Now the equation that is obtained by setting Δ_{rr} equal to zero is the frequency equation of that system which is obtained from the original one by locking it in such a way as only to prevent variation of q_r without adding mass or elasticity at any point. It follows that the equation

$$\Delta_{rr}=0 \quad . \quad . \quad . \quad . \quad . \quad . \quad . \quad (11)$$

has $n-1$ roots which are all real and positive and they will be denoted by $\Omega_1^2, \Omega_2^2, \ldots . \Omega_{n-1}^2$. Thus a *direct* receptance may be written, not only in the form (9) but more particularly as

$$\alpha_{rr}=K\frac{(\Omega_1^2-\omega^2)(\Omega_2^2-\omega^2)\ldots(\Omega_{n-1}^2-\omega^2)}{(\omega_1^2-\omega^2)(\omega_2^2-\omega^2)\ldots(\omega_n^2-\omega^2)} \quad . \quad . \quad . \quad (12)$$

where K is a constant. The frequencies ω_j are the natural frequencies and the Ω_j are the so-called "anti-resonance frequencies." When ω coincides with one of these anti-resonance frequencies, no motion occurs at the driving point q_r.

The anti-resonance frequencies of a mechanical system are spaced between the natural frequencies in order of magnitude. With this limitation, values of these two sets of frequencies may vary between limits which are set by the possibility of having repeated roots of equations (8) and (11). These special limiting cases (which of course, cannot be realised *exactly* in a practical system) have been examined by Bishop and Johnson[7].

2.3. Motion in Principal Modes

A second property of the receptances α_{rs} of equation (9) is that all of them may be expressed as series of partial fractions. Thus α_{rs} may be expressed in the form

$$\alpha_{rs}=\frac{{}_1A_{rs}}{\omega_1^2-\omega^2}+\frac{{}_2A_{rs}}{\omega_2^2-\omega^2}+\ldots .+\frac{{}_nA_{rs}}{\omega_n^2-\omega^2} \quad . \quad . \quad . \quad (13)$$

where the numerators are all real constants.

The significance of this expansion can easily be seen by writing down the

responses at the co-ordinates $q_1, q_2, \ldots q_n$ due to harmonic forcing at one co-ordinate only—the s^{th} say. They are

$$\left.\begin{aligned}
q_1 &= \left[\frac{{}_1A_{1s}}{\omega_1^2-\omega^2}+\frac{{}_2A_{1s}}{\omega_2^2-\omega^2}+\ldots\ldots+\frac{{}_nA_{1s}}{\omega_n^2-\omega^2}\right]\Phi_s e^{i\omega t}\\
q_2 &= \left[\frac{{}_1A_{2s}}{\omega_1^2-\omega^2}+\frac{{}_2A_{2s}}{\omega_2^2-\omega^2}+\ldots\ldots+\frac{{}_nA_{2s}}{\omega_n^2-\omega^2}\right]\Phi_s e^{i\omega t}\\
&\cdots\cdots\cdots\cdots\cdots\cdots\cdots\cdots\cdots\\
&\cdots\cdots\cdots\cdots\cdots\cdots\cdots\cdots\cdots\\
q_n &= \left[\frac{{}_1A_{ns}}{\omega_1^2-\omega^2}+\frac{{}_2A_{ns}}{\omega_2^2-\omega^2}+\ldots\ldots+\frac{{}_nA_{ns}}{\omega_n^2-\omega^2}\right]\Phi_s e^{i\omega t}
\end{aligned}\right\} \quad . \quad . \quad (14)$$

If excitation is applied at more co-ordinates than just the s^{th}, then other expressions of the same form as these must be added, but the general form of the solutions is retained.

Each column of terms in equation (14) represents motion in a principal mode. Let ω approach the m^{th} natural frequency ω_m and, at the same time, Φ_s be diminished such that the fraction $\Phi_s/(\omega_m^2-\omega^2)$ retains a finite and constant value. As this limiting process proceeds, the harmonic distortion acquires a definite shape which is given by

$$q_1 : q_2 : \ldots : q_n :: {}_mA_{1s} : {}_mA_{2s} : \ldots : {}_mA_{ns} \quad . \quad . \quad . \quad (15)$$

This shape of distortion is, of course, independent of the co-ordinate q_s at which the vanishingly small excitation $\Phi_s e^{i\omega t}$ is applied; in fact, the appearance of the suffix s in the relation (15) merely indicates that, while the ratios between the A's are determined by the system, their actual values depend upon the co-ordinate q_s at which forcing occurs.

When ω does not coincide with a natural frequency, equation (14) shows that, in general, all the principal modes are excited. Moreover, if a principal co-ordinate p_m is associated with distortion in the m^{th} principal mode—that is with distortion according to the m^{th} column of partial fractions—then p_m varies in the same way with ω as does the deflection of a simple spring-suspended mass when it is subjected to a harmonic force.

2.4. The Addition of Damping

The various results that have been quoted for conservative systems are well known. They are modified when damping is included and it is difficult to see the ways in which they are altered by viscous damping, because of the algebraic complications which accompany viscous damping terms. Now heavier algebra is evidently inescapable when damping is introduced, but it will next be shown that the theory does not lose its previous form and indeed retains much of its simplicity when the existence of *hysteretic* (instead of viscous) damping is postulated.

3. Hysteretic Damping of Systems with n Degrees of Freedom

3.1. The General Solution

The mathematical theory of hysteretic damping has been presented in a previous paper[3], and it will now be supposed that all the damping forces are of this type. It was shown that the equations of motion governing the variation of $q_1, q_2, \ldots q_n$ are of the form

$$\left.\begin{aligned}[a_{1r}\ddot{q}_1+(c_{1r}+id_{1r})\,q_1]+[a_{2r}\ddot{q}_2+(c_{2r}+id_{2r})\,q_2]+\ldots\\ \ldots+[a_{nr}\ddot{q}_n+(c_{nr}+id_{nr})\,q_n]=\Phi_r e^{i\omega t}\qquad(r=1,2,\ldots n)\end{aligned}\right\} \quad (16)$$

where the effects of the hysteretic damping are embodied entirely in the constants $d_{1r}, d_{2r} \ldots$, and where the applied harmonic forces give rise to generalised forces, as in equation (3). The algebraic consequence of introducing the damping into a conservative system is thus to add an imaginary part to each of the stability coefficients c_{rs} of the potential energy function (1). If the harmonic solutions of equation (4) are now sought as before, n algebraic equations are found for the amplitudes Ψ_j. They are

$$(c_{1r}+id_{1r}-\omega^2a_{1r})\,\Psi_1+(c_{2r}+id_{2r}-\omega^2a_{2r})\Psi_2+\ldots+(c_{nr}+id_{nr}-\omega^2a_{nr})\,\Psi_n=\Phi_r \quad (17)$$

and the same technique of solution as before may be used.

The amplitude of the response at q_r due to excitation by a force $\Phi_s e^{i\omega t}$ is again found to be given by equation (7), where the receptance

$$\alpha_{rs}=(-1)^{r+s}\frac{\Delta_{rs}}{\Delta}. \quad (18)$$

is now complex. This means that the response is no longer in phase (or in exact anti-phase) with the excitation. The complexity of α_{rs} arises because the determinant Δ is similar to that of equation (6) but has the real constants c_{rs} of that expression augmented by the imaginary parts id_{rs}, and also the determinant Δ_{rs} which is formed from it is complex for the same reason.

When it is expanded, the determinant Δ yields a polynomial of degree n in ω^2 whose coefficients are now, in general, complex. Equation (8) will have n complex roots, which will be denoted by $\xi_1, \xi_2, \ldots \xi_n$, so that the receptances have the form

$$\alpha_{rs}=\frac{f(\omega^2)}{(\xi_1-\omega^2)(\xi_2-\omega^2)\ldots\ldots(\xi_n-\omega^2)} \quad (19)$$

where $f(\omega^2)$ is now a complex polynomial in ω^2 of maximum degree $n-1$. The receptances may be manipulated as before to show (*i*) the properties of direct receptances and (*ii*) the nature of motion in modes although these modes are no longer the " principal modes."

3.2. Direct Receptances

The direct receptance α_{rr} is given by $\alpha_{rr}=\Delta_{rr}/\Delta$ and, just as $\Delta=0$ has n complex roots, so $\Delta_{rr}=0$ has $n-1$ complex roots which will be denoted by $\eta_1, \eta_2, \ldots\ldots \eta_{n-1}$. The receptance may therefore be written in the form

$$\alpha_{rr}=K\frac{(\eta_1-\omega^2)(\eta_2-\omega^2)\ldots\ldots(\eta_{n-1}-\omega^2)}{(\xi_1-\omega^2)(\xi_2-\omega^2)\ldots\ldots(\xi_n-\omega^2)} \quad . \quad . \quad . \quad (20)$$

where K is a constant.

If all the damping forces are made smaller and smaller then, in this expression

$$\left.\begin{aligned}&\mathscr{R}(\eta_i)\longrightarrow\Omega_i^2\,; \quad \mathscr{I}(\eta_i)\longrightarrow 0 \quad (i=1,2,\ldots n-1)\\ &\mathscr{R}(\xi_j)\longrightarrow\omega_j^2\,; \quad \mathscr{I}(\xi_j)\longrightarrow 0 \quad (j-1,2,\ldots n)\end{aligned}\right\} \quad . \quad . \quad (21)$$

in order that the result (12) may be arrived at for the conservative system.

The quantity ω^2 is essentially real and positive because the motion is restricted in this way so that, in general, $|\alpha_{rr}|$ can never be made infinite or zero by adjustment of the excitation frequency. The amplitude $|\Psi_r|$ which is given by

$$|\Psi_r| = |\alpha_{rr}|\Phi_r \quad . \quad . \quad . \quad . \quad . \quad (22)$$

may be said, somewhat loosely, to have minimum values when

$$\omega^2=\mathscr{R}(\eta_i) \qquad (i=1,2,\ldots n-1) \quad . \quad . \quad . \quad . \quad (23)$$

and maximum values when

$$\omega^2=\mathscr{R}(\xi_j) \qquad (j=1,2,\ldots n) \quad . \quad . \quad . \quad . \quad (24)$$

where it is assumed that the introduction of damping does not modify the quantities Ω_i^2 and ω_j^2 to the extent of making the real parts of η_i and ξ_j negative. This assumption is justified as normally damped systems do give minimum and maximum amplitudes in the manner just stated.

3.3. Motion in "Modes"

The receptances α_{rs} have been shown to be of the form (19) where $f(\omega^2)$ is a polynomial of maximum degree $n-1$ in ω^2 whose coefficients are complex. It follows that they can still be expressed as series of partial fractions as in equation (13) so that

$$\alpha_{rs}=\frac{{}_1B_{rs}}{\xi_1-\omega^2}+\frac{{}_2B_{rs}}{\xi_2-\omega^2}+\ldots\ldots+\frac{{}_nB_{rs}}{\xi_n-\omega^2} \quad . \quad . \quad . \quad (25)$$

where the constants ${}_mB_{rs}$ and (of course) the ξ's are complex.

As before, it is instructive to write down the expressions giving the responses at the co-ordinates q which are caused by harmonic forcing of amount $Q_s = \Phi_s e^{i\omega t}$. They are

$$\left.\begin{aligned} q_1 &= \left[\frac{{}_1B_{1s}}{\xi_1 - \omega^2} + \frac{{}_2B_{1s}}{\xi_2 - \omega^2} + \ldots + \frac{{}_nB_{1s}}{\xi_n - \omega^2}\right]\Phi_s e^{i\omega t} \\ q_2 &= \left[\frac{{}_1B_{2s}}{\xi_1 - \omega^2} + \frac{{}_2B_{2s}}{\xi_2 - \omega^2} + \ldots + \frac{{}_nB_{2s}}{\xi_n - \omega^2}\right]\Phi_s e^{i\omega t} \\ &\cdots\cdots\cdots\cdots \\ q_n &= \left[\frac{{}_1B_{ns}}{\xi_1 - \omega^2} + \frac{{}_2B_{ns}}{\xi_2 - \omega^2} + \ldots + \frac{{}_nB_{ns}}{\xi_n - \omega^2}\right]\Phi_s e^{i\omega t} \end{aligned}\right\} \quad . \quad (26)$$

Once again, if more of the generalised forces than just Q_s are non-zero, then other, similar, solutions must be added to these; but they will not alter the general character of the equations. However, there is no longer any assurance that the ratios between the constants ${}_mB_{rs}$ in any column of partial fractions are the same for all co-ordinates q_s at which excitation is applied, since the previous limiting condition cannot now be used. Thus the shapes of the "modes" which are associated with the various columns depend upon the nature of the applied harmonic excitation.

It will be seen from equations (26) that, for any value of ω, all the modes will be excited in general; but one mode, the m^{th} say, will predominate if

$$\left.\begin{aligned} \mathscr{R}(\xi_m) &\fallingdotseq \omega^2 \\ \mathscr{I}(\xi_m) &\fallingdotseq 0 \end{aligned}\right\} \quad . \quad . \quad . \quad . \quad . \quad . \quad (27)$$

Also, the amplitude of the motion can never be infinite unless these approximations are realised exactly.

If a particle of mass M is suspended by a light spring of stiffness k which has in parallel with it a hysteretic damper whose coefficient is h, the equation governing extensional displacement x if a harmonic force $Fe^{i\omega t}$ is applied to the particle is[2]

$$M\ddot{x} + (k + ih)\,x = Fe^{i\omega t} \quad . \quad . \quad . \quad . \quad . \quad (28)$$

The steady-state solution of this is

$$x = \frac{Fe^{i\omega t}}{(k + ih) - M\omega^2} \quad . \quad . \quad . \quad . \quad . \quad (29)$$

This result has the same form as the contributions of individual partial fractions to the variations of the q's in equations (26). The nature of the approximation which is made when a damped system is treated as if it possesses but one degree of freedom when it is excited at a near-resonant frequency may thus be seen clearly.

Equations (26) provide a means of assessing the errors arising in a vibration analysis which ignores damping altogether. This latter technique is, of course, only feasible when the frequency ω is not near a natural frequency, as will be seen on inspection of the equations. When the damping is not light, it will often be possible to use only a few of the partial fractions instead of all of them; the decision to make a selection of this sort may be made when numerical values of the various parameters are known.

4. Systems with Small Damping

4.1. The General Solution

In engineering one is mainly concerned with systems which embody "small" damping, as these are the most prone to violent oscillation near resonances. It is worth while, therefore, to discuss the form that the theory of Section 3 takes when the damping forces are small. It is convenient, in doing this, to quote certain mathematical results, the validity of which is dealt with in the Appendices.

Suppose that a conservative system is modified by the introduction of small damping forces, so that the coefficients c_{ij} have, added to them, small imaginary parts id_{ij}. The quantities $\xi_1, \xi_2, \ldots \xi_n$, which are the roots of $\Delta=0$, may be regarded as functions of the coefficients $(c_{ij}+id_{ij})$. By means of Taylor's theorem for a function of several variables, it is shown (*see* Appendix I) that

$$\left.\begin{aligned}\xi_m = \omega_m^2 + i\,[\text{real function of order } (d_{ij})\,] + \\ +\,[\text{functions of higher orders of } (d_{ij})\,] \quad (m=1, 2, \ldots n)\end{aligned}\right\} \quad . \quad (30)$$

The condition under which the first term in square brackets is small and the second is negligible is that of "small damping," and its nature is discussed in Appendix I. Thus, for small damping, any receptance may be written in the form

$$\alpha_{rs} \fallingdotseq \frac{f(\omega^2)}{(\omega_1^2 + iO\,[d_{ij}] - \omega^2)\,(\omega_2^2 + iO\,[d_{ij}] - \omega^2) \ldots \ldots (\omega_n^2 + iO\,[d_{ij}] - \omega^2)} \cdot \quad (31)$$

Once more it is convenient to examine separately (*i*) the properties of direct receptances and (*ii*) the nature of the motion in modes.

4.2. Direct Receptances

The roots of $\Delta_{rr}=0$ are modified in a similar fashion to those of $\Delta=0$, so that

$$\eta_m \fallingdotseq \Omega_m^2 + iO\,[d_{ij}] \qquad (m=1, 2, \ldots n-1) \quad . \quad . \quad . \quad (32)$$

where the function of order (d_{ij}) is a real one. Direct receptances may therefore be written in the form

$$\alpha_{rr} \fallingdotseq K\,\frac{(\Omega_1^2 + iO\,[d_{ij}] - \omega^2)\,(\Omega_2^2 + iO\,[d_{ij}] - \omega^2) \ldots \ldots (\Omega_{n-1}^2 + iO\,[d_{ij}] - \omega^2)}{(\omega_1^2 + iO\,[d_{ij}] - \omega^2)\,(\omega_2^2 + iO\,[d_{ij}] - \omega^2) \ldots \ldots (\omega_n^2 + iO\,[d_{ij}] - \omega^2)} \quad (33)$$

It is now seen that, for small damping, the frequencies which correspond to the minimum motions at q_r are very close to the original anti-resonance frequencies of the undamped system. Furthermore, these minimum responses are small. Equally, maximum motions occur at excitation frequencies which are very close to the natural frequencies of the conservative system; these motions are large.

4.3. Motion in Modes

In Appendix II it is shown that any receptance α_{rs} of the form (25) is such that, for small damping,

$$ {}_mB_{rs} \fallingdotseq {}_mA_{rs} + iO\,[d_{ij}] \qquad (m = 1, 2, \ldots n) \quad . \quad . \quad . \quad (34) $$

where, again, the function of order (d_{ij}) is real. It follows therefore that, if excitation is applied at q_s as before,

$$ \left.\begin{aligned}
q_1 &\fallingdotseq \left[\frac{{}_1A_{1s} + iO\,[d_{ij}]}{{\omega_1}^2 + iO\,[d_{ij}] - \omega^2} + \frac{{}_2A_{1s} + iO\,[d_{ij}]}{{\omega_2}^2 + iO\,[d_{ij}] - \omega^2} + \ldots + \frac{{}_nA_{1s} + iO\,[d_{ij}]}{{\omega_n}^2 + iO\,[d_{ij}] - \omega^2}\right] \Phi_s e^{i\omega t} \\
q_2 &\fallingdotseq \left[\frac{{}_1A_{2s} + iO\,[d_{ij}]}{{\omega_1}^2 + iO\,[d_{ij}] - \omega^2} + \frac{{}_2A_{2s} + iO\,[d_{ij}]}{{\omega_2}^2 + iO\,[d_{ij}] - \omega^2} + \ldots + \frac{{}_nA_{2s} + iO\,[d_{ij}]}{{\omega_n}^2 + iO\,[d_{ij}] - \omega^2}\right] \Phi_s e^{i\omega t} \\
&\cdots\cdots\cdots\cdots\cdots\cdots\cdots\cdots\cdots\cdots\cdots\cdots\cdots\cdots\cdots \\
&\cdots\cdots\cdots\cdots\cdots\cdots\cdots\cdots\cdots\cdots\cdots\cdots\cdots\cdots\cdots \\
q_n &\fallingdotseq \left[\frac{{}_1A_{ns} + iO\,[d_{ij}]}{{\omega_1}^2 + iO\,[d_{ij}] - \omega^2} + \frac{{}_2A_{ns} + iO\,[d_{ij}]}{{\omega_2}^2 + iO\,[d_{ij}] - \omega^2} + \ldots + \frac{{}_nA_{ns} + iO\,[d_{ij}]}{{\omega_n}^2 + iO\,[d_{ij}] - \omega^2}\right] \Phi_s e^{i\omega t}
\end{aligned}\right\} \quad . \quad . \quad . \quad . \quad (35) $$

The modes are seen to be still complex but the complexity, that is the amount by which the displacements are out of phase in a given mode, is small. The modes are very nearly the same as the principal modes but no longer represent motions which are exactly in phase.

5. Conclusion

The theory of small forced harmonic motions of conservative systems is well-known and is mathematically straightforward. But when damping is included in the theory, added complication of the equations is inescapable. The usually adopted theory is that of viscous damping and, by its use, it is possible to derive several important results for the case of small damping. These results are not easily established and the general theory of viscous damping is, analytically speaking, unwieldy. Problems in which the damping is not small are by no means easy to tackle on this account.

It has been shown in this paper, that the motion of damped systems is more easily dealt with under the assumption of *hysteretic* damping. The same general conclusions are arrived at as may be found from viscous damping theory, but their

extraction is much simpler. The hysteretic damping theory also provides a simpler means of dealing with systems whose damping is not small.

ACKNOWLEDGMENT

The author wishes to acknowledge the help which he has received from discussions with Professor D. C. Johnson on the subject matter of this paper.

REFERENCES

1. YATES, H. G. Vibration Diagnosis in Marine Geared Turbines. *Transactions of the N.E. Coast Institution of Engineers and Shipbuilders*, Vol. 65, 4, 225-261, 1949.

2. BISHOP, R. E. D. The Treatment of Damping Forces in Vibration Theory. *Journal of the Royal Aeronautical Society*, November 1955.

3. BISHOP, R. E. D. The General Theory of "Hysteretic Damping." *The Aeronautical Quarterly*, February 1956.

4. DUNCAN, W. J. Mechanical Admittances and Their Applications to Oscillation Problems. R. & M. 2000, 1947.

5. JOHNSON, D. C. The Application of Admittance Methods to the Classical Theory of Small Oscillations. *Engineering*, Vol. 171, No. 4453, p. 650, 1951.

6. BISHOP, R. E. D. The Analysis and Synthesis of Vibrating Systems. *Journal of the Royal Aeronautical Society*, October 1954.

7. BISHOP, R. E. D. and JOHNSON, D. C. Some Properties of Nodes in Vibrating Systems. *The Aeronautical Quarterly*, February 1955.

Appendix I

THE EFFECT OF SMALL DAMPING ON ROOTS OF THE EQUATION $\Delta=0$

The equation

$$\Delta=0 \quad . \quad . \quad . \quad . \quad . \quad . \quad . \quad (36)$$

may be regarded as one relating any of its roots $\omega^2=\xi_r$ to the complex quantities

$$z_{ij}=c_{ij}+id_{ij}, \quad . \quad . \quad . \quad . \quad . \quad . \quad (37)$$

in which only the imaginary parts will be supposed to vary. Thus, equation (36) may be written as

$$f(\xi_r, z_{11}, z_{22}, \ldots z_{nn}, z_{12} \ldots)=0, \quad . \quad . \quad . \quad . \quad (38)$$

the quantity ξ_r being given as an implicit function of the z_{ij}. The value of ξ_r varies if the z_{ij} are varied, and, in particular, if all the imaginary parts of the z_{ij} are zero, then $\xi_r=\omega_r^2$.

According to Taylor's theorem for several complex variables

$$\xi_r=\omega_r^2+\sum_{i=1}^{n}\sum_{j=1}^{n}\left[\frac{\partial\xi_r}{\partial z_{ij}}(id_{ij})\right]+\ldots \quad . \quad . \quad . \quad . \quad (39)$$

where the derivatives are all evaluated at the real values of the z_{ij}, (that is at $\xi_r=\omega_r^2$).

Now, in order to obtain these derivatives, it is necessary to differentiate the implicit function (38) of ξ_r and the complex variable z_{ij}. This may be done by means of a result in the theory of complex variables which states that, provided that conditions of analyticity are met and that equation (36) has no repeated roots,

$$\left[\frac{\partial \xi_r}{\partial z_{ij}}\right]_{\xi_r=\omega_r^2} = -\left[\frac{\partial f}{\partial z_{ij}}\right]_{\xi_r=\omega_r^2} \Big/ \left[\frac{\partial f}{\partial \xi_r}\right]_{\xi_r=\omega_r^2} . \quad . \quad . \quad (40)$$

For any physical system, the conditions under which this result holds good are fulfilled.

The two derivatives on the right hand side of equation (40) are real. It follows that the one on the left hand side is also real and hence that the second terms of the Taylor series (39) are all imaginary, containing the d_{ij} to the first power.

This result provides a mathematical specification for " small damping," namely that

$$\left[\frac{\partial \xi_r}{\partial z_{ij}}\right]_{\xi_r=\omega_r^2} \times d_{ij} << \omega_r^2 \quad . \quad . \quad . \quad . \quad (41)$$

for all i, j and r. This implies that all the $| d_{ij} |$ must be much smaller than the absolute values $| c_{uv} |$ of these stability coefficients which are non-zero.

Appendix II

The Effect of Small Damping on the Constants ${}_iB_{rs}$

The constants ${}_iB_{rs}$ of equation (25) can be expressed in a standard form, as may be seen by starting from the equation

$$\alpha_{rs} = (-1)^{r+s} \frac{\Delta_{rs}}{\Delta} = \sum_{i=1}^{n} \frac{{}_iB_{rs}}{\xi_i - \omega^2} . \quad . \quad . \quad . \quad . \quad (42)$$

If both sides of this equation are multiplied by Δ and then ω^2 is made equal to ξ_i, it is found that, provided that $\Delta = 0$ has no repeated roots,

$${}_iB_{rs} = \frac{(-1)^{r+s} (\Delta_{rs})_{\omega^2=\xi_i}}{\left(\dfrac{\Delta}{\xi_i - \omega^2}\right)_{\omega^2=\xi_i}} . \quad . \quad . \quad . \quad . \quad (43)$$

This equation defines ${}_iB_{rs}$ as an analytic function of the quantities z_{uv} (*see* equation (37)) and the ξ's. But, since the ξ's are analytic functions of the z's, it follows that the ${}_iB_{rs}$ are analytic functions of the z's.

Taylor's theorem may now be used in the same manner as before to trace the effect upon the constants ${}_iB_{rs}$ of varying the damping coefficients d_{uv}. It will be recalled that, when all the d_{uv} are zero, ${}_iB_{rs}$ is the same as ${}_iA_{rs}$ of the conservative system, so that

$${}_iB_{rs} = {}_iA_{rs} + \sum_{u=1}^{n} \sum^{n} \left[\frac{\partial {}_iB_{rs}}{\partial z_{uv}} (id_{uv})\right] + \ldots \quad . \quad . \quad . \quad (44)$$

where all the derivatives are evaluated at one of the values $\xi = \omega_j^2$ (when all the z's are real). From inspection it is clear that the derivatives in the second terms of equation (44) are all real so that, to the first power of the d_{uv}, ${}_iA_{rs}$ is modified by the addition of an imaginary term only.